Electronic Theses and Dissertations

Theses, Dissertations, and Major Papers

2013

Study of the Door Closing Performance of an Aluminum Door

Maurizio Mozzone
University of Windsor

STUDY OF THE DOOR CLOSING PERFORMANCE OF AN ALUMINUM DOOR

By

Maurizio Mozzone

A Thesis

Submitted to the Faculty of Graduate Studies

through the **Department of Mechanical, Automotive and Materials Engineering**

in Partial Fulfillment of the Requirements for

the Degree of **Master of Applied Science**

at the University of Windsor

Windsor, Ontario, Canada

2013

STUDY OF THE DOOR CLOSING PERFORMANCE OF AN ALUMINUM DOOR

by

Maurizio Mozzone

APPROVED BY:

_____
Jill Urbanic
Department of Industrial and Manufacturing Systems Engineering

_____
Daniel Green
Department of Mechanical, Automotive and Materials Engineering

_____
Jennifer Johrendt, Advisor
Department of Mechanical, Automotive and Materials Engineering

July 30, 2013

DECLARATION OF ORIGINALITY

I hereby certify that I am the sole author of this thesis and that no part of this thesis has been published or submitted for publication.

I certify that, to the best of my knowledge, my thesis does not infringe upon anyone's copyright nor violate any proprietary rights and that any ideas, techniques, quotations, or any other material from the work of other people included in my thesis, published or otherwise, are fully acknowledged in accordance with the standard referencing practices. Furthermore, to the extent that I have included copyrighted material that surpasses the bounds of fair dealing within the meaning of the Canada Copyright Act, I certify that I have obtained a written permission from the copyright owner(s) to include such material(s) in my thesis and have included copies of such copyright clearances to my appendix.

I declare that this is a true copy of my thesis, including any final revisions, as approved by my thesis committee and the Graduate Studies office, and that this thesis has not been submitted for a higher degree to any other University or Institution.

ABSTRACT

When purchasing a product, and in particular when many different brands compete in the market, the first impression will consistently affect a customer's choice. When buying a car, the ease with which the doors close, the speed and the sound of the closure must give the customer the impression of a quality car.

The recent stringent regulations on fuel economy and pollution have forced car makers to look for new solutions to lower the fuel consumption of the vehicles of their fleet and meet the standards imposed. The most obvious solutions to reach the target are the improvement in the efficiency of engines and the reduction in vehicle weight. In the recent past, the use of aluminum (mainly in the form of alloy) in the automotive industry has increased due to its lower weight with respect to steel, even if the higher costs remain a big hindrance to the large-scale use of this metal. When dealing with door closing effort, the use of aluminum introduces some issues that relate directly to the lower weight of the door and possibly to other factors dependent on the different materials. The closing performance of the door is therefore expected to change, and the variations in the contributors to the closing effort need to be analyzed and discussed.

In this work, the door closing performance of an aluminum door and of a steel door of a C segment vehicle are fully compared to study what changes, and to which extent, in the closing effort, due to the lighter alloy used. Two means are used, the physical testing of the doors in the body shop with the EZ Slam technology, and the simulation of the closing event with an existing closing effort predictive model. Particular focus is put on the contribution of the check system to the closing effort and how its final profile affects the closing event of the door.

DEDICATION

To family and friends, who, regardless of distance, never felt far away.

ACKNOWLEDGEMENTS

TABLE OF CONTENTS

LIST OF TABLES

LIST OF FIGURES

xiii

LIST OF ABBREVIATIONS/SYMBOLS

c_{seal}: coefficient used to correct the seal compression model in the OU Model.

c_m: door center of mass position (OU Model).

CLD: compression Load Deflection.

DFSS: Design For Six Sigma.

DP: Dual Phase.

d_{latch}: latch displacement (OU Model).

d_{seal}: compression distance (OU Model).

$\bar{D}$: normalized compression distance.

E_{air}: energy sunk by the air bind effect during closure (OU Model).

E_{latch}: energy sunk by the latch-striker system during door closure (OU Model).

E_g: gravitational potential energy.

E_{hinge}: energy sunk by the friction at the hinges during closure (OU Model).

E_{weight}: energy that will help door closure due to the weight of the door (OU Model).

F_{latch}: latch force (OU Model).

f_{seal}: seal force (OU Model).

FAST: Ford Advanced Super Plastic Forming Technology.

HSLA: High Strength Low Alloy.

HVAC: Heating Ventilation Air Conditioning.

I_{Adoor}: door's moment of inertia (OU Model).

I_{CM}: moment of inertia of an object around its center of mass.

IQS: Initial Quality Study.

g: acceleration of gravity.

h: distance between the upper and lower hinges (OU Model).

l: length of a seal segment (OU Model).

$\bar{L}$: normalized compression force

l_{seal}: seal lip interference (OU Model).

k_{latch}: constant of proportionality between latch force and latch displacement (OU Model).

MDO: Multidisciplinary Design Optimisation.

mmAq: millimeters of water.

NVH: Noise Vibration Harshness.

OU Model: Oakland University Model.

p_{atm}: atmospheric pressure .

$\overline{\Delta p}$: change in pressure inside the vehicle cabin due to door closure (OU Model).

PA/PE: polyamide/polyethylene

PP100: Problems per 100 vehicles.

QPF: Quick Plastic Forming.

r_{cm}: distance of the door center of mass from door hinge (OU Model).

r_h: door hinge pin radius (OU Model).

r_{latch}: distance of the latch system from door hinge axis (OU Model).

S: vent hole's area.

S_D: door area.

SPF: Super Plastic Forming.

STAR: Simplified Total Aluminum Reinforced.

T_{air}: torque opposing to door closure due to the air bind effect (OU Model).

T_{hinge}: total contrasting torque given by the friction at the door hinges during closure (OU Model).

T_{weight}: torque due to door weight helping door closure (OU Model).

T_{seal}: torque opposing to door closure exerted by all the seal segments (OU Model).

T'_{seal}: corrected seal torque value (OU Model).

ULSAC: Ultra-light Steel Auto Closure.

UTS: Ultimate Tensile Strength.

V_c: vehicle cabin volume.

v_{vent}: velocity of air at the vent (OU Model).

YS: Yield Strength.

ρ_{atm}: density of air at atmospheric pressure (OU Model).

μ_h: hinge friction coefficient (OU Model).

ω: door's angular velocity.

θ_c: door opening angle at which the seals start to compress (OU Model).

θ_h: door opening angle at which the contact between latch and striker takes place (OU Model).

NOMENCLATURE

- Airtight Integrity: closure or fitting that prevents the passage of air.
- Latch: component in the door assembly that allows the complete closure of the door hooking to the striker.
- Lightweighting: term to indicate the decrease in weight of the automotive structures or subsystems.
- Fully latched position: position of the door in which the latching mechanism is fully engaged. The door can be closed in a primary position (the latch is partially engaged so the door cannot open but it is not fully closed), and in a secondary position, corresponding to the fully latched position.
- Overslam: distance the door travels past the final rest position during closure in order to reach a complete latching. Overslam depends on the closing speed, the higher the speed the higher its value.
- Residual Energy: is the energy retained by the door system once the door is shut; if the kinetic energy of the closing door goes to zero before the latched position is reached, the door will not close. A certain amount of kinetic energy (minimum kinetic energy) is needed in order to fully latch the door.
- Seal Gap: it is an indicator of the amount of compression of the seals on the body when the door is fully latched.
- Striker: component screwed on the car body (in correspondence of the latch system) to which the latch hooks in order to completely close the door.

1. INTRODUCTION

Car makers have to deal with many different problems, often related to governmental regulations, standards to be respected and safety issues. Another of the main factors leading car companies' choices is customers' perception and impression on the quality of the product sold.

Door closing performance is strictly related to this last aspect. After the visual impact the vehicle has on the customer, when the customer buys a car the doors are most likely the very first part of the vehicle he/she comes into contact with, to access and exit the vehicle. One of the customer's very first impressions about the quality of the car will then be given by the behaviour of the doors when opening and closing, the speed and the energy that are required to obtain a full latching, and the sound that the door makes when closed by the user. Moreover, an incomplete closure of the door or an excessive speed required to fully latch it might give rise to safety issues that must be avoided or to unpleasant sounds during closure.

Another point of focus for car companies is represented by the lightweighting of structures, required in order to lower the total weight of the vehicle to reduce fuel consumption and pollutants emissions. One of the most obvious ways to reduce the weight of a car (even though not yet sufficient to solve the problems of fuel consumption and excessive pollution levels) is to use lightweight materials (e.g. aluminum and magnesium alloys) to replace the use of steel in components such as the frame or the door panels (side doors, trunk lid, and hood). The use of doors built with an aluminum frame is therefore of great interest for car companies that must take into account the effects that the use of a much lighter door might have.

The purpose of this study is to evaluate the consequences, in terms of door closing effort, of the use of a lightweight aluminum door in place of a common steel door, analyzing all the differences that the use of a different material creates in the door closing process and understanding which actions might be taken, in case of the worsening of the performance, to obtain acceptable door closing performance. The term closing effort can be intended as the total energy needed to fully latch the door, but the greatest focus is put on the effort

that the customer needs to put in order to shut the door (which, as explained later in the document, does not coincide with the total effort). The best way to perform such a study is to have the values of the parameters pertaining to door closing effort both for a steel frame and for an aluminum frame, in order to be able to directly compare all the contributions that hinder or help the door closure and detect the factors that change the most with the change of frame material. Once the values of the energy contributions are known from the tests, it is possible to understand on what parameters it is necessary to work either to lower the value of the energy sinks during closure or to increase the amount of energy given by the factors that help the user in closing the door. To obtain all the parameters related to the effort, the two doors will be tested with the same equipment (provided by EZ Metrology and described in Chapter 5), testing first the steel door and then swapping all the components from the steel frame onto the aluminum frame in order to maintain all the door's features and changing only the frame material. Using an available door closing predictive model, the OU (Oakland University) Model described in Chapter 5, the parameters relative to the two doors will be input to the model to perform an additional comparison of the doors and to correlate the results. Both methods have assumptions and approximations in the calculations, but the results of the two comparisons (between steel and aluminum frames) should point in the same direction, as the two doors will be treated exactly in the same way during the testing and the running of the predictive model.

The document is subdivided into 6 main sections. In Chapter 2 the research work found in the literature about the lightweighting of automotive structures, in particular of side doors, and the use of aluminum in the automotive industry is presented together with past work done on door closing effort. In Chapter 3 a brief review of the theoretical background and of the physical phenomena behind door closing effort is done. Finally, Chapters 4 and 5 focus on the methodologies that have been used to evaluate the door closing effort and on the results obtained with the physical tests on the doors Chapter 6 presents the conclusions, summarizing the results obtained and suggests the future work to be done to improve the results of the research.

The main components of the door assembly are here briefly described to allow an easier understanding of the topic treated.

1.1 Automotive Door Assembly

An automotive door can be divided into eleven main sub-assemblies, each of which is made up of several other parts. In this section a brief description is given of the main parts of the door that will be considered in the following sections in order to facilitate the understanding of the discussion and analysis of the results.

- *Door frame*: composed of the outer and inner panels and an anti-intrusion beam for side crash protection. As described in the literature review section, the frame assembly can change and may have different configurations in terms of inner panel, hinge and belt reinforcements and anti-intrusion safety elements. The door frame exploded view is shown in Figure 1-1.
- *Inner panel*: the exterior panel of the door assembly pointing towards the inside of the cabin; includes the armrest, the handle and other inserts. The trim panel is attached to the door frame by push pins, and it is shown in Figure 1-3, item 1.
- *Door mechanism*: includes the door lock and latching system, the latch support and the latch anchor (placed on the body).
- *Window system*: includes the glass and the window motor and regulator.
- *Sealing system*: all the weather strips and the moldings that provide insulation from sound and external agents. The seal system is divided between the seals attached to the door and the seals attached to the car body. The seals on the door frame and car body are shown in Figure 1-2.
- *Hinges*: upper and lower hinges situated on the door, they are coupled with the hinges mounted on the body and allow the door to swing.
- *Power system*: it is made up of the wiring harness.
- *Mirror system*: includes the mirror glass, frame, external shell, attaching plate, wiring harness and all the insulation.
- *Power controls*: include all the door switches.
- *Speaker system*: includes the speaker and wiring harness connection to the vehicle.

- *Function carrier (or module)*: allows the installation of all the power controls, wiring harness and speaker in the door. The component is screwed directly to the door frame's inner panel (Figure 1-3, item 2).

An exploded view of a front left door is shown in Figure 1-3
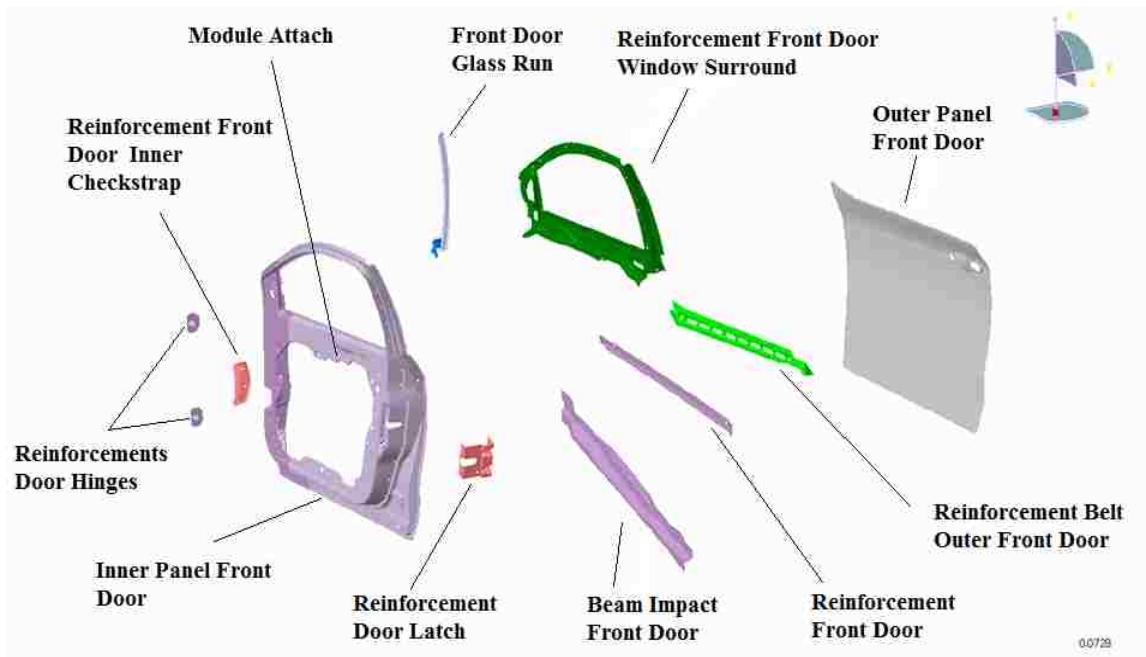
Figure 1-1: Door frame exploded view. In the picture are listed all the components and the reinforcements included in the door frame.

Figure 1-2: Weatherstrip seal system on door frame and car body [1]. The sealing system includes both the seals on the door and the ones applied to the vehicle body where the door fits when closed.

4
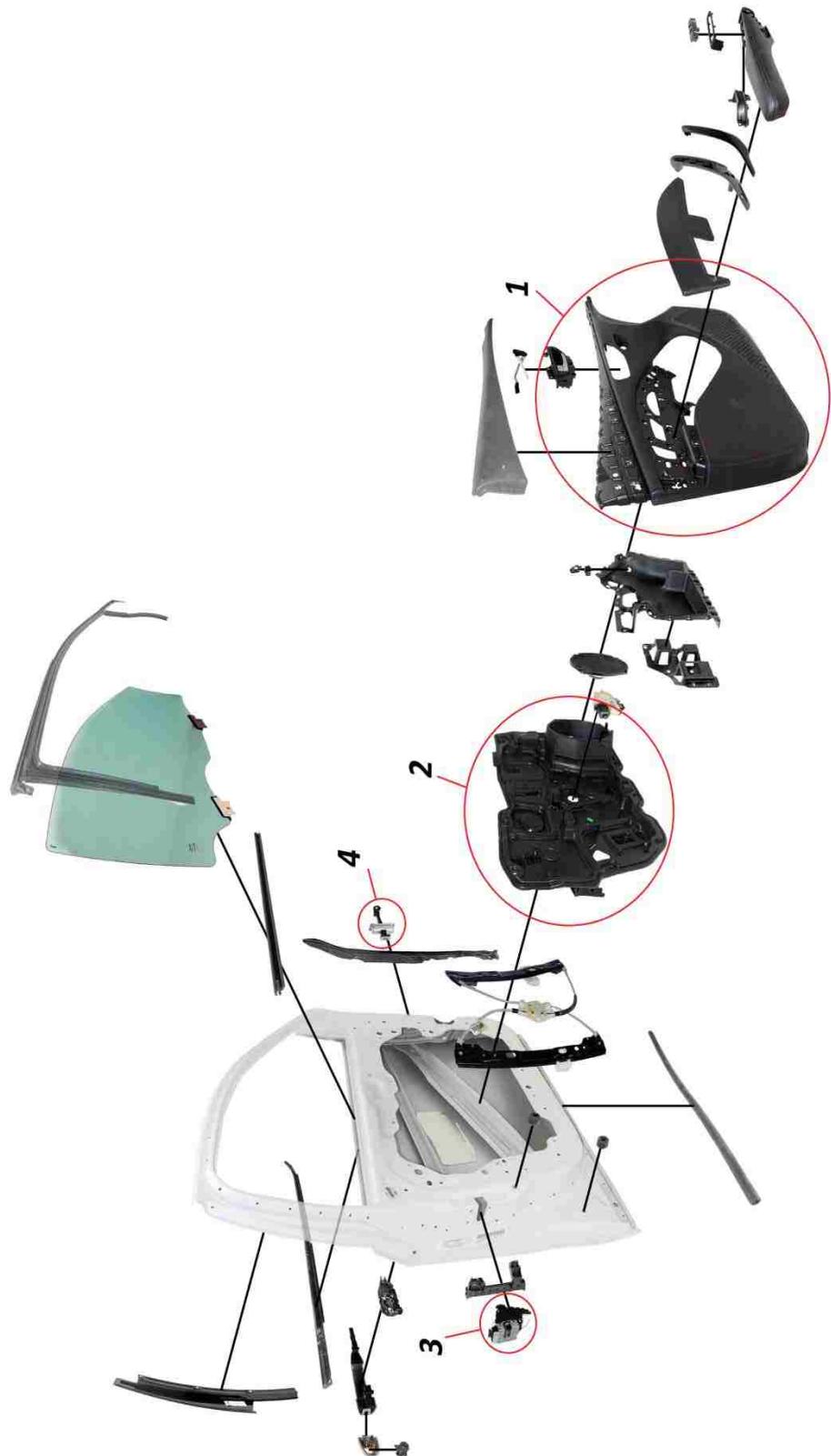
Figure 1-3: Exploded view of a front left door [1]. Specifically numbered from 1 to 4 are the following components: 1) Door trim panel, 2) Door module, 3) Door latching mechanism, 4) Door check system.

1.2 Door latching mechanism and striker (or latch anchor)
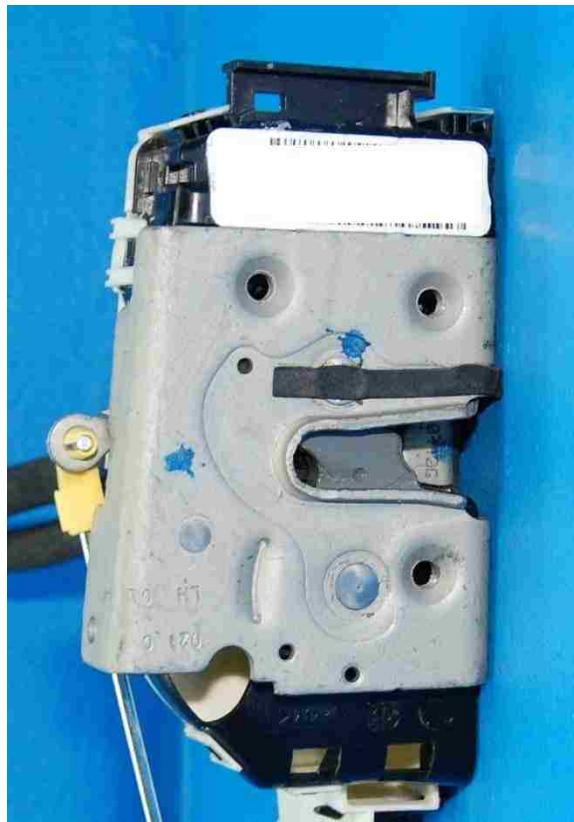
Figure 1-4: Door latching mechanism [1].

Each door of a car is equipped with a latch to lock the door to the body in the closed position. The other main use of the latch is to prevent unauthorized entry to the vehicle. The latch system (shown in Figure 1-4) also has to perform to a specific level during car accidents, having a minimum strength that reduces the possibility of occupants of being ejected during a crash. Tests are performed to verify the minimum strength of door latch (or, better, of the latch-striker combination) in a longitudinal direction (parallel to the direction of vehicular travel) and in a lateral direction (perpendicular to the vehicle's direction of travel). The requirements involve a minimum performance in terms of loads both in the primary position (fully latched door) and in the secondary position (partially engaged system) [2]. Since the latching system is exposed to the environment, it must also withstand exposure to water, ice, dust and dirt, and also to very high and very low temperatures. The system is placed as shown in Figure 1-3, item 3. The latching system features a lock that can be actuated either from the inside or the outside of the vehicle and

it is usually coupled to electromechanical systems of rotation or rotation-translation. The latch can be either manually operated or powered by a motor and it usually consists of rigid and elastic elements (articulated bars, cams, springs and levers) and an actuator in the form of a locking lever. The latch is connected to the inside and outside handles via attached rods and cables [3]. Over the years the latching system has evolved and many different features were added to the mechanism increasing its functionality but also its complexity and weight. As explained in [4], in the 1970's central locking was added (allowing the simultaneous unlocking of all the doors with the push of a button) while in the 1980's remote keyless entry was introduced (thanks to the use of radio frequency transmitters and receivers placed in the key and in the car). The introduction of "Super Locking" allowed an improvement in safety, neutralizing the interior windowsill control knob and all of the door handles to prevent theft. Other features that have been introduced or are in the design phase are the door Passive Entry, that allows the recognition of the owner and the unlocking of the door even before he/she presses the button on the key, the Electric Child Safety (that neutralizes the inside handles of the rear doors to prevent accidental openings by children) and the Power Closing and Release, that allow a tighter closure of the door during vehicle motion to reduce wind and road noise, and an automatic release of the claw of the latch to open the door. The main issues regarding these improved features are, as said before, the increase in weight of the system and also the increased costs. Usually the mechanical solutions that allow all the newly introduced functions require electric powered motors that include compressors, solenoid valves, ECUs and extensive wiring that can add as much as 7 kg of weight to the system. Moreover, these systems are usually complex and time consuming to assemble. However, solutions are available, such as the one presented in [4], that allow all the functions requested in a state-of-the-art latching system while maintaining lower prices (thanks to the use of fewer motors, drivers, wires, and connectors), lower weight (thanks to the simpler system used), smaller packaging envelope, easier installation and system design, and flexibility.

The latch locks the door by hooking to the striker (or latch anchor), shown in Figure 1-5, that is placed on the car body. When trying to reach the best fitting of the door on the body and a perfect closure without unwanted frictions between the components, the

striker can be left loose, the door is shut and the striker is left to adjust itself in order to provide the best closure. The striker is then tightened in its final position.

Figure 1-5: Door striker (anchor) [1].

1.3 Door check system

The check strap, presented in the exploded view in Figure 1-6, is a system connecting the door to the car body and placed as shown in Figure 1-3, item 4.
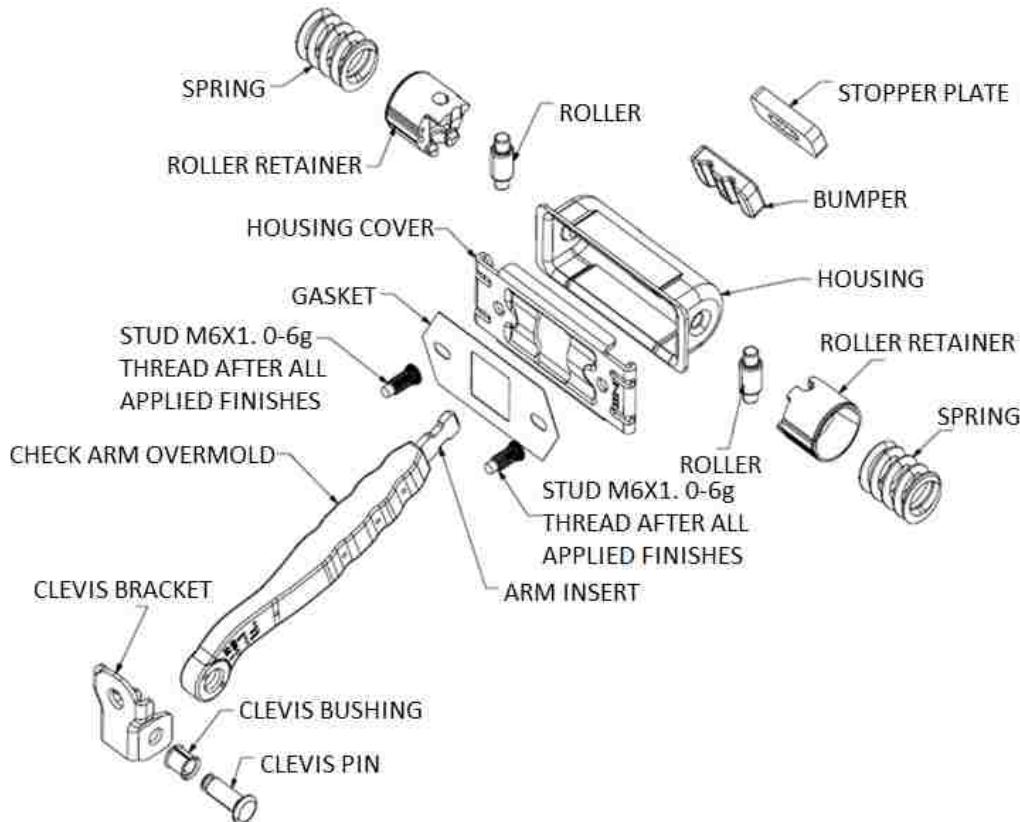
Figure 1-6: Exploded view of the door check system.

The shape of the component is symmetrical with respect to the horizontal axis and the forces are exerted on the check arm through two springs and two rollers. As the door is moved along its arc trajectory, the rollers travel forwards (during closing) and backwards (during opening) on the check arm following the profile of this last component. A section of the check strap is shown in Figure 1-7.
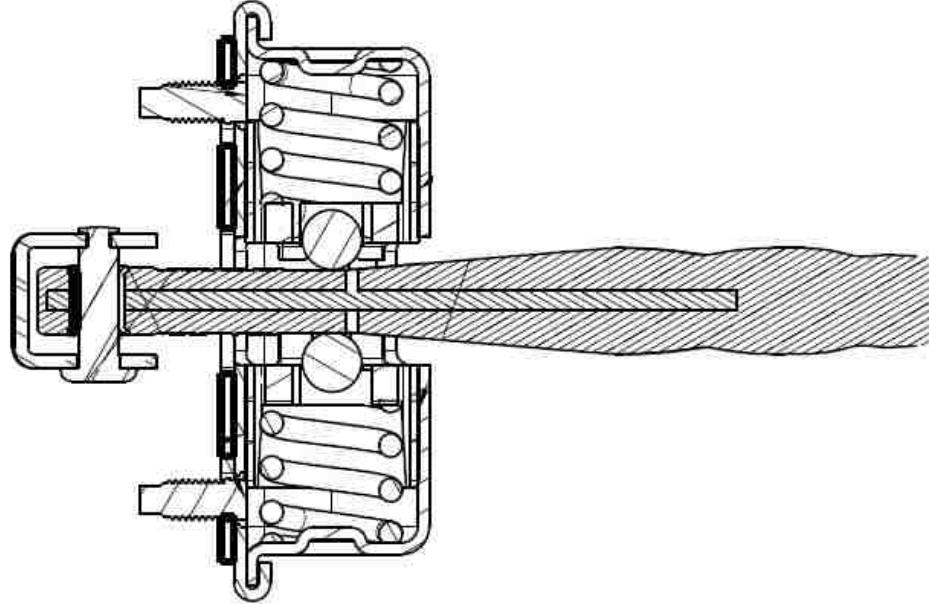
Figure 1-7: Check arm section. In the picture it is possible to see the two springs and the two roller bearings that allow the motion of the door along the check arm.

The left-hand side of the picture shows the clevis bracket that connects the check link to the pillar while the "case" that contains the springs and the rollers is screwed to the door. The check arm has three indents corresponding to positions at which the door will stop if it is operated sufficiently slowly. The presence of these indents causes the closing speed profile that is shown in Figure 1-8. The door is pushed by the user up to a certain angle and then it is let go to close by itself. While the user pushes the door the speed increases, while it starts decreasing when the user lets go and the roller bearings of the check system start "climbing" the profile. Every time the check arm's profile shows a slope, the speed of the door increases; the speed increase is particularly evident during the last slope of the check arm, from approximately 30 degrees of opening angle to the latched position. This last part of the profile of the check is defined close assist. The plot in Figure 1-8, that will be re-presented in the next Chapters 4 and Chapter 5, is to be read from right to left

because it represents the door closing phenomenon that starts when the door is in the fully open position (in the example 67 degrees) and ends when the door is fully latched. When the door is opened the springs store energy, which is released during closure.

The explanation provided describes why the energy contribution of the springs is considered positive on closing the door and negative during opening. During the portion of the profile where the slope increases (the rollers "climb" the check arm) the springs are compressed and store energy that is released during the motion on the portion of the profile showing a negative slope.

The entire weight of the door is carried by the hinges; the clevis bracket that connects the check arm to the car body has a small amount of vertical float allowed and so none of the weight is carried by the check, that has very little rigidity in the up/down direction.
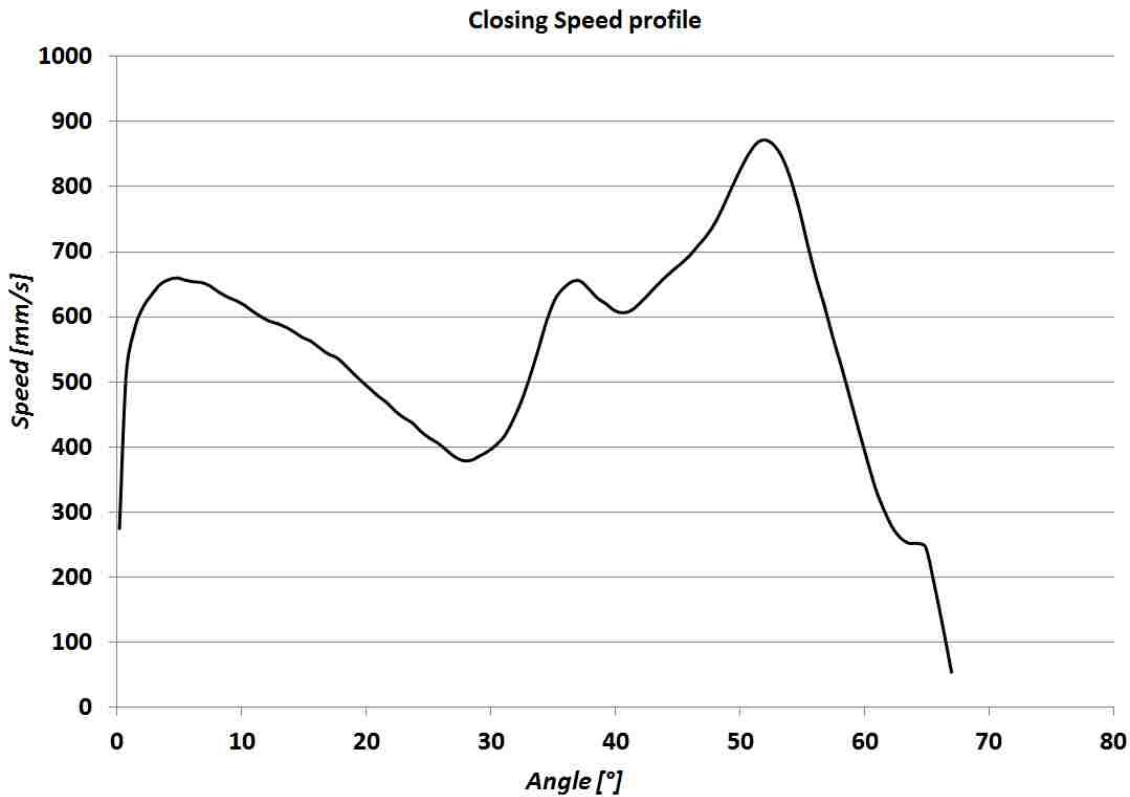
Figure 1-8: Typical closing speed profile of a door pushed by the user. The trend of the curve is dependent on check arm profile and the graph is to be read from right (fully open position) to left (fully latched position).

2. REVIEW OF LITERATURE

2.1 Lightweighting

The regulations on fuel economy, which have become more stringent in the latest period, force car makers to develop different fuel-saving technologies that allow them to meet the standards imposed by the government. These standards are expected to increase in severity even more in the next years; an example would be the 54.5 mpg as average fuel economy required on cars and light trucks by 2025.

From very recent surveys [5], [6], two main technology trends will probably be most helpful for automakers to reach their goals in terms of fuel saving: the use of lightweight materials, and engine downsizing. Other possible ways to be considered are the integration of different components in order to reduce the overall mass of the vehicle (design optimization), improvements in the aerodynamic efficiency of the vehicle and increases in thermodynamic efficiency of engines. During the last IEEE iTec conference on electrification and transportation held in Dearborn, Michigan, in June 2013, it was pointed out how the lightweighting of structures and the engine downsizing will probably not be sufficient to reach the targets on fuel economy and low pollutant emissions, but they will need to be coupled to the use of hybrid propulsion systems such as electric motors. This solution is expected to allow also an improvement in vehicle performance.

Fuel economy concerns and changing government regulations are driving the need to introduce lightweight alternatives for vehicle components. The areas that will probably be the most targeted by lightweighting will be car body and powertrain, followed by the chassis. The reason for this lies in the fact that these areas are all characterized as heavy systems and therefore offer the greatest possibilities for weight reduction: engine and chassis each weigh about 20-30% of the total vehicle weight and auto-body weighs approximately 40-50% of total weight, leaving a 10% for the remaining parts. Amongst the available lightweight materials, aluminum and composites are thought to be, at least at the moment but probably also for several years more, the best choices to obtain a consistent decrease in the weight of components and consequently of the vehicles, but many solutions involving high strength steels in particular have also been studied.

11

Starting back in 1994, significant vehicle weight reductions were achieved with the introduction of high strength steel (mostly in the framework) that allowed an increase in structural resistance and stiffness together with a decrease in weight of around 12-13%. These benefits were realized due to the higher mechanical properties of high strength steel. However, cost-related issues arose due to the more expensive shaping techniques required, the better anti-corrosion treatments needed and, in general, the higher cost of the high-strength steel with respect to common steel. The aluminum alloys have interesting qualities such as low density, good mechanical properties and high corrosion resistance. A comparative study in 2001 of Kelkar et al. [7] analyzed the production costs relative to three small cars; one was built entirely in steel (VW Lupo), one built with an hybrid steel-aluminum structure (VW Lupo Hybrid, built with doors, bonnet and fenders made of aluminum) and a last one designed to be a fully aluminum car (Audi A2). Although as highlighted before aluminum has a much lower density than steel (and thus lower weight) and satisfies the stiffness and torsion requirements for automotive components, the cost by weight is much higher than that of steel and therefore requires optimized design and production of the components in order to be cost effective and maintain the advantages of the weight saving. In this research the Technical Cost Modeling (TCM) of MIT's Material System Laboratory was used to break down the total cost into its components (material parameters, processing parameters and production parameters) in fixed and variable costs.

With respect to the steel version, the hybrid version of the Lupo was more expensive due both to the higher material costs and to the added tooling costs required to stamp all the parts. The problems in stamping aluminum involve a tendency of the aluminum to tear, thus requiring slow stampings and extra hits. Even though neglected in the research, another additional cost to be considered was the joining of the aluminum closures to the steel body. The Audi A2 (full aluminum) was comparable, in cost, with the Lupo Hybrid; this was possible because the A2 was designed to be a fully aluminum car and allowed the spaceframe to be optimized using large, cost effective castings instead of aluminum stampings. The total production costs analyzed in the research are presented in Figure 2-1. In order to reach satisfactory results a net decrease of the cost of aluminum is needed

together with a complete review of the design and manufacturing aspects with respect to steel to obtain a cost-effective process.
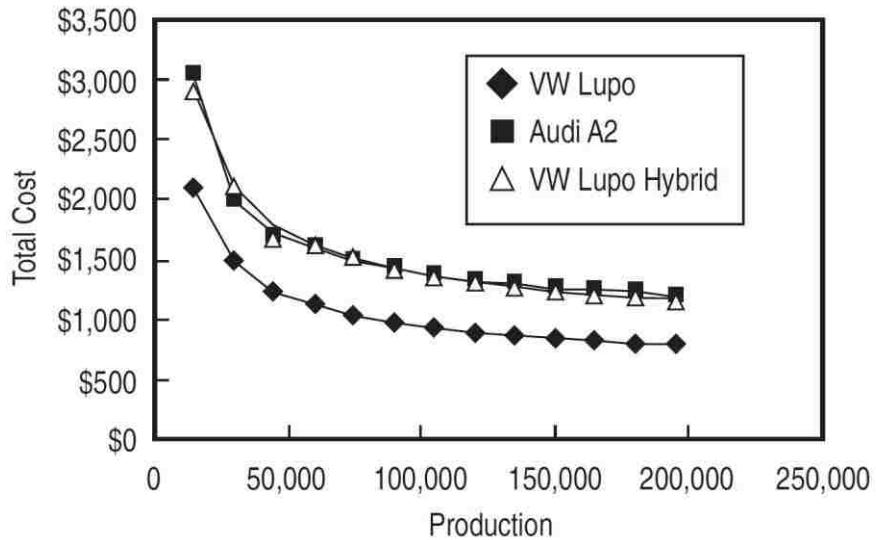
Figure 2-1: Total production costs for the three small cars analyzed in [7]: VW Lupo, Audi A2 and VW Lupo Hybrid.

An even greater weight reduction can be obtained with magnesium alloys, characterized by a density of two-thirds that of aluminum, but showing a lower resistance at high temperatures.

Looking ahead in the future however, the results of the surveys have shown that the greatest weight reductions will probably come from the use of a mixed-materials design approach more than from the use of a single lightweight material.

The costs of the modifications needed on the vehicles of their fleets and of the research and development stages that are necessary to introduce the use of lightweight materials into mass production represent a big investment for car makers, but the cost savings that will result from the lower fuel consumption are thought to outweigh those costs. Despite this fact, the increase in costs probably still represents the biggest challenge for industries in terms of lightweighting.

2.1.1 Lightweight door solutions

Some research was done in 1993 to study the feasibility of the production of a door with die cast magnesium and an extruded aluminum frame using a common steel door design [8]. The steel door used for comparison was that of a mid-size 4 doors sedan of medium-high production volume (> 100000 units). The proposed solution included a one-piece magnesium die casting to consolidate inner panel, upper frame, hinge, lock and waist reinforcements, glass window channels and hinges. For the remaining parts (outer panel, side intrusion beam and window frame) aluminum was chosen. High pressure die casting was chosen for the magnesium parts because of its good design flexibility, dimensional stability and repeatability and overall integrity. The proposed attachment method of the door panel was a flange hemming operation (the operation of folding a panel over another panel, often with the use of a binding element). All the internal components of the door were installed in the exact same position as in the steel frame. From the predicted deflections the magnesium door met the stiffness requirements apart from localized points for the lower torsional rigidity case. From the business analysis done in the research, with a 40% weight saving with respect to the steel door, an estimated unit cost saving of $14.66 may be reached with the magnesium/aluminum solution. Another study was carried out in 2006 by Luckey & al. [9] to investigate the feasibility of superplastic forming (SPF) to reduce the cost of the manufacturing of aluminum sheets and achieve weight savings of the order of at least 30-40% with respect to conventional steel. The superplastic forming allows to achieve large strains to failure and low flow stresses in the panels. It is typically accomplished with a single sided die (less expensive than matched tooling) where the sheet is heated to a high temperature and gas pressure is applied to push the sheet into the tool. Thanks to aspects such as flexible automation for blank heating and loading, automated part extraction and cooling and use of CAE to determine optimal forming parameters that allow a decrease in the overall cycle time, the Ford Advanced Super-Plastic Forming Technology allows cost-effective, higher volume applications of the SPF. The castings, stampings and extrusions necessary to produce a common door architecture were substituted with fewer, less-expensive parts formed with the FAST system, reaching an 80% saving in tooling cost for the door inner.

In 2007 Schrot & al. [10] studied a new design of aluminum front and rear doors using quick plastic forming (QPF) and a multi-purpose reinforced panel named "STAR". The exploded view of the front door is shown in Figure 2-2. The Quick Plastic Forming process was developed by General Motors as a hot sheet blow forming technology to allow the manufacturing of complex aluminum shapes at automotive volumes (up to 100000/yr) [11].
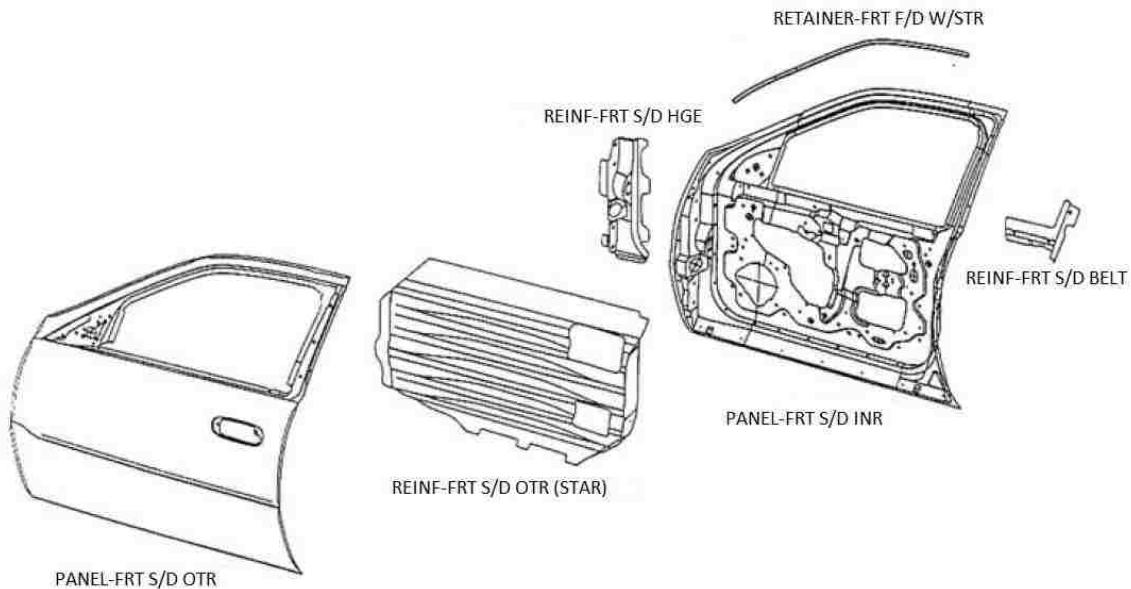
Figure 2-2: Exploded view of the aluminum front door [10].

This type of technology was targeted at forming an automotive panel from a cost-effective aluminum sheet with tooling appropriate for high-volume production. High-volume manufacturing capability was sought. To support the high volume of automotive production the automation of the forming cells was needed. The hydraulic press with heated, insulated tool system offered advantages in terms of performance and flexibility. The higher costs coming from a greater complexity of the system were amortized over a larger number of parts produced. In the QPF process, after the aluminum sheet is brought to the forming cell in blanked and lubricated form, a conduction preheater does the blank preheating outside the press. The cycle time is reduced thanks to an automated material handling. The formed panels can be removed from the tool in a repeatable manner thanks to tool-based extraction mechanisms.

Completing the structure of the door designed in [10] were the inner and the outer panels. The outer panel thickness was increased by 50% with respect to the steel counterpart in order to provide the required rigidity and the inner panel replicated the steel door inner panel, with the same geometry, in order to fit the trim panel without modifications. Maintaining the same outer dimensions, the greater thickness of the panel was driven toward the center of the door section. The main innovation in [10] was the replacement of the conventional impact beam of the door with an open-ended multifunctional Simplified Total Aluminum Reinforced panel (STAR), that allowed the forming in a simple single-piece tool. The front door inner panel and STAR panel are shown in Figure 2-3 and Figure 2-4.
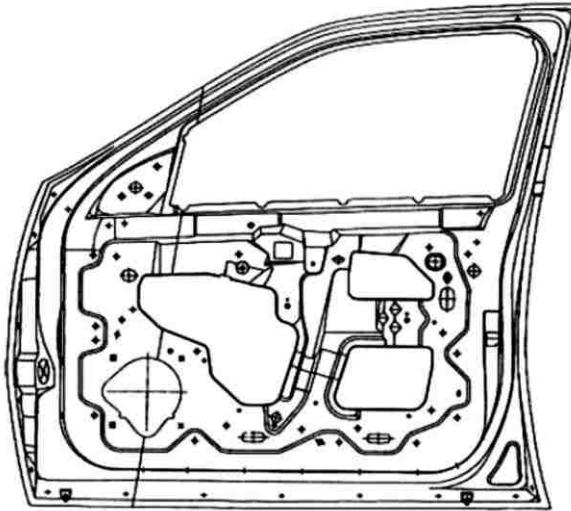
Figure 2-3: Front door inner panel geometry [10].

The corrugated geometry of the STAR panel was designed based on the computer modeling of the static and dynamic performance of the panel; the panel was designed to allow high-volume assembly with traditional assembly fixtures. A separate hinge reinforcement was added. The weight saving with the new front door aluminum structure with respect to its steel counterpart was of 5.7 kg. In terms of performance of the aluminum door, Table 2-1 summarizes the results (for deflection and maximum load for several load cases) predicted in [10] making a comparison with the steel door. The structural performance of the aluminum door was satisfactory and almost all deflection metrics met the target values; a very large deflection at the upper B-pillar position was recorded, but consistent with the steel door performance and dependent on the baseline

16

door design. During the dynamic loading case (dynamic side impact test) the STAR panel was found to distribute the load along the entire periphery of the door below the beltline.
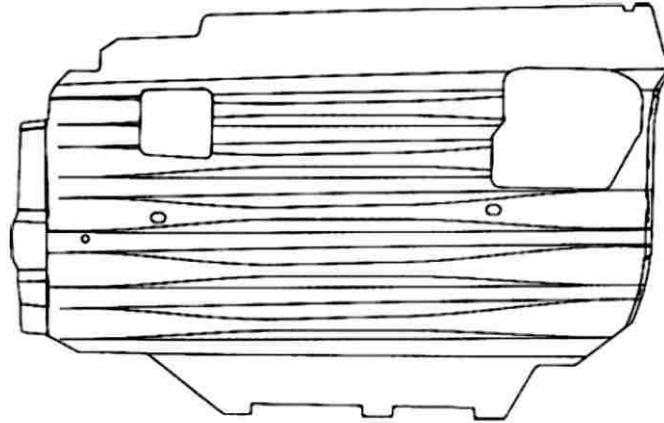
Figure 2-4: Front door STAR panel geometry [10].

Suggestions for an improved door design in [10] were to increase header rigidity and reduce door mass by downgauging the panels, as for many load cases the aluminum door was found to perform even better than the steel prototype.

Table 2-1: Aluminum and Steel predicted structural performance (in terms of deflection and maximum load for several load cases) [10].

	Aluminum front door	Steel proto. front door
Vertical Rigidity	7.44 mm	6.4 mm
	280 MPa	491 MPa
Inner Belt Stiffness	8.9 mm	9.1 mm
	163 MPa	579 MPa
Outer Belt Stiffness	9.0 mm	11.8 mm
	303 MPa	445 MPa
Upper Torsion	2.7 mm	2.6 mm
	101 MPa	372 MPa
Lower Torsion	2.4 mm	3.9 mm
	106 MPa	511 MPa
Upper Frame (Forward)	18.6 mm	12.5 mm
	106 MPa	209 MPa
Upper Frame (Aft)	21.0 mm	18.4 mm
	148 MPa	339 MPa
Mass	14.8 kg	20.5 kg

Amongst the investigations aimed at reaching lower weight doors using steel, in 2000 the UltraLight Steel Auto Closure Consortium achieved a significant 22% weight saving over the lightest benchmark framed door at that time.

The results were achieved by using high and ultra-high strength steels combined with technologies such as tailored blanks and hydroforming. Even greater achievements and further mass reduction were reached using sheet hydroforming for the door outer [12].

When designing a light vehicle, in order to achieve an optimum solution the constraints coming from three main areas need to be considered simultaneously: design, manufacturing and materials. Zuidema [13] defines the process that leads to the correct management and interaction between these three aspects, that starts with the determination of the mechanical properties combination to achieve the required performance in strength, energy absorption and stiffness of the component. The second step is to determine the requirements that assure the manufacturability of the component, and thus mechanisms like work hardening and thinning during manufacturing need to be taken into account. Once the first two aspects are defined, the steel grade development team is in charge of finding the suitable microstructure of the material that will achieve the desired properties. Finally the thermomechanical processes needed to reach the necessary microstructure are defined. Zuidema analyzes how, in the door area of the safety cage, components like the vertical pillars, the roof and the floor cross members need to resist bending collapse and axial buckling. The suggested steel grades for the safety cage components are therefore dual phase grades up to 1180 MPa ultimate tensile strength (UTS) and other complex phase or martensitic and press hardening grades of similar UTS.

In his work Zuidema presents also the design of a door in DP490 steel and 55% Advanced High Strength Steel. First the constraints relative to all the different parts of the door were identified: the door inner is limited by global stiffness and torsional stiffness considerations, the door outer panel is limited by dent resistance and global stiffness considerations while the beltline reinforcement has constraints relative to the elastic axial buckling during transfer of frontal crash loads to the rear of the structure. As for the other components, the door beam is limited by bending collapse and the hinge reinforcement by strength due to door sag requirements. A 20% weight saving with

respect to an initial reference structure with conventional tailor-welded mild steel inner was reached using a monolithic medium-strength grade of lighter gauge and a different door impact beam geometry to make up for the stiffness loss due to the inner panel downgauging. The dent performance of the outer panel was maintained thanks to the use of the lighter and stronger DP490 steel and an additional stiffener was used between the belt line reinforcement and the door beam to offset the lower stiffness of the DP steel and gain back oil canning (slight buckling in the sheet metal that causes an uneven appearance) and panel flutter (self-excited dynamic-aeroelastic instability of panels) resistance. The beltline reinforcement and the door beam were replaced with higher strength, lighter gauge grades. As for the hinge reinforcement, a separate press-hardened steel reinforcement of the highest available yield strength was added, contributing to a good overall door stiffness.

In 2012, the "InCar" project, by ThyssenKrupp, presented two solutions for the lightweighting of steel doors with a focus on cost savings and improved functionality [14]. Amongst the many requirements that a door has to satisfy (e.g side impact protection, dent resistance, oil canning, fatigue, over opening, frame stiffness and torsional stiffness) the majority are stiffness dependent and make it very challenging to develop a lightweight steel door. Reduction in weight is nonetheless achievable in various components (e.g. door inner, window frame and belt reinforcement) through geometry optimization, minimal weld flanges and part consolidation with tailored blanks. With regard to door impact beams, with the use of steel grades with at least 1900 MPa minimum tensile strength a 25% reduction in mass is possible. The increase in material strength allows the decrease of the thickness of the panels and beams needed to meet the imposed stiffness and strength requirements. With thickness reduction, however, other problems, like the decrease in oil canning performance, may show up, requiring the use of additional structures. In order to reduce the total weight of outer panels while keeping a constant thickness (to maintain resistance to oil canning) a sandwich material with two ultra-thin steel sheets around a plastic core can be used. In the project [14] a reference door was chosen with a modular design including an equipment mounting plate to support window lifter mechanism, loud speakers and central locking motor. The list of the parts for the reference door is shown in Table 2-2.

Tailor welded blanks were used for the inner panel and for the window frame. The door weight was in the mid-range with respect to the results of benchmark studies on doors weight.

Table 2-2: Material information for the reference door structure [14].

Part #	Part Name	Material	Gauge (mm)
1a	Inner Panel Front	IF 160	1.50
1b	Inner Panel Rear	Mild Steel	0.70
2a	Sash Front	IF 220	1.80
2b	Sash Rear	IF 180	1.00
3	Window Guide	HSLA 250	0.70
4	Belt Rnf. Outer	HSLA 340	0.70
5	Latch Rnf.	HSLA 250	0.90
6	Outer Panel	BH 220	0.75
7	Crash Bracket	CP 780	1.20
8	Hinge Rnf. Lower	HSLA 340	1.80
9	Intrusion Beam	MS 1200	1.70
10	Carrier Plate	-	-
11	Lift Rail	-	-

The two lightweight solutions were called "Lightweight steel door concept" and "Advanced door concept", and are explained in Sections 2.1.1.1 and 2.1.1.2 respectively.

2.1.1.1   Lightweight steel door concept

The aim of the lightweight door concept was to reduce the overall weight of the door keeping the same conventional door architecture and minimizing any increase in cost [14].

Weight reduction was obtained using modern steel grades, semi-finished products and joining methods; a 4-pieced tailored blank inner panel was used, compliant with the stiffness and sheet thickness requirements, achieving a weight reduction of 5% with respect to the conventional door but maintaining the same stiffness performances, but the greatest weight saving was reached using a stiffness optimized sandwich material for the outer panel. A thick PE/PA (polyamide/polyethylene) core surrounded by two mild steel

outer sheets was used, reaching excellent dent resistance and oil canning performance. The parts that comprise the structure are listed in Table 2-3.

The thickness of intrusion beam and crash bracket was reduced using steels of higher grades.

The use of laser welding instead of conventional spot welding in the window frame area enabled a reduction in flange width. The total weight reduction of this model was 13%. From the manufacturing and assembly perspective, the lightweight steel door concept required reworking some tools (although the majority of tools needed were unchanged with respect to the reference door case), and non-heat intensive joining processes, such as hemming, riveting or adhesive bonding, were required not to damage the PA/PE compound. All components but the window frame and the outer panel were assembled in a conventional way.

Table 2-3: Material information for the Lightweight steel door concept [14].

Part #	Part Name	Material	Gauge (mm)
1a	Inner Panel	Mild Steel	0.70
1b	Inner Panel	Mild Ste	1.50
1c	Inner Panel	IF 160	0.90
1d	Inner Panel	IF 160	1.50
2a	Sash Front	IF 220	1.80
2b	Sash Rear	IF 180	1.00
3	Window Guide	HSLA 250	0.70
4	Belt Rnf. Outer	HSLA 340	0.70
5	Latch Rnf.	HSLA 250	0.90
6	Outer Panel	Sandwich	0.25/0.40/0.25
7	Crash Bracket	DP 980	1.00
8	Hinge Rnf.	HSLA 340	1.90
9	Intrusion Beam	MnB 1500	1.20
10	Carrier Plate	-	-
11	Lift Rail	-	-

2.1.1.2   Advanced door concept

In the advanced door concept the goal was to achieve a considerable mass reduction through part consolidation. A monolithic design was used for the inner door panel, and for the mid panel two solutions were developed: one using hot stamped MnB steel and HSLA steel, and the other using cold stamped DP980 steel and trip steel. Due to the change of design, an increase in thickness of the tailored blank window frame and the use of support struts to help meet oil canning requirements were needed.
Nevertheless, the total weight saving achieved was 11% with respect to the reference door. The material information for the advanced door concept is shown in Table 2-4.

The two lightweight doors resulted to be comparable to the reference door in stiffness, oil canning and dent performance, while with regard to crash performance, all the doors met the necessary requirements and the advanced door concept showed even improved performance thanks to the unique architecture used. As for the corrosion protection performance, all the doors met the production requirements. For the manufacturing and assembly of the advanced door concept, several simulations were needed to validate the feasibility of both the hot and cold stamped mid panels using the 2-piece tailored blank design. Added to the intense computer simulation, completely new prototype stamping tooling was required due to the totally innovative design of the advanced door concept. As a joining technique, laser welding was used in the frame window area to improve stiffness and to connect the mid panel to the monolithic inner panel. For the rest of the door, common assembly processes were used. A cost analysis was performed to compare the overall costs of the three door types: based on a production volume of 200,000 vehicles per year for an 8-year life cycle, the lightweight door concept resulted to cost around 11% more than the reference door (due to the cost of the stiffness optimized sandwich material for the outer panel), while the advanced door concept showed to have higher material (for the cold stamped variant) and assembly costs with respect to the reference door. Due to the lower material cost of the hot stamped door, its final cost was slightly lower than that of the reference door, while the cost of the cold stamped variant resulted slightly higher in the overall. The costs are shown in the bar chart in Figure 2-5.
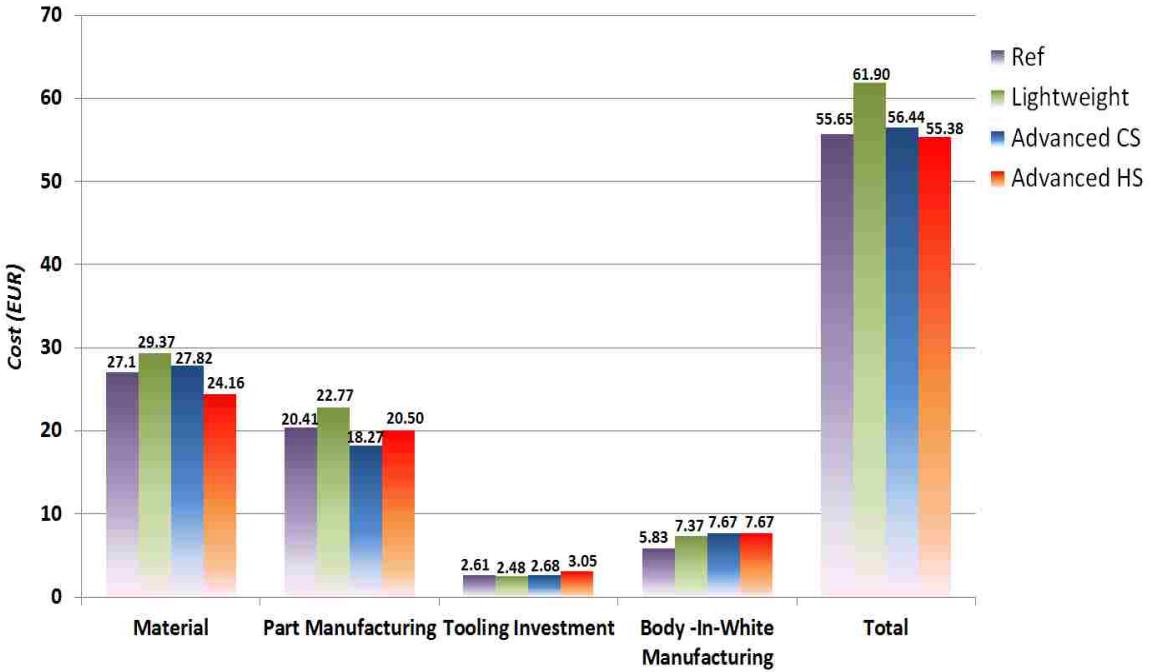
Figure 2-5: Bar chart showing the costs for the door solutions presented in [14]

Table 2-4: Material information for the Advanced Door Concept [14].

Part #	Part Name	Material	Gauge (mm)
1a	Inner Panel	IF 160	0.75
2a	Sash Front	IF 220	2.30
2b	Sash Rear	IF 180	1.00
3	Window Guide	HSLA 250	0.70
4a	Inner Panel Outer	TRIP 700	0.70
4b	Inner Panel Outer	DP 980	1.10
4c	Inner Panel Outer	HSLA 340	0.70
4d	Inner Panel Outer	HSLA 1500	1.10
5	Outer Panel	DP 500	0.55
6	Intrusion Beam	HSLA 340	2.40
7	Carrier Plate	-	-
8	Lift Rail	-	-

2.2 Door closing effort

There are different performance requirements that car doors need to meet, and they can be divided into approximately five categories as explained in a study of 2008 aimed at

23

designing an aluminum door with performance comparable to that of a reference steel door. Multidisciplinary Design Optimization was used [15]:

- Structure performance requirements (door frame rigidity and sag resistance): The door must not undergo excessive deflection when closed, due to the difference of pressure between the exterior and interior sides of the door when travelling. This difference of pressure is associated with the aerodynamic effects that take place at high speed. Moreover, when the door is open and subjected to its own weight, it must not show an excessive deflection in the vertical direction.

- NVH requirements (Noise Vibration Harshness; the lowest natural frequency of the closed door must not go below a certain value): This requirement is taken into account during the design phase of the part considering the frequencies of excitation the vehicle undergoes most frequently. For example in [15] the lowest natural frequency for the door to be designed was found to be 30.7 Hz with a corresponding modal shape as shown in Figure 2-6.

- Crashworthiness (the protection of the car occupants during side impacts): The requirements to be met are coming from several regulations and standards.

- Durability requirements (the durability of the component can be controlled either by damage inflicted, or corrosion action or fatigue failure): Since spot-welding is the most used technique to join automotive sub-assemblies, the presence of spot welds often gives rise to stress concentrations that can lead to fracture either along the plane of the weld or in the sheet metal around the weld. The cyclic loading of the door can depend on different factors like the source of loading (engine and wheel vibrations), vehicle driving speed, road condition and way the door is mounted on the body.

- Manufacturability requirements.

The door closing effort in a car represents a key point affecting customer's choice. When buying a car, the door is probably the very first part the customer comes in contact with, getting in the vehicle and getting out. The ease with which the door is closed, both from the inside and from the outside, the speed with which it closes and the sound of the closure, must give the customer the impression of a quality car.
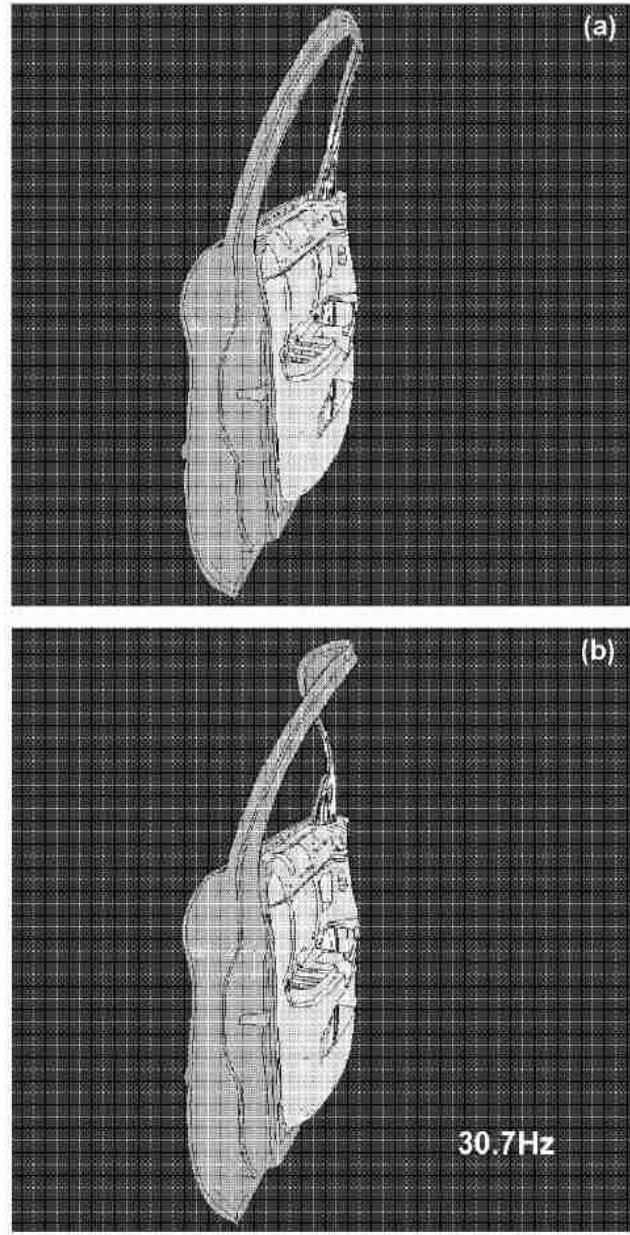
Figure 2-6: Modal shape presented by the door in the simulation carried out in [15].

A good way to estimate a door's difficulty of opening and closing is to evaluate the IQS (Initial Quality Study) score of the door. Research has been done to correlate the subjective evaluation of customers, the numerical results obtained with the physical testing of the doors in closing and opening and the IQS score, to find ways to improve the value of this last index by reducing the minimum closing velocity of the door. A lower closing velocity represents the ability of the user to close the door easily and smoothly [16]. The J.D. Power IQS study uses problems per 100 vehicles (PP100) as a measure of

25

initial quality, giving a lower score to better quality vehicles. From the data based on a three year survey it was seen that the IQS score is not influenced by the door closing velocity for scores lower than 0.8 PP100 (front door) and 0.6 PP100 (rear door); front door velocity must be lower than 0.9 m/s and, for the rear door, lower than 1.0 m/s. The IQS score could include behavioral intention and it is influenced by attitudes and subjective norms. During the subjective evaluation performed, higher numbers meant better feelings to the user and cars with high rankings in the IQS resulted also having higher subjective evaluation.

The survey also identified some factors affecting the side door closure:

- Weatherstrip: the door's seals play a role in increasing door closing effort, isolating the passenger compartment from water and wind noise. The weatherstrip appears to make one of the biggest contributions to the minimum closing velocity.

- Area of the extractor chamber: the pressure difference between the exterior and the interior of the vehicle is another factor affecting door closing velocity; a wide extractor chamber area leads to lower closing velocities.

- Weight and center of gravity: the moment of inertia of the door can be obtained through experimentation and calculations, and it is thought that a larger distance between the center of gravity and the hinge axis would improve closing velocity.

- Door hinge axis: the door hinge axis is not perfectly vertical but it is tilted inwards towards the inside of the vehicle to take advantage of gravity during door closure. By optimizing the inclination of the hinge axis it is possible to reduce the closing effort.

Different studies, such as [17] and [18], were carried out to assess the influence of door sound quality on customers' first impression. In a 2004 study by Kuwano et al. [18], sounds of the closing doors of different passenger cars were recorded and presented via head-phones in a sound-proof room to two different groups of participants (German and Japanese); based on the sounds heard, the participants formed mental images of the cars involved and gave an evaluation of the quality of the sounds. A correlation was found between the image formed and the impressions on the sounds' quality, thus suggesting that the image of a car is related to the sound of its doors closing.

The experiment was subdivided into three parts. In the first part the sounds were presented three times to the audience, with a 1 second interval between them, and the participants were instructed to evaluate the impression of the sound using semantic differential. The jurors were informed that the sounds were from a car door closure and had to choose between fifteen pairs of adjectives scales.

In the second part of the experiment the participants listened to the sounds again and formed the mental image of the car starting from a list of five types of cars (luxurious sedan, expensive sporty car, economic sedan, pick-up truck and another category of their description). Part 3 involved again the evaluation of the impression of the sounds (presented again) using a semantic differential. In the results of the study, three factors were extracted, "pleasant", "metallic" and "powerful/hard". In general high correlation was found between the Japanese and the German group and the different sounds were described with a series of adjectives like deep, pleasant, heavy, gentle, metallic, powerful etc. The sounds described by good adjectives were associated in a high percentage with the class "luxurious sedan", while the sounds in the unpleasant category were mostly associated with the "economy sedan" car image. A slight difference was found on some sounds between the two groups, but in general a good correlation between car image and the quality of sound was found in both groups.

A considerable effort is made by car makers to reach the best closing performance possible, and all the variables affecting this performance must be carefully studied taking into account all the other aspects related to the functionality of the doors.

In general, five main contributions (or energy sinks) are seen to affect door closing effort:

1. Check and hinge friction.
2. Latch effort.
3. Seal compression.
4. Door weight.
5. Air bind.

Airtight integrity considerably affects a vehicle's habitability from the stand point of both air conditioning amplification and sound insulation. However, the greater the improvements in the airtight performance, the greater the reactive force of the air in the cabin that impedes the door closure thus worsening the door closing performance [19].

A very early survey was conducted in 1981 by Nagayama and Fujihara to understand human response to a vehicle's airtight integrity and its influence on door shutting performance [19].

The minimum closing velocity is reached when the kinetic energy equals exactly the contrasting energy. The change in door cabin pressure when the door is shut is felt in different ways by the occupants, based on whether it is the occupant who is shutting the door or another person. In the survey the feelings experienced by the occupants were analyzed and revealed that a pressure level increase of 30 mmAq (2.94 mbar) is not considered to be unpleasant by 95% of the occupants, even if another person shuts the door.

Airtight integrity has been studied in the same research analyzing which factors affect it the most. The relationship between the velocity at which the door is shut and the pressure inside the cabin was found to be linear from the tests. Plotting this relationship for varying values of the ratio:

$$\frac{V_c}{S_D} \tag{2.1}$$

being the cabin volume and S_D being the door area, considered constant, produced the results shown in Figure 2-7.

When the door is shut, a rise in pressure is experienced in the vehicle's cabin, starting around 0.2 seconds before the door is completely closed and reaching a peak as soon as the door is fully closed. In [19] the closing process is divided into three main stages:

1. The door is wide open and starts closing. Due to the large door's gap areas around the door's frame the air is not pushed into the compartment but is allowed to escape;

2. Just before the door is closed, due to the sharp reduction of the door gap area and to the contact between the door and the body sealing the air starts being pushed inside the cabin and simultaneously partially flowing out the vent-hole;

3. After the door is completely shut and the peak pressure is reached, the pressure gradually decreases due to the flow of air out the vent-hole.
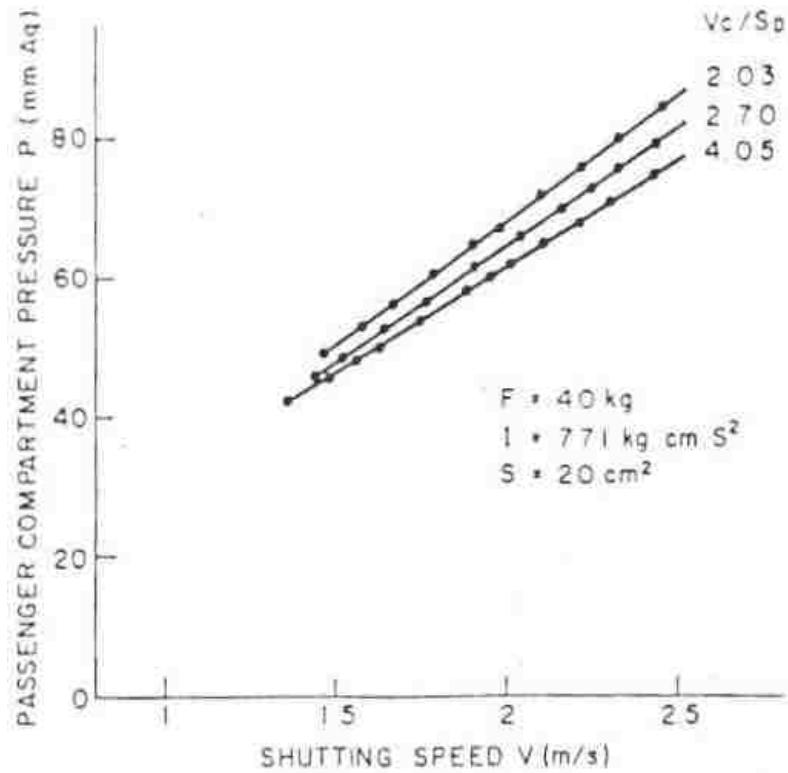
Figure 2-7: Passenger compartment pressure compared to door shutting speed [19].

As a result it is concluded that the factors affecting the pressure increase in the passenger compartment are the speed at which the door is closed, the door's area, the cabin's volume and the air vent hole's area.

In order for the door to close, its kinetic energy must be greater than all the energy contributions that hinder it from shutting.

The pressure rise rate was studied as a function of the area of the vent hole S, showing a great dependency on this parameter. It was found that the greater the vent hole area, the smaller the pressure rise rate; the change in the factor $\frac{V_C}{S_D}$ affects the pressure rise rate for values of the vent-hole area smaller than 500 cm^2. From the point of view of cabin pressure rise, the vent hole area should be as large as possible.

From the relationship between pressure rise rate and the factor $\frac{V_C}{S_D}$ it is clear that the smaller the ratio between cabin volume and door area, the greater will be the pressure rise rate inside the cabin, thus requiring a greater vent area. This is shown in Figure 2-8.

29
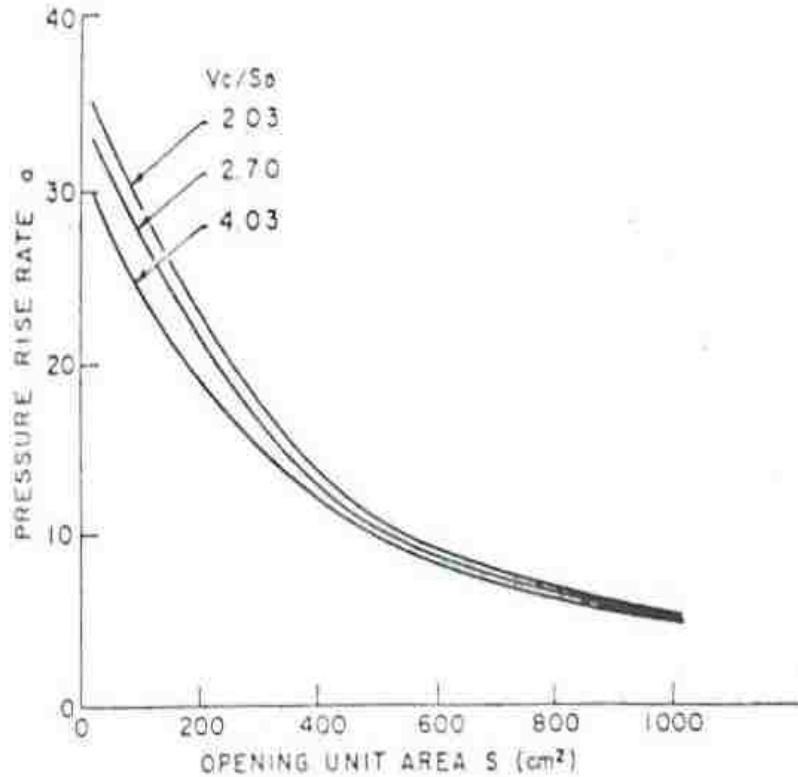
Figure 2-8: Pressure rising rate compared to opening unit area [19].

The "shutting force" (weatherstrip, bumper rubber and lock interlocking resistance) and the door's moment of inertia were found to have a negligible effect on the cabin pressure rise rate with respect to the change in factor $\frac{V_c}{S_D}$, as shown in Figure 2-9. Increasing the vent area decreases the minimum speed; when the vent area reaches a sufficiently big value, the change in velocity becomes negligible, as shown in Figure 2-10.

The reason for this behavior is that in order to completely latch the door a certain amount of resisting energy, not depending on the air bind phenomenon, needs to be overcome. This quantity is called static resistance. The door's moment of inertia strongly affects the door shutting performance, as shown in Figure 2-11. When the inertia of the door decreases, the influence of airtight on door closing performance increases.
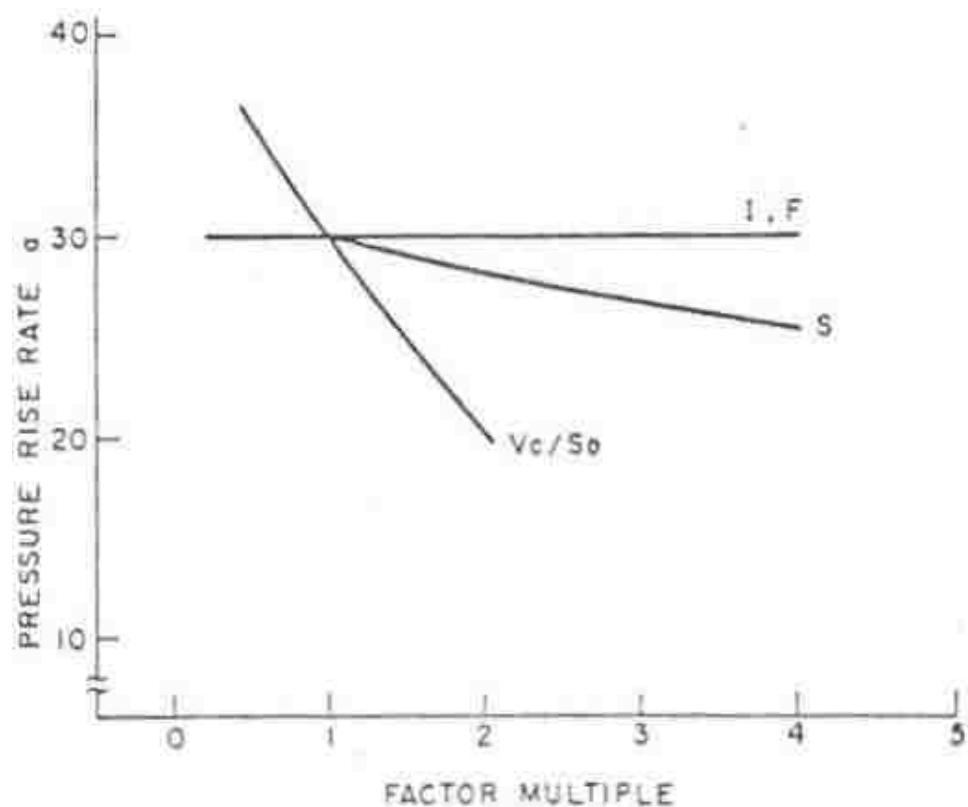
Figure 2-9: Different factors influences on pressure rise rate inside the cabin [19].
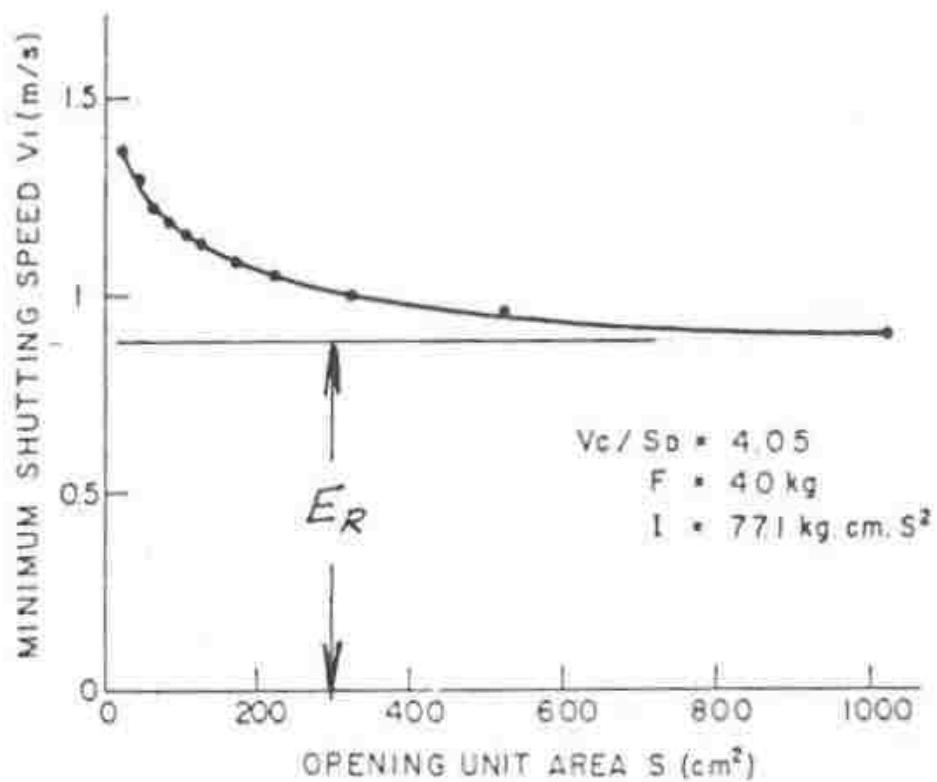
Figure 2-11: Minimum shutting speed compared to moment of Inertia [19].

From the study it is concluded that, in order to meet both the requirements of maximum acceptable cabin pressure rise and minimum reachable closing speed, a tradeoff between the two requirements must be achieved. The vent hole area must be properly designed as well as the ratio between cabin volume and door area, all the while carefully taking into account the weight and inertia of the door.

2.2.1 Predictive models for door closing energy and closing speed

The possibility to predict with sufficient precision the minimum closing speed and closing energy that will be necessary to fully latch the door allows the designer to make different simulations already in the design phase of the door system. The obvious benefit is the possibility to find the best possible configurations that allow to meet all the requirements in terms of safety and door closing performance without performing too many tests, always much more expensive than numerical simulation. For this purpose, different predictive models have been implemented during the years to give an idea of the

entity of all the contributors that will sink energy during the door closing process and finally the minimum speed that will be required to reach complete closure.

In 2003 a simulation model was implemented using ADAMS® to estimate the minimum closing speed and closing energy during the closure of an automotive side door [20]. The model was designed to take into account the entire swing of the door, thus considering the contributions given by latch, weather seals, air bind effect, hinge axis inclination and check link. The reason for choosing this methodology was because the customer usually closes the door starting from a fully open (or almost fully open) position and not from a nearly closed position; because it is important to correlate door closing effort to customer satisfaction indicators (as the JD Power ratings), it is important to simulate exactly what the customer experiences. Moreover, when simulating just the last few degrees of door closure, it is nearly impossible to clearly take into account the contributions of check link and hinge axis inclination, as these factors affect door closure from the fully open position to the nearly closed position, at which point the other factors (latch, seal compression and air bind effect) come into play. The model used in [20] is presented in Figure 2-12.
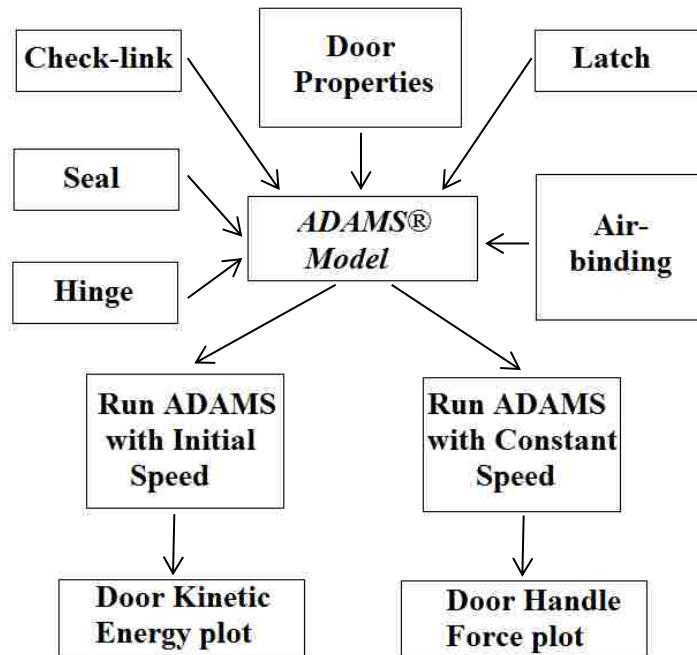
Figure 2-12: Door closing/opening effort model with ADAMS [20].

All the information relative to the door properties (weight, center of gravity, inertia) and to the other factors necessary to calculate all the different contributions (vent area through which air is allowed to escape, seal position and compression load deflection (CLD) curves, hinges position to evaluate hinge axis inclination) were input to the model that was run in two different modes. Running the model giving an estimated angular velocity it was possible to evaluate the kinetic energy and the residual energy at the end of the closing event; if the kinetic energy went to zero before the swing of the door was finished, that meant a complete latching of the door was not achieved. If a large amount of residual energy remained after closure, it meant that the initial input velocity (and thus input energy) was more than the amount strictly necessary to latch the door. So with a trial and error procedure, the value of the initial angular velocity input was changed in the system until the kinetic energy became zero exactly at the time the door latched or slightly after that point, and the model predicted the minimum door closing speed and energy. The second way in which this model was used was to analyze the door closure while running the simulation at constant speed; by doing so it was possible to predict the force applied by the user to the handle for example when closing the door from the inside.

Another model was developed in 2010 [21] to predict the final closing energy (divided in all of the contributing areas) and the minimum closing speed, by subdividing the door closing event into six different subsystems, each of which was described by a mathematical model. The energy sink contributions included are those recognized by most researchers ([12], [19], [20]) on closing effort: weather strip seals, air-binding, door weight, hinge, check-link and latch.

The weather strip seal model included both the energy sink given by the non-linear compression load deflection resistance, due to the elastic reaction to compression of the rubber of the seals, and the non-linear damping resistance given by the air escaping from the seal bulbs vent holes, modeled as shown in Figure 2-13. To evaluate the air-bind contribution due to the mass of air pushed into the cabin when the door is closed, the laws of conservation of mass, of isentropic processes and the Bernoulli's equation for incompressible fluids were used, to evaluate the rise in pressure into the cabin that will act with an opposite force on the door, thus hindering its closure.
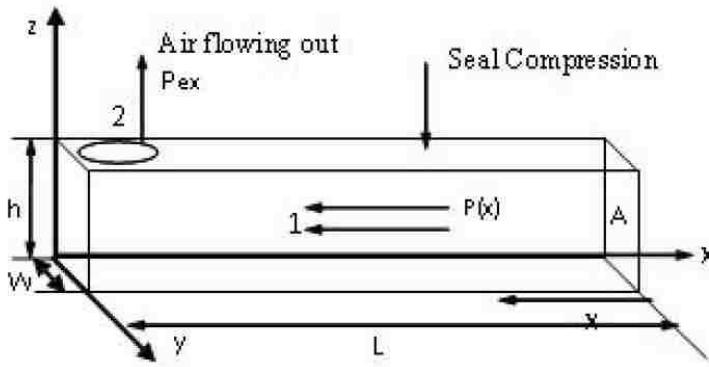
Figure 2-13: Seal modeling for air bind dampening evaluation [21].

The evaluation of the weight contribution to closing effort was instead based on the inclination of the hinge axis of the door. Based on this inclination, the door center of gravity will in fact rise or decrease its height (with respect to the fully open starting position) during the closing process, thus either sinking energy or helping door closure. An inward inclination of the door hinges axis will cause the center of gravity to be in a position lower with respect to its initial position during closure; the weight of the door will therefore push the door towards the cabin giving a positive contribution to the closure

$$E_g = mg\Delta h \qquad (2.2)$$

where m is the mass of the door, g is the acceleration of gravity and Δh is the difference in height between the initial and final position of the center of gravity. The check-link system and the latch models were instead based on check torque characteristics and latch force resistance.

In 2010, another model [22] was developed to predict the minimum closing speed using the principle of inner pressure increment due to air-bind and a modified air bag algorithm. Door seals and latch resistance, air density and door moment of inertia were taken into account to evaluate and simulate the door closing performance. The air flow in the cabin was simulated with the air flow in an airbag assuming that the air flowed in through the door area and out from the extractor in the cabin and from the door gap before reaching the contact with the seals. The minimum closing velocity was evaluated considering the seals reaction force and the air properties as input in a closing solver written in C++.

2.2.2 The DFSS project (Door Closing Effort T-method)

The DFSS Project was developed by an Automotive Original Equipment Manufacturer (OEM) to find a correlation between the JDP IQS PP100 score for the questions ("Is the front door hard to close?" and "Is the rear door hard to close?") and engineering measurables. In a JD Power test the customer is asked to answer "yes" or "no" to a certain question and the rating of the vehicle depends on the number of yes (or no) out of 100.

The project involved the acquisition of data on door closing effort from physical testing of the doors and the input of these data and other variables to the T-method processor (an analytical tool used to establish a correlation between data and a signal, in this case the JD Power score for door closing effort). Thirty-two vehicle samples were examined.

Based on the results of the research, the factors that had the strongest correlation with the JD Power scores were minimum closing speed, air bind contribution and seals and latch force (for what concerns the front doors). A decrease in these factors meant an increase in the JD Power score. For the rear door also increasing the height of the belt line and the length of the door were important to improve the score.

A lot of work has been found in the literature that describes the door closing event, the factors that affect it and the models that can be implemented to predict the closing speed and the closing energy of a door. However, no such a direct comparison, as the one carried out in this project through the physical testing of the doors, between the closing performance of a production steel door and an aluminum door has been found in the research work studied. The work presented in this paper gives immediate information, in terms of energies, speeds and other physical parameters on the closing performance of the two doors tested, analyzing and discussing every contributor in the door closing event.

3 THEORETICAL BACKGROUND

3.1 Aluminum properties review

Aluminum is currently second to iron in terms of production and consumption and is one of the most prevalent metals present in the earth's crust. This metal is also highly recyclable and the energy required for the recycling is approximately 5% of the energy needed for the production of aluminum from electrolytic reduction of aluminum oxides. With a density of only 2.7 g/cm^3 aluminum offers the great advantage of light weight, corrosion resistance, ease of fabrication and good surface finish properties. Even though the material strength is lower than the strength of steel, aluminum has a strength-to-density ratio which is around three times that of structural steel [23]. Aluminum can be produced in flat rolled sheets and plates, tubes, rods, bars and wires. Common castings, forging and stampings are also possible. Aluminum for structural applications is always used in the form of an alloy. The other main characteristics are high thermal and electrical conductivity, high reflectivity and non-catalytic action. Aluminum alloys are classified on the basis of the main alloying elements with which aluminum is combined, as presented in Table 3-1.

Table 3-1: Wrought Aluminum and Aluminum Alloy Designation [23].

Series designation	Alloying materials
1XXX	99.9% min. Al
2XXX	Al-Cu, Al-Cu-Mg, Al-Cu-Mg-Li, Al-Cu-Mg-Si
3XXX	Al-Mn, Al-Mn-Mg
4XXX	Al-Si
5XXX	Al-Mg, Al-Mg-Mn
6XXX	Al-Mg-Si, Al-Mg-Si-Mn, Al-Mg-Si, Cu
7XXX	Al-Zn, Al-Zn-Mg, Al-Zn-Mg-Mn, Al-Zn-Mg-Cu

Elements such as chromium, manganese and zirconium are added for grain control during solidification of large ingots while copper, magnesium, nickel and zinc are added to increase strength, formability and stability at elevated temperatures. Many other elements are also present in aluminum alloys that can combine with one another producing intermetallic compounds that can be soluble or insoluble in the aluminum matrix. The alloys can be divided in heat-treatable and non-heat-treatable. In the first category the

strengthening is usually obtained with solution heat treatment (400-565°C), quenching to retain the alloying elements in solid solution and aging treatments to precipitate the elements in optimum size. Amongst the non-heat-treatable alloys, the strongest are the ones belonging to the 5XXX series (with Magnesium as the main alloying element) and the most common ways to achieve a strengthening of the material are by strain-hardening, solid solution and dispersion hardening. These alloys also show a high resistance to general corrosion. The mechanical properties (Ultimate Tensile Strength and Yield Strength) of some of the most commonly used alloys of the 5XXX and 6XXX series are listed in Table 3-2 as an example.

Table 3-2: Typical tensile properties for some of the most commonly used aluminum alloys in the automotive field [23].

Alloy and temper	Ultimate Tensile Strength (UTS) [MPa]	Yield Strength (YS) [MPa]
5052-O	195	90
-H34	260	215
-H38	290	255
5454-O	250	115
-H32	274	205
-H34	305	240
5456-O	310	160
-H111	325	230
-H112	310	165
6061-O	125	55
-T4, T451	240	145
-T6, T651	310	275
6063-O	90	50
-T5	185	145
-T6	240	215
-T83	255	240

The elements with the most positive effects on mechanical properties are magnesium, copper, silicon and silver; magnesium is widely used in percentage of up to 3% of the

weight to obtain a severe strengthening of the alloy. The designations T and H refer to the type of heat treatment and to the type of strain hardening of the alloy.

3.2 Physical phenomena behind Door Closing Effort

The OU model has been developed to mathematically predict the automotive door closing effort, in terms of minimum required velocity and energy, of a vehicle's side swing door between secondary check position and closed position. The energy required to close the door from a nearly closed position is therefore predicted under the assumption that the check link has ceased to function [24].

The predictive model was developed taking into account cabin pressure, cabin volume and vehicle vent area, seal compression, door weight and inclination of the hinge axis, latch effort and hinge friction.

In this section the ways the different contributions are modeled in the OU model are briefly explained as in [24] where the physical laws behind the evaluation of the different energy sink contributions that influence door closing effort were analyzed.

3.2.1 Air bind

The simplified diagram for the air bind model is shown in Figure 3-1.
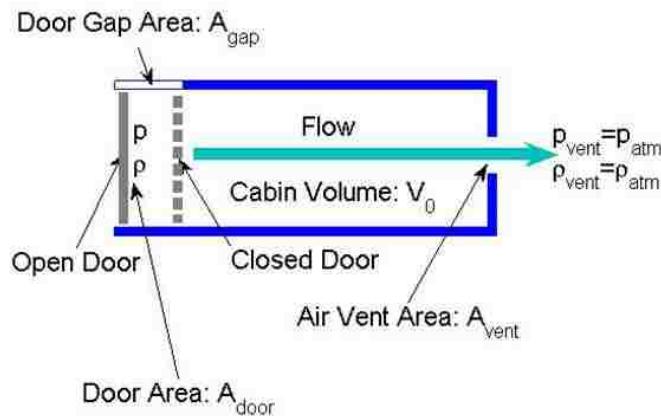
Figure 3-1: A diagram for a simplified air bind model [24].

As highlighted before, the energy loss due to air bind is caused by the pressure rise in the cabin when the closing door pushes the air ahead inside the cabin. This pressure pushes the door in the direction opposite to the closing direction. In the OU model the air bind

effect is represented through a mono-dimensional ideal fluid dynamic model. Air pressure and density at the door are assumed to be the same as in the cabin.

The cabin is represented by a tube with cross sectional area equal to door area. The air vent area (area through which the air is allowed to escape out of the cabin) includes also the door gap area.

To evaluate the pressure in the cabin that acts on the inner surface of the door during closure, Bernoulli's equation, conservation of mass and the ideal gas law are used.

Assuming the mass and temperature of air to be constant, from the equation of state for the air

$$p = \rho R T \tag{3.1}$$

Where p represents the pressure, ρ represents the air density, R is the universal gas constant and T is the temperature.

The change in cabin pressure will be proportional to the change in cabin air volume

$$\frac{\Delta p}{p} = -\frac{\Delta V}{V} \tag{3.2}$$

and

$$\frac{\Delta p}{p} = \frac{\Delta \rho}{\rho} \tag{3.3}$$

The continuity of mass flow rate is used at the door and vent area and incompressibility of air is assumed. The average speed of the air at the vent v_{vent} can be calculated from the Bernoulli equation for an incompressible flow

$$p = p_{atm} + \frac{1}{2} \rho_{atm} v_{vent}^2 \tag{3.4}$$

$$v_{vent} = \sqrt{\frac{2(p - p_{atm})}{\rho_{atm}}} \tag{3.5}$$

From the change in volume ΔV for a time Δt, given by the change in the air volume due to the displacement of the door minus the volume of air escaping from the vent area and the door gap area

$$-\frac{V}{p} \Delta p = \Delta V = \left[\left(1 + \frac{\Delta \rho}{\rho} \right) \omega I_{A_{door}} - A'_{vent} v_{vent} \right] \Delta t \tag{3.6}$$

and recalling that $\frac{\Delta\rho}{\rho} = \frac{\Delta p}{p}$, it is possible to evaluate the change in pressure $\overline{\Delta p}$ that will cause the torque acting on the door in opposition to door closure. A'_{vent} represents the total area through which air escapes, $I_{A_{door}}$ is the area moment of inertia of the door about the hinge axis.

$$\overline{\Delta p} = -\frac{p}{V}\left[\left(1 + \frac{\Delta p}{p}\right)\omega I_{A_{door}} - A'_{vent}\sqrt{\frac{2(p - p_{atm})}{\rho_{atm}}}\right]\Delta t$$

$$\overline{\Delta p} = -\frac{\bar{p} + p_{atm}}{V + \omega I_{A_{door}}\Delta t}\left[\omega I_{A_{door}} - A'_{vent}\sqrt{\frac{2\bar{p}}{\rho_{atm}}}\right]\Delta t \tag{3.7}$$

$\bar{p} = p - p_{atm}$ is the pressure difference referenced to atmospheric pressure. At this level of pressure the torque on the door about the hinge axis is

$$T_{air} = \int_{A_{door}} r\bar{p}dA = I_{A_{door}}\bar{p} \tag{3.8}$$

The energy sink increment due to this torque in the time interval Δt will be

$$\Delta E_{air} = T_{air}\Delta\theta = T_{air}\omega\Delta t \tag{3.9}$$

The pressure difference at the door will then be

$$\bar{p} = \bar{p} + \Delta\bar{p} \tag{3.10}$$

And the energy sink due to air bind will be

$$\boldsymbol{E_{air} = E_{air} + \Delta E_{air}} \tag{3.11}$$

As highlighted in some studies [25], the air bind effect coming from the flow of air through the ventilation holes present in the seals (and spaced at regular intervals in the seal system to expedite the flow of air during the closing process) should be taken into account, as it represents a damping dissipative force that depends upon the rate at which the seal is being compressed. From the studies it appears that the damping component of seal force per unit length generated during seal compression is proportional to $\frac{L^2}{D^2}$ where L represents the spacing distance between the air ventilation holes and D the diameter of the holes.

3.2.2   Latch effort

The latching system is presented in Figure 3-2.
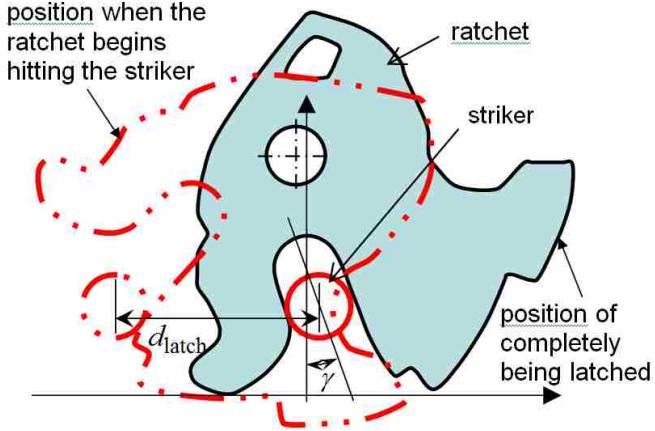
Figure 3-2: A schematic diagram for a latching system [24].

The contact between the latch (which is at a distance r_{latch} from the door hinge axis) and the striker takes place when the closing door reaches a door open angle $\theta_h = \frac{r_{latch}}{h_{striker}}$.
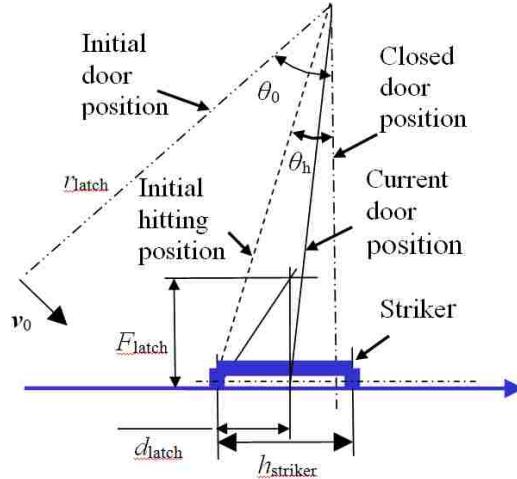
Figure 3-3: A schematic diagram for latch effort [24].

The ratchet of the latch is displaced by the striker with a force F_{latch} of a displacement

$$d_{latch} = \begin{cases} 0 \ \ for \ \theta > \theta_h \\ r_{latch}(\theta_h - \theta) \ \ for \ \ \theta \le \theta_h \end{cases} \tag{3.12}$$

The latch force and the latch displacement are assumed to have a linear relationship of the type

$$F_{latch} = k_{latch}d_{latch} \tag{3.13}$$

The torque effort of the latch will therefore be

$$T_{latch} = F_{latch}r_{latch} \tag{3.14}$$

The energy sink due to latch effort will be

$$E_{latch} = \frac{1}{2} k_{latch} (d_{latch})^2 \qquad (3.15)$$

The k_{latch} constant is calibrated based on experimental data.

3.2.3 Seal compression

In1997, a research by Wagner & al. [26] described how the weatherstrip seals are considered as one of the major contributors in door closing effort (even though, as it will be explained in the test results in Chapter 5, they are not primary energy sink during door closure). As explained in [26] the seals are usually dual extrusion bulbs of sponge and rubber and are attached both on the door frame and on the car body. On the door frame the seals are attached through push pins while on the body side they are simply inserted on the frame and under the internal panels covering the roof from the inside. The seal bulbs are usually round, triangular or free form in shape with a height of approximately 15-30 mm. The main properties of the seals are a great extensibility (up to 500% strains without permanent deformation), low extensional and shear moduli and nonlinear load vs. deflection behavior.

In order to model the seal, it is discretized into small segments along the seal line, and each segment is modeled with a spring connecting a certain point on the door seal line to a certain point on the body seal line, as shown in Figure 3-4 [24].
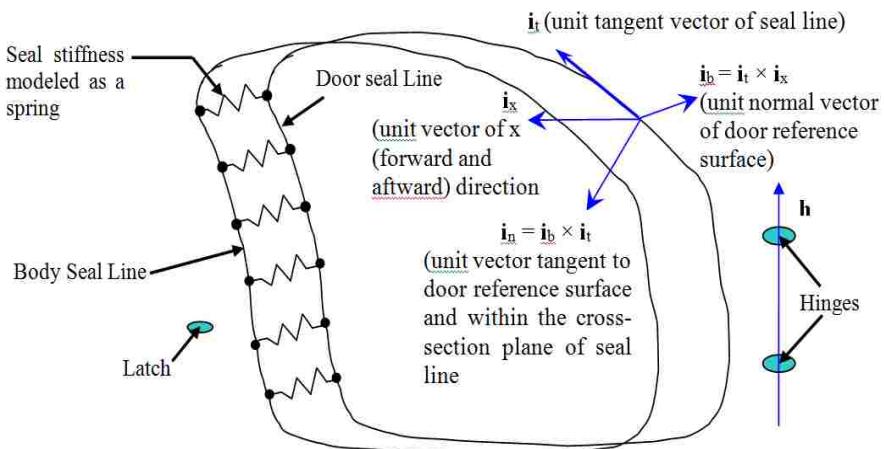
Figure 3-4: A schematic diagram of door/seal/body system [24].

At a certain closing angle $\theta = \theta_c$ the seal between the door and the body begins to be compressed along the door and body seal lines. θ_c is called the seal contact angle; the seal line can be subdivided in different seal points, each of which will have different seal contact angles. When $\theta < \theta_c$ there is no more door gap and so air venting is not possible (no air can therefore flow into or out of the cabin).

In Figure 3-5 the travel of the seal bulb during the last part of door closing is presented. The patch A-C-B is part of the circular trajectory followed by the seal contact point during its rotation about hinge axis. The seal lip interference, l_{seal}, is the amount of interference of the seal lip with the seal mounting surface. The seal stiffness is described by a Compression Load Deflection (CLD) curve (shown in Figure 3-6), given by the relation between the normalized compression force $\bar{L}$ and the normalized compression distance $\bar{D}$.

Considering a seal segment of length l, compression distance d_{seal} and compression force f_{seal}

$$\bar{L} = \frac{f_{seal}}{l} \tag{3.16}$$

And therefore the force for the seal segment will be

$$f_{seal} = l\bar{L}(d_{seal}) \tag{3.17}$$

Summing all the elements of seal segments

$$T_{seal} = \sum_i f_{seal,i}\, r_i \tag{3.18}$$

$$T_{seal}{}' = c_{seal} T_{seal} \tag{3.19}$$

c_{seal} is a coefficient used to correct the seal model error. Finally the energy sink increment for a time Δt will be

$$\Delta E_{seal} = T_{seal}{}' \Delta\theta \tag{3.20}$$

So the torque on the door is determined calculating and summing the torque that each seal segment applies on the door based on seal segment length, segment compression, CLD curve and distance of the segment from the hinge axis [27].
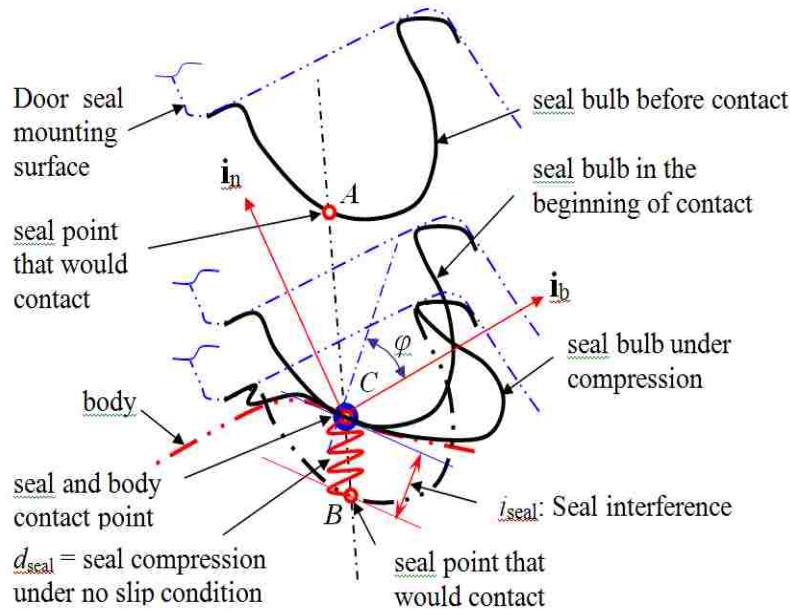
Figure 3-5: Seal compression under no slip condition [24].
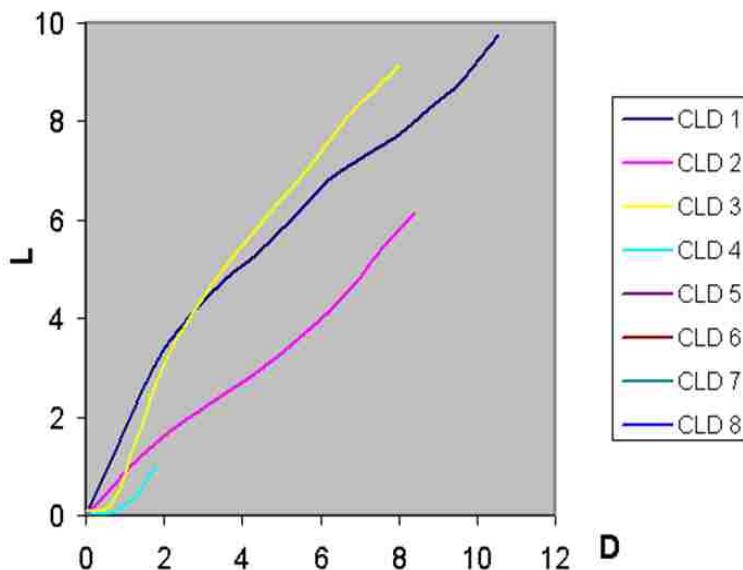
Figure 3-6: Force (L)/Compression(D) relation for Seal (per 100 mm) [24].

45
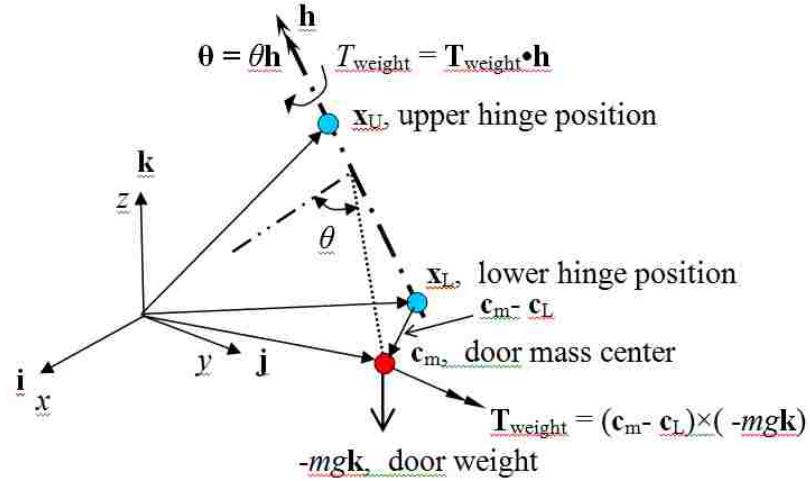
3.2.4 Door Weight

Figure 3-7: A schematic diagram for door weight effort model [24].

The non-verticality of the door hinge axis gives rise to a helping torque $T_{weight} = T_{weight}(\theta)$ given by the door weight $-mg\mathbf{k}$. The door mass center $c_m = c_m(\theta)$ is approximately at the geometric center of the door plane.

$$T_{weight} = [(c_m - c_L) \times (-mg\mathbf{k})] \cdot \mathbf{h} \tag{3.21}$$

The energy contributed by the door weight will be

$$\boldsymbol{E_{weight} = mg[c_m - c_m(0)] \cdot k} \tag{3.22}$$

3.2.5 Hinge friction

For the energy sink due to hinge friction prediction, the OU model uses a constant torque model under quasi-static state, assuming a vertical hinge axis. The system is shown in Figure 3-8.
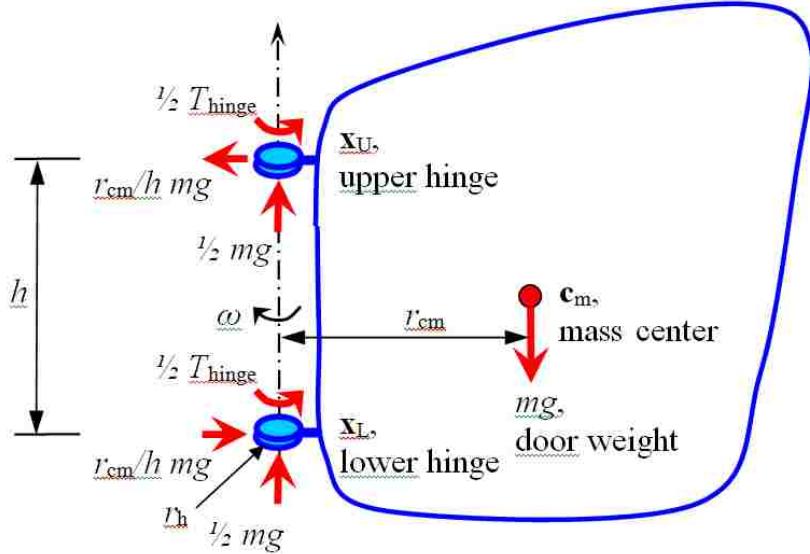
Figure 3-8: A schematic diagram for hinge friction effort model [24].

The door leans on the bottom of the upper and lower hinges, each of which carries half of the weight.

The center of mass of the door is r_{cm} away from the hinge axis, so from the equilibrium equations, there are two reactions of magnitude $\frac{r_{cm}}{h}mg$ from the sides of the two hinge pins to balance the moment induced by the door weight. Considering a hinge pin radius r_h and a hinge friction coefficient μ_h the torque from the two pin sides will be

$$T_{side} = 2\mu_h \frac{r_{cm}}{h} mgr_h \tag{3.23}$$

The torque from the two pin bottoms will be

$$T_{bottom} = 2\mu_h mgr_h \tag{3.24}$$

The total torque, given by the sum of the two will therefore be

$$T_{hinge} = 2\mu_h \left(\frac{r_{cm}}{h} + 1\right) mgr_h \tag{3.25}$$

The energy sink from hinge friction is

$$\Delta E_{hinge} = T_{hinge}\Delta\theta \tag{3.26}$$

And finally

$$\boldsymbol{E_{hinge} = E_{hinge} + \Delta E_{hinge}} \tag{3.27}$$

The solution procedure of the model involves a one dimensional nonlinear dynamic equation:

47

$$I_{door}\ddot{\theta} = T_{total} \tag{3.28}$$

The term T_{total} involves all the contributions explained before (T_{air}, T_{seal}, T_{weight}, T_{hinge} and T_{latch}).

3.3 Pendulum test for moment of inertia and center of gravity calculation

In order to have accurate information on the tested doors' moments of inertia, weight and center of gravity position, a pendulum test was performed on the doors and is briefly explained here.

The center of gravity of the door was found using intersecting plumb lines. The complete door assembly was suspended by the upper hinge bracket for one plumb line and from the lower hinge bracket for the other plumb line. The center of gravity was found at the intersection of the two lines.

A pendulum is generally a rigid body free to rotate about a horizontal axis under the influence of gravity. The period of motion is mainly dependent on the geometry of the body and on the value of the gravity acceleration constant g [28]. A pendulum is usually made up by a mass placed at the end of a very light rod (or a cord) of length L; in a simple pendulum the assumption that the rod is weightless is made. The point mass m is then placed at a distance L from the pivot point (the axis of rotation) P.
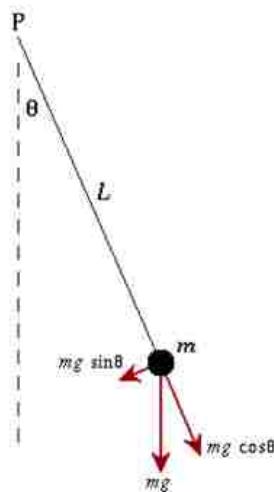
Figure 3-9: Simple pendulum schematic diagram. A mass m placed at a distance L from the pivot point P oscillates due to the effect of the force of gravity [29].

48

For the simple pendulum, for which the moment of inertia is defined as $I = mL^2$, and assuming sufficiently small angles of oscillation θ, the period of oscillation T is given by:

$$T = 2\pi \sqrt{\frac{L}{g}}$$

(3.29)

A rigid body, free to rotate about a horizontal axis, but that is not a simple mass attached at the end of a light rod, is called a compound pendulum. The schematic diagram of a compound pendulum is shown in Figure 3-10. "P" represents the axis of oscillation and "C" the center of gravity of the object. The distance d is the distance of the center of mass of the body from the pivot point.
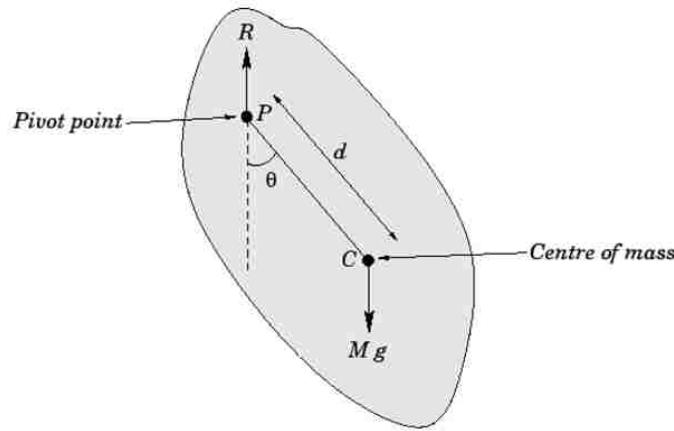
Figure 3-10: Schematic diagram of a compound (physical) pendulum [30].

The weight of the object Mg, where M is the mass of the object, acts on the center of gravity of the body.

For the compound pendulum the equivalent length L to be used for the calculation of the period in equation 3.29 is given by:

$$L = \frac{I}{Md}$$

(3.30)

The period T for a complete oscillation of the pendulum is then given by:

$$T = 2\pi \sqrt{\frac{I}{Mgd}}$$

(3.31)

where I is the moment of inertia of the body about the oscillation axis.

During the pendulum test performed on the door the hinges of the door were drilled larger and a steel bar was inserted inside the holes. The whole door was placed

49

horizontally with the hinges pointing upwards and the latch pointing downwards. The door was left to oscillate freely about the door hinge axis for more than ten times; the swing of the first ten times was timed with a stop watch and the inertia was calculated from the pendulum equation for the period of oscillation (3.31). The test was repeated for five times showing a very high accuracy of the calculation (within 2.3% deviation). The moment of inertia calculated with this methodology can be directly used in the calculations and analysis of the closing event because it is directly calculated about the axis of interest (the hinge axis); therefore no centrifugal moments need to be taken into account.

4 DESIGN AND METHODOLOGY

The study of the door closing effort has been divided into different steps. To understand the differences and be able to compare the door closing performance of an aluminum door with the performance of a steel door, two different but parallel methods have been followed, including both laboratory testing with the EZ Slam device by EZ Metrology and closing effort prediction with the OU model, the theoretical background of which has been described in the Chapter 3.

4.1 EZ Slam testing

In order to have a direct measurement of the overall closing performance of a car's door the EZ Slam device was used on the test vehicle, and is briefly described in this section [31].

4.1.1 Test set up

The EZ Slam system is made up by three main units:

- The **door unit**, shown in Figure 4-1, is mounted on the door to be tested through suction cups and contains the majority of the sensors of the System.

Figure 4-1: EZ Slam Door Unit [31].

This unit needs to be parallel to the floor and is placed at the height corresponding to the latching system of the door and the striker on the car body. Once the end corresponding to the handle (left part in Figure 4-1) is fixed through the suction cup as close as possible to the hem of the door, the other end of the unit is placed as close as possible to the door hinges through a second suction cup, while still allowing a complete opening of the door without interference. The length of the

door unit is adjustable thanks to two carbon fiber telescopic arms fixed in the desired position by two screws operated by the user.

- The **cabin unit** (Figure 4-2) is placed inside the cabin on the seat closest to the door being tested and captures small and rapid pressure variations inside the cabin of the vehicle.

Figure 4-2: EZ Slam Cabin Unit [31].

- The **body unit** is placed very close to (but without touching) the door unit, and contains the vision system to record the two dimensional motion of the last 90 mm of door travel before latching. The body unit is shown in Figure 4-3.

Figure 4-3: EZ Slam Body Unit [31].

The position of this unit can be adjusted through three mechanisms. The red screw shown in Figure 4-3 allows placement of the main body of the unit parallel to the door unit; the two-piece arm connecting the suction cup to the main body of the unit allows the setting of the vertical and horizontal position of the unit on the rear

door (in case a front door is being tested) and finally a screw placed at the base of the arm on the side of the suction cup allows final adjustments of the body unit. The closing velocity is detected thanks to a laser-sensor system; a laser beam is produced by the door unit during the whole duration of the slam test and its passage during the last 90 mm of door travel is detected and timed by a sensor placed on the body unit. Knowing the distance travelled and the time, the device can calculate the closing speed.

The system also includes a **base station** (Figure 4-4) that provides communication between the computer and the different units. All the units are wirelessly connected to the base station which is connected via USB to the computer. The software provided with the equipment allows the data collection and processing and allows exportation of the results of the different tests to Microsoft® Excel. After the completion of a test, the measurement data set is also available in text file format.

Figure 4-4: EZ Slam Base Station [31].

The complete test set up with the position of the units on the vehicle is shown in Figure 4-5.

When analysing the closing performance of a door with the EZ Slam, four different types of tests are performed: the **Slam test**, the **Push test**, the **Wiggle test** and the **Sweep test**. Every test must be performed within a 15 second time window. The tests are briefly explained in sections 4.1.1.1 to 4.1.1.4.

Figure 4-5: Fully equipped door with the door and body units [31].

4.1.1.1   Slam test

In the Slam test the door is shut from the fully open position to the latched position by operating the EZ Slam device by the green handle of the door unit. The closure will be perceived by the sensors as *fast* closure, *medium velocity* closure or *slow* closure. A minimum number of four valid runs for each type of closure should be performed in order to have a sufficient number of points for the creation of the best fitting lines, that will be explained in section 4.1.2 (Test Outputs). The door must not be moving at the beginning and at the end of the data acquisition. The door must be closed, as explained before, with different velocities; different inputs, in terms of energy put by the user when closing the door, will therefore be necessary during the slam test. However, even though the inputs are different in amplitude (more or less energy), the impulse must be given by the user always in the same window, in terms of angle, in order not to affect the results (e.g. the door must be pushed for 20 degrees and then released, no matter if the user is looking for a fast, medium or low velocity closure).

The goal of the test is to evaluate the minimum closing speed of the door and estimate the minimum input energy necessary to reach a fully latched position; it is then necessary to have at least one run in which the latch is not engaged (incomplete closure). Attention must be paid to always have the HVAC system open in order to allow the proper air evacuation from the cabin. A closed HVAC system strongly affects the air bind effect

causing a much greater pressure rise inside the cabin during closure. To evaluate minimum effort and minimum speed the outputs of the slam tests are used in combination with the outputs of the other three tests described in the following sections.

4.1.1.2   Push test

In the push test the door is placed in a nearly closed position at the beginning of the test and must be in the position of natural rest when the data acquisition begins. In this test the door is pushed using the green handle in slow motion until the fully latched position is reached.
The goal of the test is to evaluate the static resistance of the seals, the force needed to latch the door and the minimum overslam with which the door latches. For the definition of overslam the reader is referred to the Nomenclature section.

4.1.1.3   Wiggle test

The wiggle test involves a rapid back and forth motion of the door to evaluate hem radius and door moment of inertia. The test is performed starting from a nearly closed position with the door at rest and then shaking it around 8-12 times with a stroke of around 100 mm. During the wiggle test the doors of the opposite side of the vehicle are kept open in order to completely eliminate the resistance of cabin air because it will have a very large area to escape from the cabin and no peak in cabin pressure will be detected.

4.1.1.4   Sweep test

The sweep test is done to measure the resistance of the door check system and the friction at the hinges. The test is performed both for door opening and closing actions. When measuring the door check resistance during opening the run starts with the door in the nearly closed position and the door is pulled very slowly using the green handle until the fully open position is reached. The test is repeated for the closing motion starting from a fully open position and finishing the test at a nearly closed position. The sweep tests should be performed at a slower constant speed. The outputs of the sweep test in terms of graphics are the trend of the energy input by the user to operate the door and the force exerted from the check system to the door.

4.1.2 Test Outputs

The starting point to evaluate the door closing performance of a door with the EZ Slam device is the "energy pie", based on the conservation of energy law.

When shutting a door, all the energy that is input into the system must be dissipated in some way; this phenomenon is shown graphically with two pie charts representing the input energy and the dissipated energy. The two charts are the same size because the total energy remains constant.

The direct sources of energy for door closure are the input from the user that pushes the door, the gravity that pulls the door toward the cabin thanks to the inclination of the hinge axis, and the springs of the check system. An example of an input energy pie is shown in Figure 4-6.
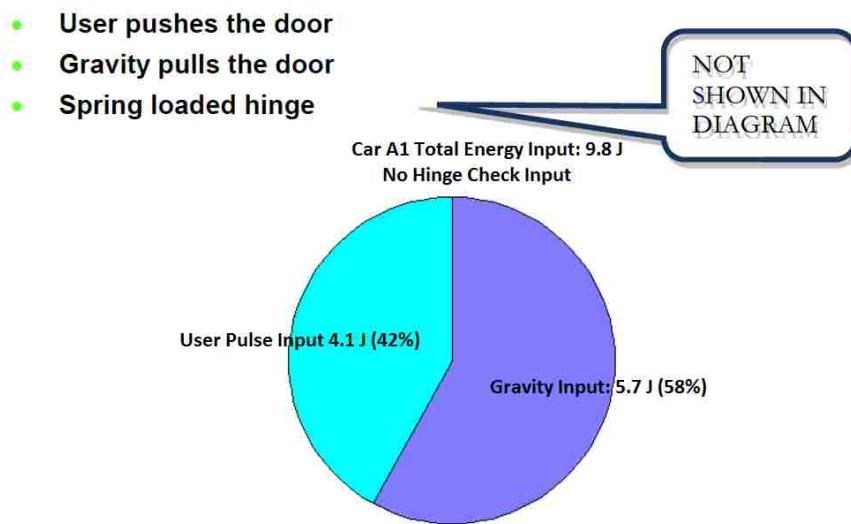
Figure 4-6: Input energy pie [31].

The energy dissipation can be divided into three main components: friction and drag, the static compression of the seal system and the effect of air bind. An example of an energy dissipation pie is presented in Figure 4-7.

When the door is at a distance of approximately 90 mm from complete closure the seals begin to compress; it is only after this point that the seal compression and the air bind contributions start acting on the door to increase the closing effort; before that point, energy is dissipated from friction at the hinges and check system, and drag. When

performing a comparison between different tests performed, the energy pies are shown as bar-charts (see Chapter 5) to allow an easier graphical comparison between the results. The principle of conservation of energy is also used by the software, as explained in Chapter 5 (Analysis of the Results), for the calculation of some of the contributions to closing effort.

- Friction and drag
- Static compression of seal system
- Dynamic dampening

Car A1 Total Energy Dissipation: 9.8 J

Static Latching (< 90 mm): 0.7 J (8%)

Drag (> 90 mm): 4.9 J (50%)

Dynamic Air Exhaustion (<90 mm): 4.1 J
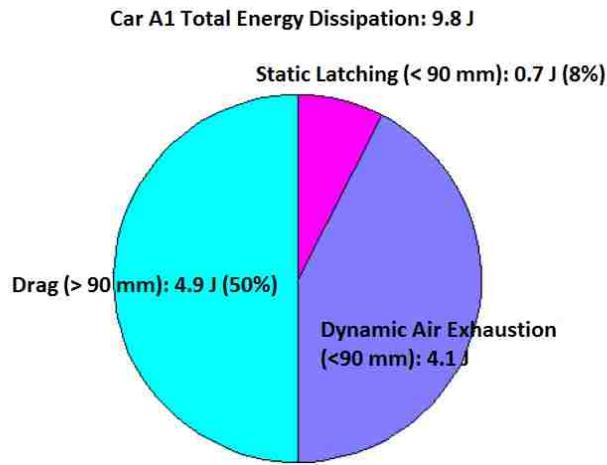
Figure 4-7: Dissipation energy pie [31].

4.1.2.1 Quality index

The quality index gives information on the overall quality of the door. All the metrics are combined in the quality index, compared to absolute values and weighted for importance. The formula used to create the index is proprietary.

To be meaningful, the reference values must be defined, and if no nominal target values are used (input by the user), generic target values are used to define the performance. Some research conducted to correlate the JD power score and the quality index showed that no particular relationship exists between the perceived quality from the customer and this index value. This index appears, therefore, not to give direct information on whether or not the user will perceive a good or bad door closing performance, but it can be used as a comparison means between the overall performance of different doors (or of the same door in different tests).

An example of quality index is given in Figure 4-8.
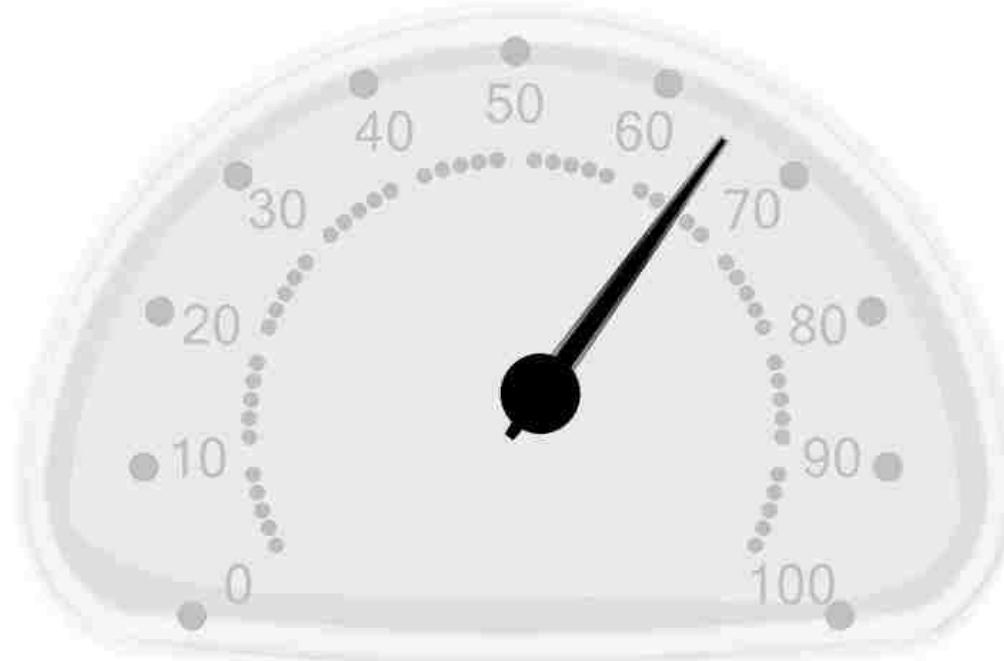
Figure 4-8: Quality index given as output of an EZ slam session.

4.1.2.2   Speed vs. Angular position

The speed of the door is calculated at the hem edge and expressed as a linear speed. The whole speed profile is recorded, from fully open to fully closed position and a combination of slams is used to create a typical speed profile of the door closure. The minimum closing speed is determined via CIM (Common Information Method), with which information from several tests is combined into one database and key characteristics can be determined. The CIM method in this case is based on Minimum Overslam and the relation between Overslam and Closing Speed.

In the typical speed vs. angular position graph example in Figure 4-9 three different areas can be underlined: *acceleration* (on the right of the cyan line, marking the releasing point), *free motion* (between the cyan and the pink line, marking the 90 mm distance) and *impact* (on the left of the pink vertical line). As explained in paragraph 1.3 the plot is to be read from right to left (and so from fully open door position to fully latched). The acceleration phase includes the input by the user and ends when the user releases the door and leaves it to close by itself. The speed profile in the free motion phase is dictated by

the shape of the check profile while in the impact phase the latch of the door hits the striker and the door reaches a complete stop. The dashed line in Figure 4-9 represents the door closing velocity scaled to minimal closing speed; the line is guessed by the software based on the results of all the different tests, because not always the real minimum closing speed is reached during the tests. If the values relative to minimum overslam and residual energy recorded in the tests suggest that the door could have been fully latched also at a speed lower than the minimum speed recorded, the new value of minimum speed is guessed by the software and its profile is plotted on the graph of Figure 4-9.
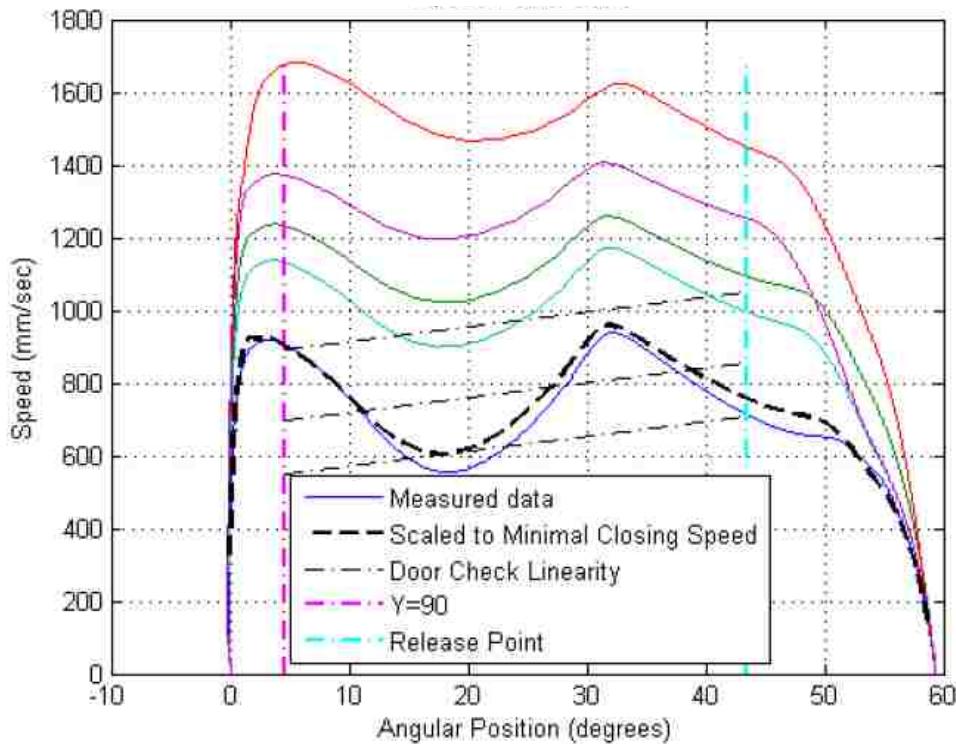
Figure 4-9: Speed vs: Angular Position graph example [31].

4.1.2.3   Y vs. Z

The program gives as output the plot of the Z coordinate of the door latch position with respect to the striker for the last millimeters of the door's linear travel. If the latch and the striker were always perfectly aligned this plot would be represented by constant horizontal lines, also in the last millimeters of door closure; however, when the door latch hits the striker, the relative position between the two components changes due to the impact. A typical plot is shown in Figure 4-10.
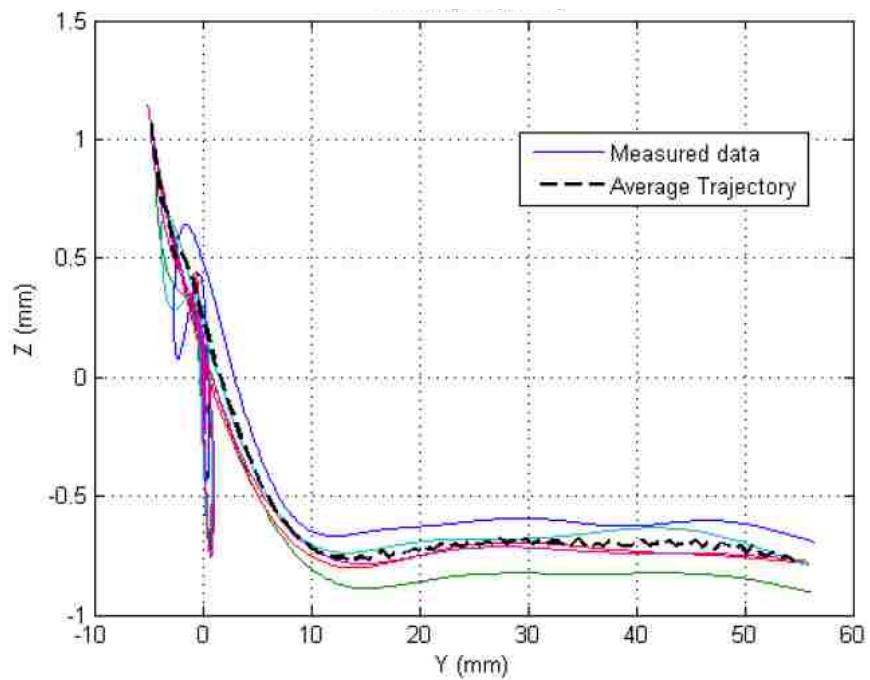
Figure 4-10: Z vs. Y trajectory graph [31].

4.1.2.4   Overslam vs. Speed

An overslam vs. speed curve is created based on a number of individual runs of the slam tests. The curve is shown in Figure 4-11.
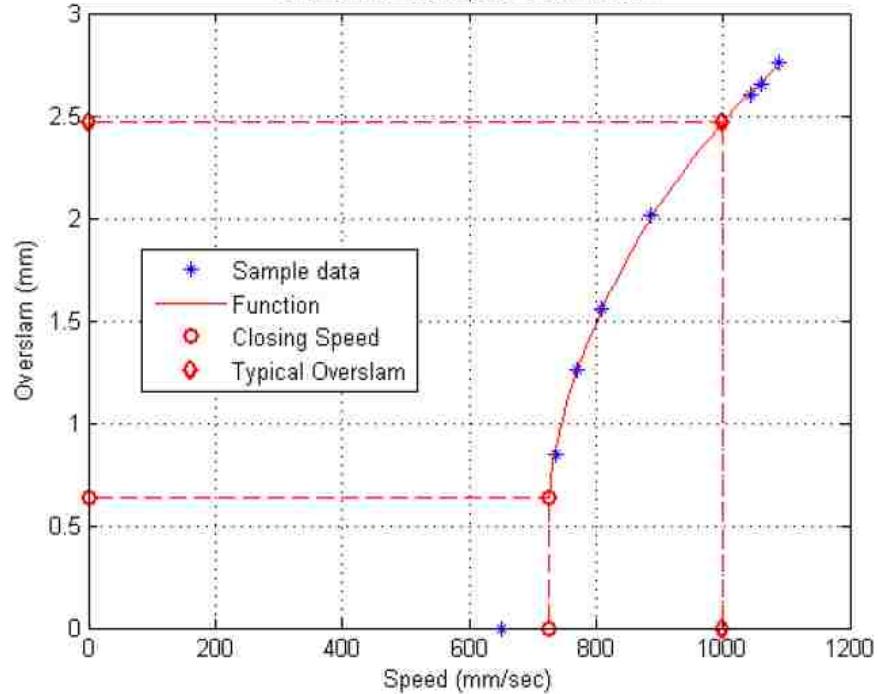
Figure 4-11: Overslam vs. Speed graph [31].

Every blue dot represents one run and shows the value of door overslam recorded as a function of door closing speed. As it can be seen, the greater the closing speed the further the door travelled past the rest position when it closed (so the greater the overslam). The red line represents, like in other plots given as outputs, the best fitting line of all the runs performed.

4.1.2.5 Overslam vs. Input impulse
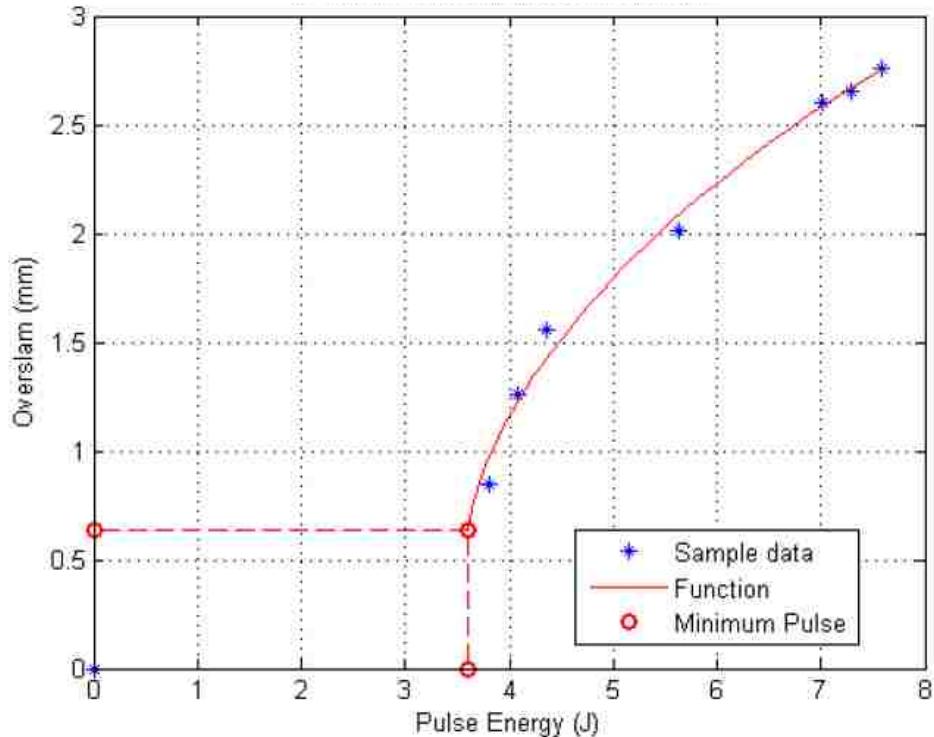
Figure 4-12: Overslam vs. Input Energy graph [31].

The graph of the overslam as a function of the input pulse is shown above in Figure 4-12. The software provides the user with the value of the impulse given as input by the user during the slam test and its correlated overslam value. The impulse value corresponding to the minimum overslam represents the *minimum input impulse*. The characteristic is used in combination with the minimum overslam measured in the static Push test, described in the following. As in the overslam vs. speed graph, the blue dots are the single run performed during the slam test and the red line is the associated best fitting line.

61

The plot is also very useful to determine an anomalous, and most likely wrong, run. The measurements taken by the sensors may be adversely affected by several factors related to the environment (a sudden flash of light interfering with a sensor, a sudden error in the connection between the units and the base station etc.) and as a result give a wrong value for the run. It is obvious that greater values of the overslam must correspond to greater input impulses. If two runs disagree and a greater overslam is detected for a smaller input pulse, the software gives a warning and one of the two or more contrasting runs can be eliminated or disregarded during data processing.

4.1.2.6 Push Force vs. Y

The graph of the static force as a function of displacement is shown in Figure 4-13.
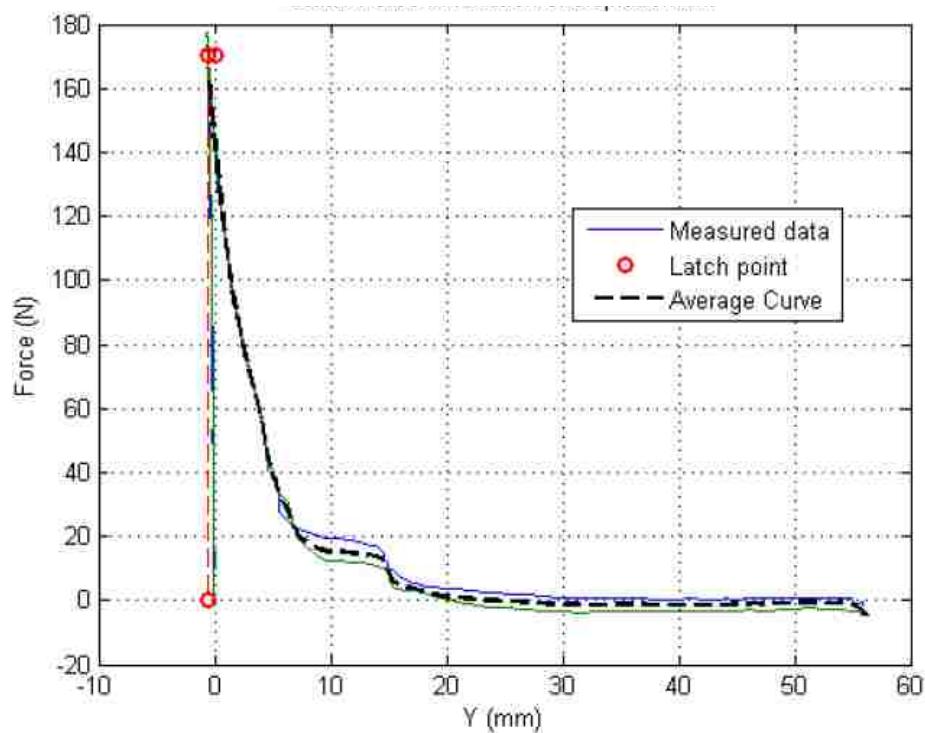
Figure 4-13: Push force vs. Displacement graph [31]. This graph is the main output of the static push test together with the value of minimum overslam.

The value of the force in the Push test is given as a function of the travel in the Y direction. In the first millimeters of travel in the Y direction the force value is very low and increases sharply when the seals start being compressed and opposing a resistance to door motion. The latch point with the smaller force and the corresponding overslam is

recorded and later used to determine the minimum speed to reach the minimum overslam. During the quasi static test the door is released immediately after latching takes place, so the recorded overslam is taken as the minimum overslam that is necessary to latch the door. This value is used as input to the Overslam vs. Speed graph of Figure 4-11: the value of speed at which the Overslam vs. Speed best fitting line intersects the value of minimum overslam is taken as the minimum necessary door closing velocity.

4.1.2.7   Speed vs. Input Energy

Another very important output is represented by the door closing speed as a function of the pulse energy of the user. Since one goal is to evaluate the minimum closing energy necessary to fully latch the door, the Slam tests are used to create a best fitting line between all the runs and correlate the closing speed of every run to the energy that was input by the user to shut the door. The value of minimum closing speed found in Figure 4-11 and based on the Push test result is input to the graph of Figure 4-14 to evaluate the minimum required closing energy. The value on the abscissa of Figure 4-14 that corresponds to the value of the minimum closing speed on the best fitting function is taken as minimum closing energy.
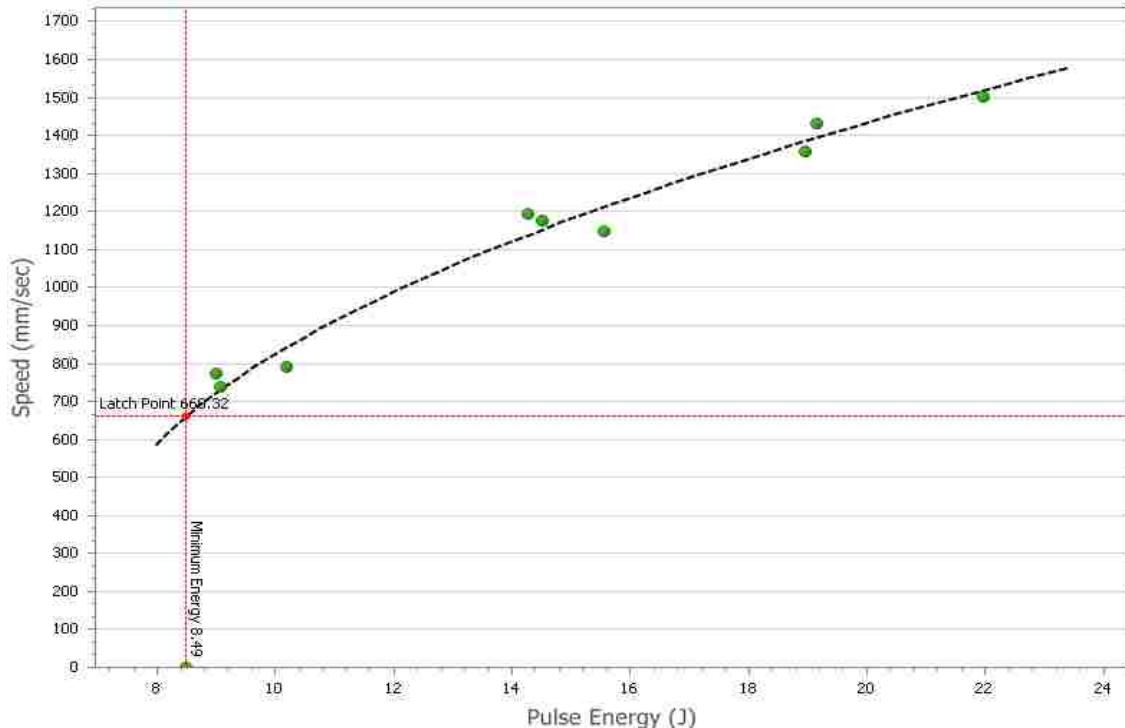
Figure 4-14: Closing Speed vs. Pulse Energy [31].

4.1.2.8   Pulse energy vs. Angular position

The pulse energy vs. angular position plot is characterized by a sharp increase in the energy when the user initially pushes the door and a constant pattern after the door is released as no more input is given to the door (Figure 4-15). The plot tells the value of the user input when the door was released.
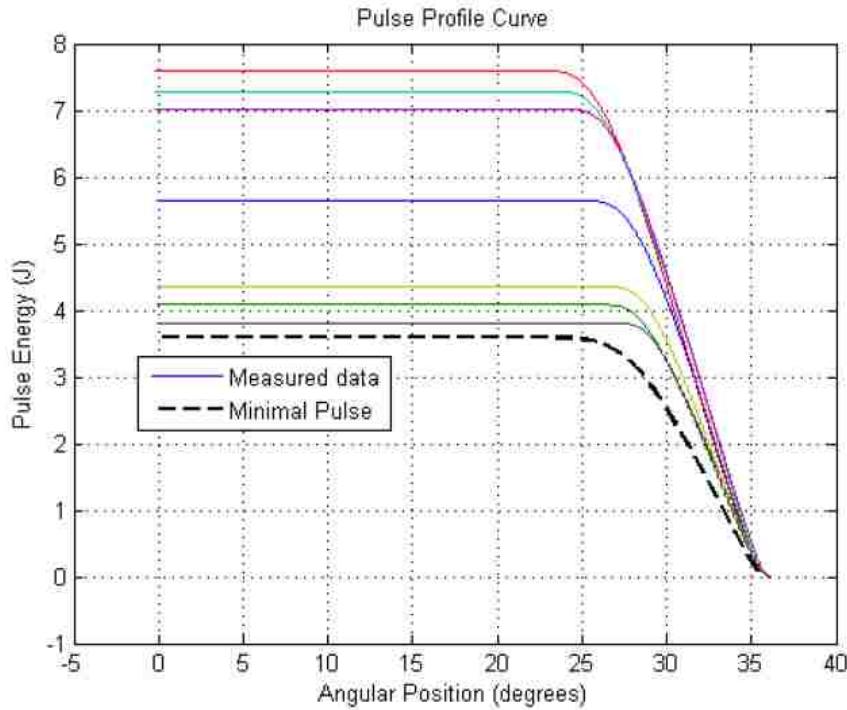
Figure 4-15: Pulse energy vs. Angular position graph [31].

4.1.2.9   Door raise vs. Angular position

The graph in Figure 4-16 shows the trajectory of the center of gravity of the door in the Z direction as a function of the angular position of the door. The change in height of the center of gravity of the door is, as explained in section 3.2.4, the cause of the positive or negative contribution that door weight gives to the closing event. If the position of the door CG is lower in height with respect to the initial position, the weight will assist during the closing process, pulling the door towards the cabin. The trajectory of the center of gravity is not really linear and in certain cases (as it will be highlighted in Chapter 5) the door center of gravity rises at the beginning of the closing event and then starts falling giving a positive contribution to closure. The value that is given as numerical output for the door rise is measured at the hem edge of the door; but the door

rise used for the calculation of the weight contribution is the value measured at the center of gravity. Since the door center of gravity is positioned at approximately 48% of the door radius, the value of door rise of the center of gravity will be about 48% of the value displayed by the software.
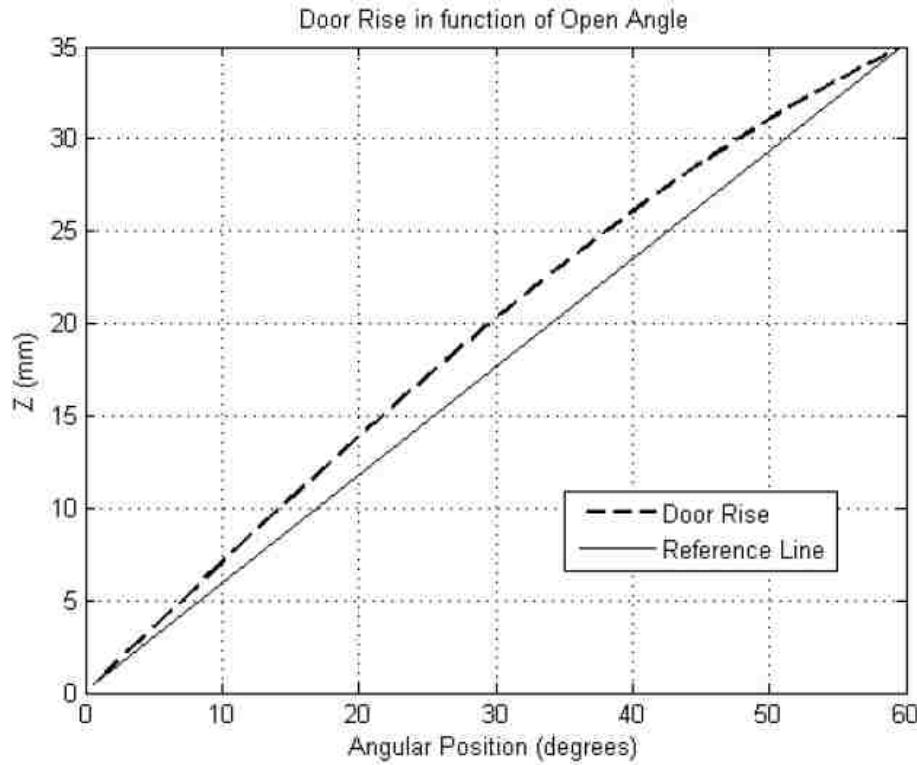
Figure 4-16: Door raise vs. Angular position graph [31].

Other graphics given as output by the program will be described during the analysis and discussion of the results in Chapter 5. The line called reference line represents a linear decrease of the height of the center of gravity during door closure, an optimal trajectory that allows the weight of the door to give a positive contribution to door closure for the entire swing of the door.

4.2 The OU model

In order to predict the minimum closing effort and the minimum closing speed for side doors, the OU Model requires some input regarding the door to be tested. The constant parameters include the values for atmospheric pressure, air density, cabin volume, air leakage rate, door mass, door area and door inertia. These parameters are needed in

particular to calculate the air bind and weight contribution. In case the values for door area and door inertia are not available or not reliable, the software uses the data regarding seal lines and mass (that must be provided by the user) to approximate these quantities.

A direct time integration method (Newark method) is used to update every one of the torque contributions described in section 3.2 at each time step and evaluate the final total counter-acting torque as a sum of all the contributions [24]. In order to use this method, some solution parameters need to be input to the software that include:

- Time step for the integration, Δt_g, usually set between 0.001 and 0.0001 seconds.

- Estimated closing velocity v_g of a point on the door at a certain distance r_m from the hinge axis and linear displacement in the cross car direction (y direction) from the car body d_0.

The input for constant and solution parameters is shown in Figure 4-17.

Constant Parameters		
$P_{atm} =$	100000	Pa
$\rho_0 =$	1.2051	kg/m^3
$V_0 =$	2.75	m^3
$q_{leak} =$	125	cfm
$M_{door} =$	36.7	kg
$A_{door} =$	1.082	m^2
$I_{door} =$	13.81	kg-m^2

Solution Parameters		
$\Delta t_g =$	0.0005	s
$v_g =$	2.72	ft/s
$d_0 =$	20	in

Figure 4-17: Constant and solution parameters input.

The d_0 value represents the distance at which the user stops pushing the door during the closing event. After that point (taken from experimental data at a distance of 20 in (508 mm)), the door is left to close by itself.

In order to evaluate hinge, latch and weight contributions the coordinates of hinges, latch and center of gravity locations must be input to the model as well.

For the calculation of the seal compression effort, data relative to the seals are required by the software. An established number of seal points is input (inserting the coordinates of the points that approximate the seal segments position) together with the seal gap information, the seal lip interference (the amount perpendicular to the mounted surface), and the seal bulb interference (the amount of seal compression displacement within the

cross section of the seal line in the direction of the normal of the seal contact line when the door is closed).

The door seal geometry based on the points input to the model is showed in the three coordinate planes (x-y, x-z and y-z) as shown in Figure 4-18.

In the simulation performed in this research the seal gap data input to the model was measured from the doors tested with the EZ Slam. With regards to the door weight and inertia information, the data retrieved with the pendulum test was used as input. Even though the last few degrees of door closing are considered for prediction, information on the check system (in particular the torque vs. angle characteristics) are also required in input and affect the overall result of the simulation. The model doesn't include the energy loss in friction due to the hinges and to the check system during the travel of the door that is covered by the user (the first 30-40 degrees), but the check strap information is used to evaluate the positive energy contribution given by the close assist of the check. From the torque vs. angle curve input to the model, the area under the curve in the last (approximately) 25 degrees of closure is calculated, and represents the check positive energy.
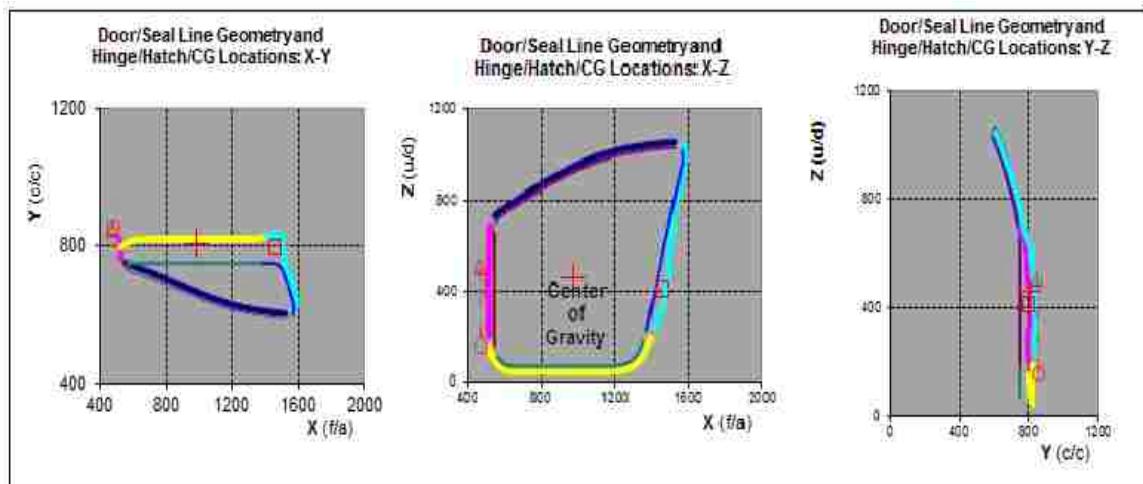
Figure 4-18: Door seals geometry shown in the three coordinate planes in the OU Model.

After the model is run, the calculated contributions to the effort and the predicted minimum closing speed are outputs; the percentage of total energy represented by each different contribution is also given in the outputs. An example of output is given in Figure 4-19.

Energy Sinks/Effort		
	J	%
E_{air} =	3.158783	68.62819
E_{seal} =	0.780109	16.94877
E_{weigh} =	-0.39989	-8.68797
E_{hinge} =	0.284031	6.17091
E_{latch} =	0.77971	16.9401
E_{total} =	4.602748	100
Closing Velocity		
v_p =	2.856196	ft/s
at t_p =	0.552174	s
d_m =	4	in

Figure 4-19: Output results from a simulation performed with the OU Model as an example.

The value d_m represents the distance at which the closing speed of the door is usually measured in laboratory testing. The software gives the predicted value of closing velocity at this point to allow a comparison with the physical measurements of the closing speed. The OU model gives also the possibility to calibrate the model in order to have more precise results in terms of hinge, latch, seals and air bind contributions. If data on the real hinge pin radius and friction coefficient are available, they need to be input to the model. Through calibration it is possible to set the correction factors used by the model for the seal compression contribution and the air bind model. The correction factors are needed because all the models used to model the different contributions (a part from the weight model that is geometrically exact) are approximations of the real physical phenomena that take place during closure. Also the latch constant k_{latch} used in section 3.2.2 is obtained through calibration and kept constant for a specific vehicle latch.

5. ANALYSIS OF THE RESULTS

The scope of the tests performed with the EZ Slam was, as mentioned before, to analyze the differences in the energy sink contributions, that hinder door closure, and in the positive energy contributions that help the user closing the door, of an aluminum door in comparison with a steel door. The tests performed were of the type described in section 4.1.1. It was hypothesized that the performance of the aluminum door would worsen with respect to the steel door in particular because of the lower weight and lower inertia to help the closing action. In view of a more widespread use of aluminum in the automotive body and in particular in closures, the closing performance of a lighter door needs to be acceptable and compliant to the standards used by car companies in terms of minimum closing speed and minimum closing effort. The specification used for maximum allowable minimum closing speed is 4.5 ft/sec (1371.6 mm/sec) while there is no specification for the allowed minimum user input necessary to fully latch the door. Even with a closing performance that falls into specifications, car makers always seek to obtain the best results possible to stay competitive. A direct correlation of the minimum closing speed and closing energy specifications with customer satisfaction has not yet been found, but these two factors are certainly to be carefully considered; closing effort and closing speed are in fact the two factors that characterize door closure from the customer perspective (together with the sound during closure). The values of closing energy and speed must be high enough to avoid the risk of an incomplete closure of the door, but low enough to allow a comfortable and easy closure by the user. The correct balance must be found, that brings the highest satisfaction of the customer in operating the doors, both during closing and opening.

The influence of a more aggressive check profile (a greater close assist after the last indent of the check arm) on door closing performance was also tested to understand if it can be adopted as a solution to decrease door closing effort. Since the research is focused on the aluminum door, the prototype check strap was tested on this door. Finally, the simulation of door closure is performed with a predictive tool available as a different means to evaluate the door closing effort and to understand if the two methods are directly comparable in their functions.

5.1 Testing Conditions

The door closing effort of a vehicle was studied through tests performed with the EZ Slam equipment on the front left door (driver's door). A steel frame and an aluminum frame were fully dressed with the same components, mounted on the same C segment vehicle, and tested with the same equipment. The seal gaps were measured on the vehicle before the steel frame was removed from the body to mount the aluminum frame. To measure the seal gaps, the seals on the body were removed, and several cone-shaped pieces of clay were placed on the car body in the positions shown in Figure 5-1.

Figure 5-1: Points used for seal gap measurements

The door was then closed very slowly to a fully latched position and then reopened in such a way to leave the clay attached to the car body. The height of the compressed clay was then measured with a caliper as an indicator of the amount of compression of the seals on the body when the door is latched. It is important when measuring door seal gaps to operate the door by the handle in order not to deform the frame in other points when closing the door, thus affecting the measurements. A common mistake is to push the door

on the top right corner when closing it, thus affecting the seal gap value in that position. All the tests were performed by the same operator.

Due to the different thickness (greater) of the aluminum frame, the fittings of some of the components removed from the steel door and placed on the new frame were not perfect. Due to some differences between the aluminum frame and the steel frame, a hole needed to be drilled in the speaker housing in order to allow the connection of the wiring harness of the electrical components inside the door module to the car body. After the aluminum door was mounted, the seal gaps were re-measured. The seal gaps were measured both for the steel frame and for the aluminum frame because the amount of compression of the seals when the door is latched gives a contribution to the closing effort that, for the type of study conducted, was required to be the same. In order to reach a value of the seal gap in the upper right corner (B pillar) closer to the one previously measured for the steel door, the upper header of the door was bent slightly. The values measured for the points used for the seal gap measurements for the steel and the aluminum case are listed in Table 5-1.

Table 5-1: Seal gap measurements.

Point	Seal gap measurement steel [mm]	Seal gap measurement aluminum [mm]
1	13	11.5
2	10	10.5
3	13.5	14
4	13.8	14.9
5	14	15.1
6	13.8	12.9
7	11.7	11

Points 1, 3, 4 and 6 are chosen where there are parts or components that could be adjusted in their position on the body in order to reach the wanted value of the seal gaps. Point 1 corresponds to the upper right corner of the door and this part of the frame can be easily bent to reach different values of the seal gap in that point. At the level of the hinges (Points 3 and 4) the door can be moved slightly up or down and forward or backward thus modifying the overall fitting on the body and the value of multiple seal gaps.

It is recommended, when moving a door from its original position on the body, to mark the position of the hinges before moving the door to be able to apply the modifications needed to reach the desired values of the seal gaps. Point 6 is aligned with the striker on the body, another component that can be easily moved in every direction thus changing the way the door latches. Points 2, 5 and 7 are reference position used to check the matching of the values of the seal gaps in those points of the frame. If all those points match, the rest of the seal gaps around the door frame will most likely match as well. Even though in the case of the aluminum door the values of the gaps were not exactly the same as for the steel frame, they were considered close enough not to affect excessively the measurements of the seals contribution to closing effort. A part from the action on the door right corner, a further change of the seal gaps in other points (angles, latch point etc.) would have negatively affected the measurements in other locations.

The mounting and fitting of the aluminum frame onto the body presented several difficulties and, even though the hinges used were the ones taken from the steel frame, and so the exact same component, door location changed slightly between the steel and the aluminum tests.

The modifications in the position of the door were needed to reach a satisfactory fitting of the door on the body. It must also be taken into account that, whenever the door is removed from the body and then remounted, its position will most likely slightly change in any case. The difficulties in reaching a good fitting of the door depended on the different thickness of the aluminum frame with respect to the steel frame and possibly on the aluminum frame dimensional tolerances, probably not exactly the same as for the steel frame. The thickness of the aluminum frame was greater than the thickness of the steel frame due to the necessity to satisfy the strength and stiffness requirements for the door.

A major change that must be underlined in the fitting of the door is the adaptation of the striker mechanism for the tests on aluminum. Although the striker was kept the same, a shim was needed and put behind the striker on the body in order to reach a correct closure of the door.

With regard to its position, the striker mechanism cannot, therefore, be considered the same for the aluminum and for the steel case, but repositioning it was unavoidable.

Having totally moved this part the "striker misalignment" value (giving the relative position between the latching system on the door and the striker on the body during the last millimeters of closure) recorded by the EZ slam during the test of the aluminum frame was obviously off with respect to the values relative to steel. The tests were performed during different days (and even different weeks) even though the car tested was never moved from its spot in the body-shop for the whole duration of the tests. The temperature varied in a window of around 4 degrees Celsius, a very small difference to have an influence on the tests.

The results presented in sections 5.2.1 and 5.3.1 are the average of three tests for the steel, four tests for the aluminum frame with the normal check and two tests for the aluminum with the prototype check. Each of the tests used for the evaluation of the results was considered reliable based on considerations made on the deviation of the runs from the best fitting line in each of the graphics given as output from the EZ Slam. Not all the tests performed during the testing sessions of the two doors were taken into account for the reasons listed here:

1. The very first run of the slam test was a non-latching; sometimes in this case the software did not recognize the non-latching and treated the run as a fully latched test thus misinterpreting the results.
2. A fatal error occurred in a run and the software was not able to disable that run and go on with the test. The software would crash for those runs and the entire test would need to be restarted.
3. The values of certain parameters at the end of the test were totally off from the tests previously performed thus suggesting that something went wrong or that the test had not been performed properly. In order to avoid averaging the results with unreliable data the test was not considered.

The coordinates system used by EZ Slam is shown in Figure 5-2. The X direction is positive towards the back of the car, the Y direction is the cross-car direction (positive in the direction of the right side of the vehicle) while Z direction is the vertical coordinate.
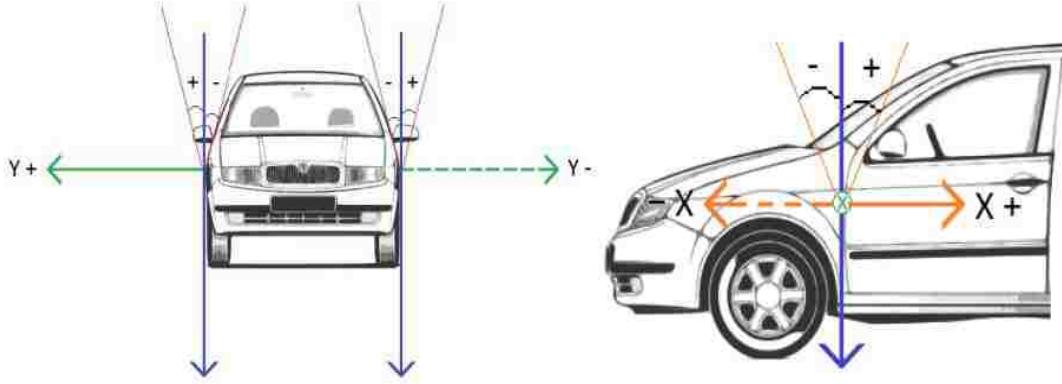
Figure 5-2. Coordinate system used by EZ Slam.

5.2 Comparison between Steel frame and Aluminum frame door closing effort

5.2.1 EZ Slam Testing

The results of the comparison between the steel door and the aluminum door closing performance are presented in Table 5-2 (numerical results of the tests) and in Figure 5-4 and Figure 5-5 under the form of bar-charts. In Figure 5-4 the energy sinks contributions are presented while in Figure 5-5 the positive input contributions are shown. For every contribution involved in the closing action it is also indicated what percentage of the total energy it represents. All the plots that will be presented are thus organized: the plots representing the best fitting lines of all the tests used to evaluate the average values shown in Table 5-2 are presented, each one followed by the plot representing just the average of all the curves for the three cases (steel tests, aluminum tests and aluminum tests with prototype check).

Table 5-2: Steel vs. Aluminum door closing performance results.

	Steel	Aluminum (normal check)	Difference [%]
Minimum closing speed [mm/s]	664.00	974.50	46.8
Total Energy to Close [J]	16.65	17.47	4.9
Minimum user Input Pulse [J]	8.53	12.12	42.1

Closing Energy Sinks

	Steel	Aluminum (normal check)	Difference [%]
Energy Loss from Gravity [J]	0.000	0.00	-
Energy Loss from Spring [J]	0.000	0.00	-
Energy Loss to Air Bind [J]	1.66 (9.9%)	2.51 (14.4%)	50.6
Energy Loss to Check [J]	10.00 (60.1%)	11.16 (63.9%)	11.6
Energy Loss to Drag [J]	4.44 (26.7%)	2.70 (15.5%)	-39.0
Energy Loss to Static Compression [J]	0.55 (3.3%)	1.10 (6.2%)	98.7

Closing Energy Inputs

	Steel	Aluminum (normal check)	Difference [%]
Energy provided by Gravity [J]	1.32 (8%)	1.10 (6.3%)	-16.5
Energy provided by Spring [J]	6.80 (41%)	4.24 (24.3%)	-37.6
Energy provided by User [J]	8.53 (51%)	12.12 (69.4%)	42.1

Opening Energies

	Steel	Aluminum (normal check)	Difference [%]
Energy provided by Gravity [J]	0.00	0.00	-
Energy provided by spring [J]	0.00	0.00	-
Energy provided by user [J]	18.12	16.50	-8.9
Energy required by check [J]	10.00	11.16	11.6
Energy required by gravity [J]	1.32	1.10	-16.5
Energy required by spring [J]	6.80	4.24	-37.6
Total Energy to Open [J]	18.12	16.50	-8.9
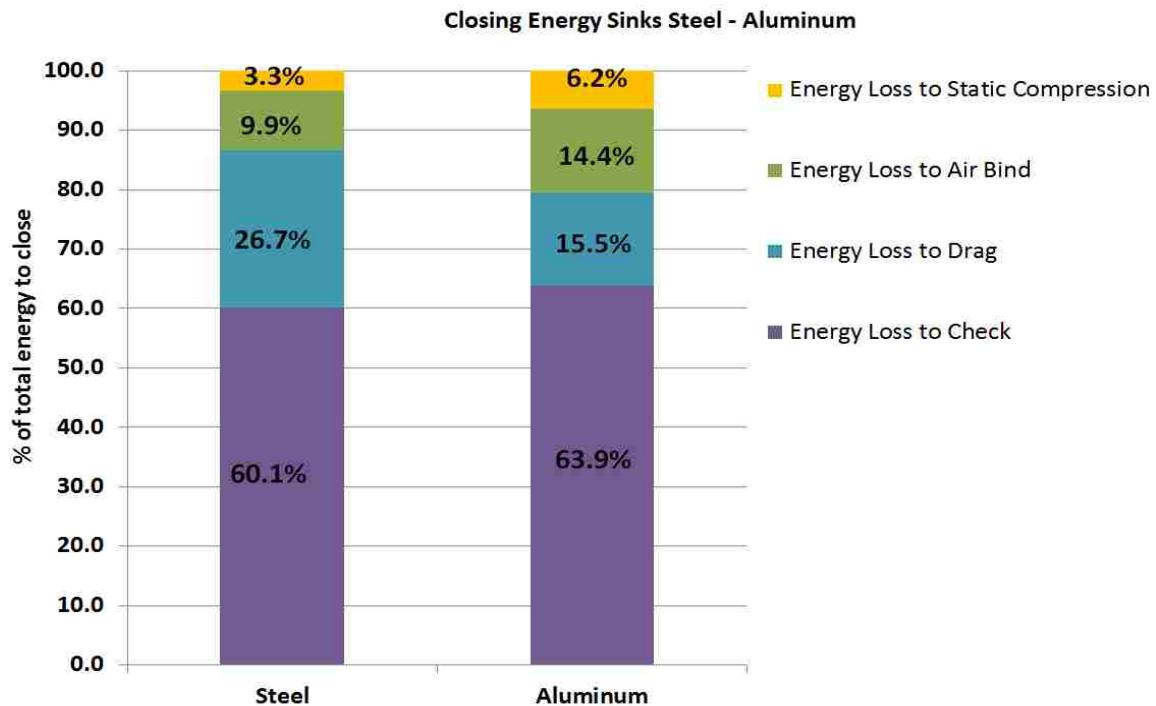
Figure 5-3: Direct visual comparison of the energy sinks percentage contributions for the tests performed on the steel and on the aluminum doors.
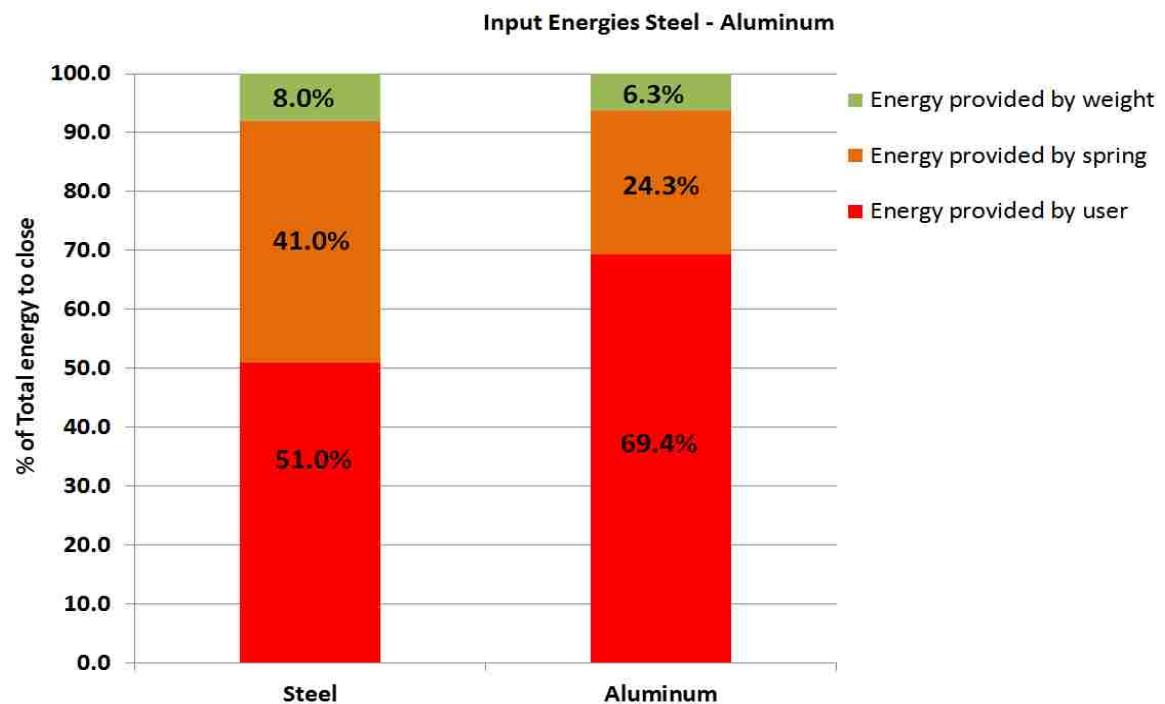
Figure 5-4: Direct visual comparison of the energy inputs for the tests performed on the steel and on the aluminum doors.

The specifications of the steel door used in the tests are shown in Table 5-3, the specifications of the aluminum door are proprietary and not publishable.

Table 5-3: Doors' weight, inertia and center of gravity information for the steel door.

Weight [kg]	36.8
Inertia [kgm^2]	13.81
Center of Gravity (x,y,z) [mm]	978.9, 804.7, 461.9

The coordinates of the center of gravity refer to a coordinate system with the origin placed at the very front of the car and in the very center. The z coordinate is calculated from the ground.

The doors' information was obtained with the pendulum test, as explained in section 3.

All the quantities named in Table 5-2 are briefly described:

1. *Minimum closing speed*: minimum speed (recorded during the last 90 mm of door travel) with which the door was able to fully latch, or minimum predicted closing speed based on the combination of all the data recorded during the different tests.

2. *Total energy to close*: total energy that was necessary in order to bring the door to full latching. It is both the sum of all the energy sink contributions or of all the positive energy inputs (given by user, weight and spring).

3. *Minimum user input pulse*: it is the minimum energy input given by the user that allowed to reach a complete closure (*Closing Energy provided by user*). It is measured through a load cell in the door unit of the device.

4. *Closing energy loss from gravity*: energy that is sunk during closure due to the weight of the door. This value is always zero as, due to the tip angle of the hinge axis and to the overall decrease in height of the center of gravity during closure, the weight always provides a positive energy contribution (*Closing Energy provided by gravity*).

5. *Closing energy loss from spring*: since the contribution of the check system during closure is positive (the check system helps pulling the door toward the closed position) this value is always zero (*Closing Energy provided by spring*). This means that part of the energy stored by the check during opening is given back during closure.

6. *Closing energy loss to air bind*: amount of energy sunk due to the air bind opposing effect.

7. *Closing energy loss to check*: energy dissipated in friction between the roller bearings and the arm of the check strap and in friction at the hinges.

8. *Closing energy loss to drag*: completes the balance equation between energy input to the system and energy dissipated by the system when the amount of energy input is greater than the sum of the energies sunk by air bind, static compression of the seals, latch engagement, and check and hinge friction.

9. *Closing energy loss to Static Compression*: energy sunk to compress the seals and to engage the latch on the striker.

10. *Opening energy provided by gravity*: this value is always zero as, during opening, gravity does not help the user but gives an opposite contribution (*Opening Energy required by gravity*).

11. *Opening energy provided by spring*: as for gravity, spring action during opening is always opposing user's input, because the energy is being stored (*Opening Energy required by spring*). So the check does not provide any help in opening the door.

12. *Opening energy provided by user*: energy input by the user to slowly open the door in the Sweep test.

13. *Opening energy required by check*: energy dissipated in friction by check and hinges during the opening sweep test. This energy is equal to the energy required to overcome friction during the closing sweep test.

The total energy necessary to close the two doors differed by only 5% resulting in a slightly higher energy in the aluminum case while the minimum closing speed necessary to latch the aluminum door was almost 50% greater with respect to the steel door, as shown by the graph in Figure 5-5 and Figure 5-6. The curves show a progressive flattening with the increase of the closing speed; when the speed is lower, the bearings of the check system follow exactly the check arm's profile and the accelerations and decelerations given by the slope of this profile are more clearly shown by the curves of the speed. When the door is shut faster and a much higher closing speed is reached, a slight floating of the bearings over the check's profile causes the flattening of the curves (particularly during the close assist of the check's arm).
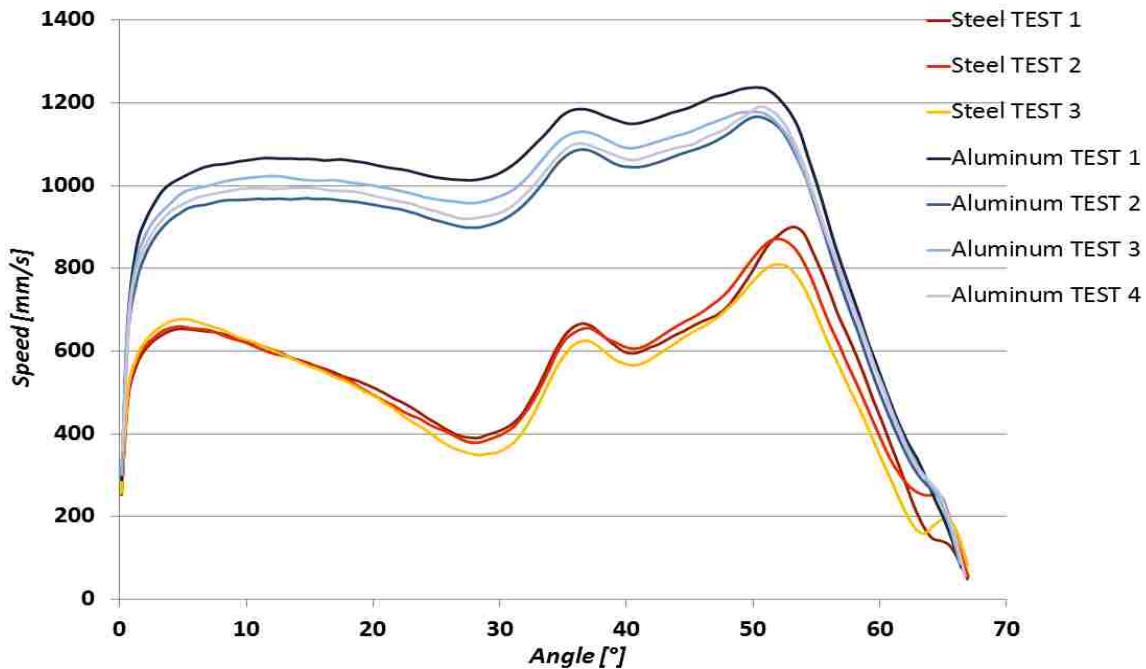
Figure 5-5: Minimum closing speed vs. Angle graph.
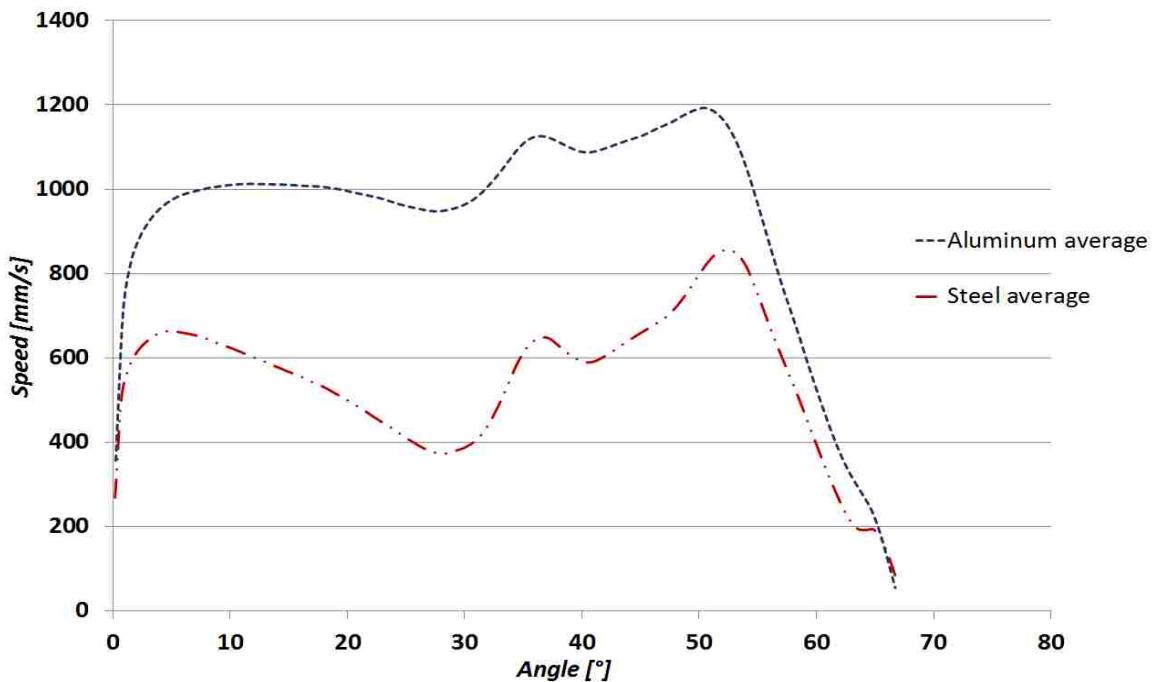
Figure 5-6: Minimum average closing speeds.

With regard to the tests performed on the steel door, the greatest energy sink was the check system (60.05% of total energy), followed by drag (26.7%), air bind (9.95%) and static compression (3.3%). In the tests performed on the aluminum frame, the energy sink contributors were the same but their influence on the closing event were different; the

79

check system required 63.9% of the total energy to close, air bind 14.3%, drag 15.55% and the static compression of the seals 6.25%. The bar charts relative to the results are shown in Figure 5-7 and Figure 5-8.
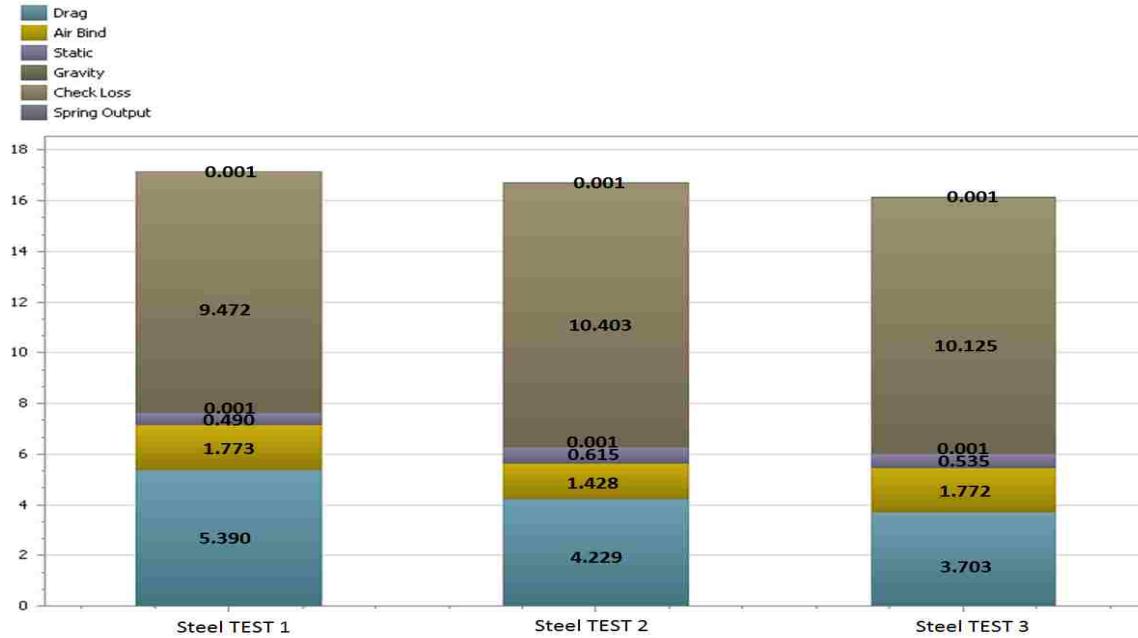
Figure 5-7: Energy sink contributions during the closing action of the steel door. Each bar corresponds to the energy values relative to one of the tests performed on the steel door and used to create the average values presented in Table 5-2.
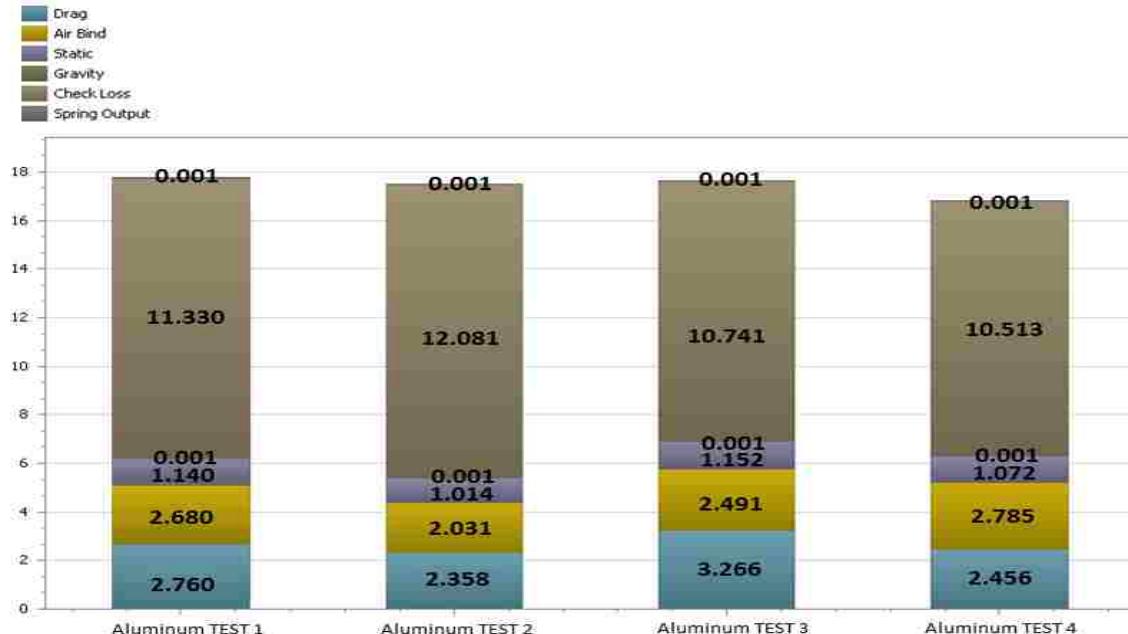
Figure 5-8: Energy sink contributions during the closing action of the aluminum door. Each bar corresponds to the energy values relative to one of the tests performed on the aluminum door and used to create the average values presented in Table 5-2.

It is evident that in both cases the friction of check system and hinges (check loss) was the greatest opposing force to door closure. In the two cases the value of energy loss due to check and hinge friction differs by about 10%; the value was expected to be the same because the check system used for the two doors was the same, but a slight difference could be simply due to the repeatability of the measurements. The second greatest contributor to the steel door closing effort was drag. In the aluminum closing effort drag was about 40% less than steel (representing just about 16% of the total loss). The huge difference in drag is due to the differences in the other energy sink contributions. The drag contribution is evaluated from the energy balance between the total energy absorbed during door closure and the total energy input to close the door (including all the contributions and not just user input). The two total energies have to be equal in order to satisfy the conservation of energy principle, so after the energy dissipated due to air bind, check and hinge friction, and seal compression is calculated, what is missing in the closing action to equate the input energy is put into the drag category.

The graphs presented in Figure 5-9 and Figure 5-10 show the closing sweep force applied from the check to the door as a function of the closing angle for the two doors.
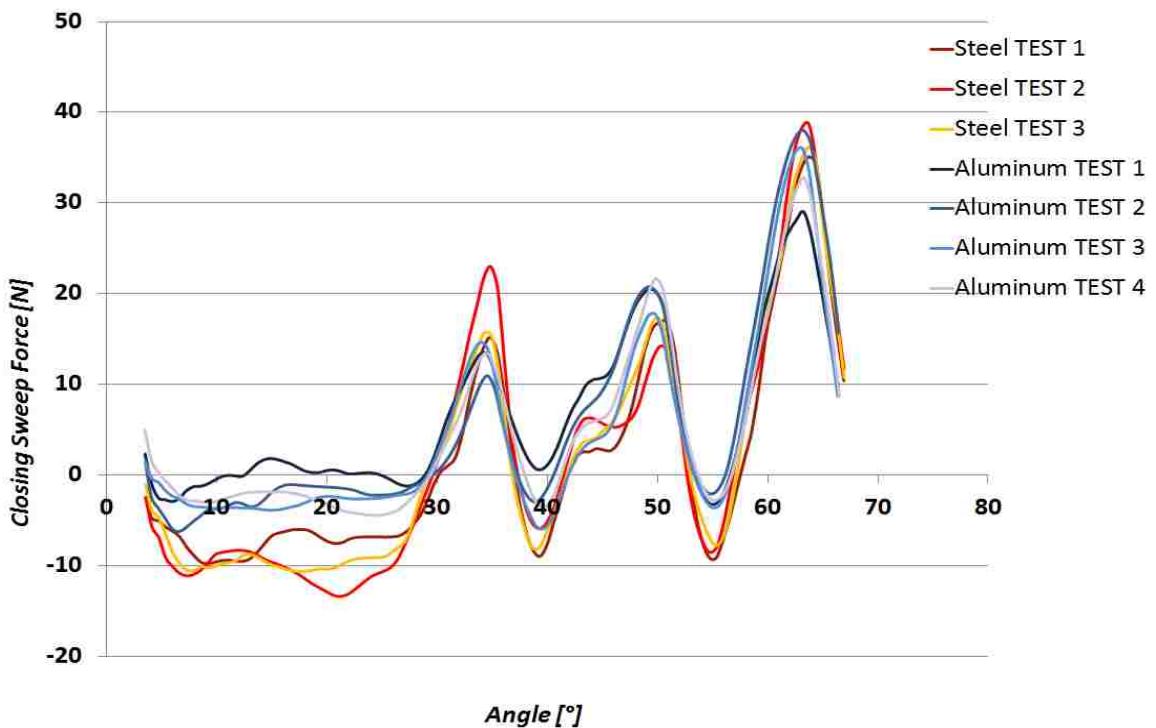
Figure 5-9: Steel vs. Aluminum Closing sweep force comparison (applied by the check to the door). The sinusoidal shape is due to the corrugated profile of the check arm.
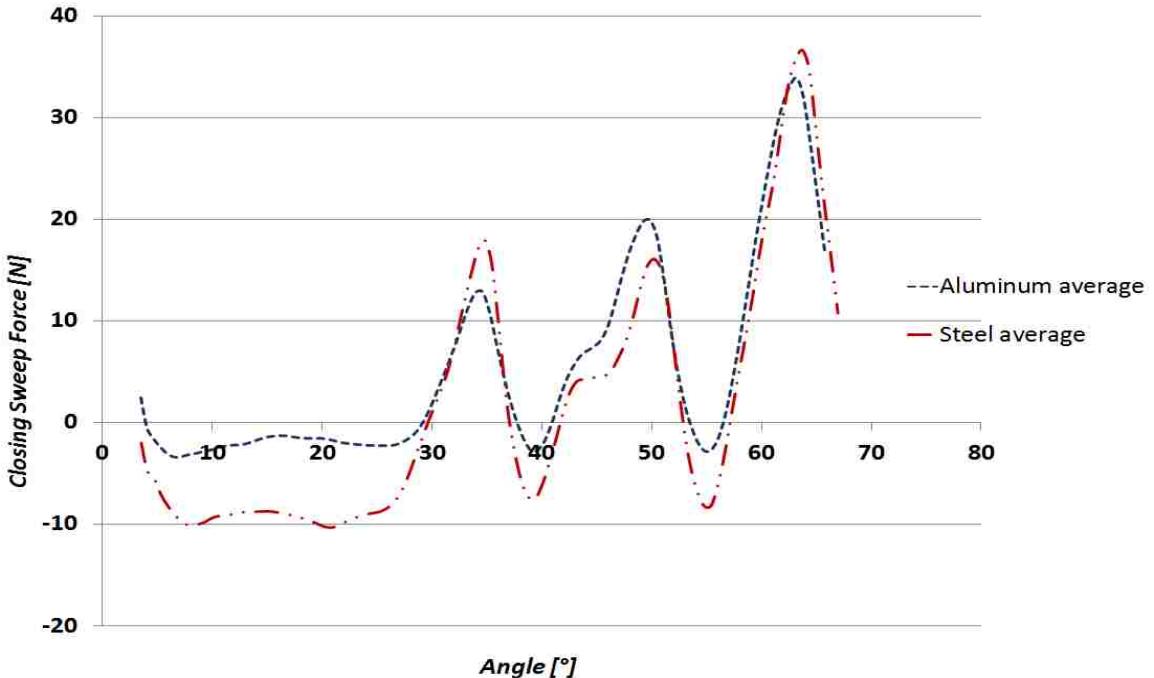
Figure 5-10: Average closing sweep forces of the tests conducted on the steel and on the aluminum frame.

During the closing sweep test, when the springs of the check system are compressed (and so after every check detent), the user needs to push the door in order to continue the closing action; the force applied has therefore positive sign. Instead, when the springs are in the extension phase, and the check is pulling the door toward the closed position (as for example in the last degrees of closure when the close assist pulls the door toward the cabin), the user has to hold the door that would otherwise accelerate, and so the force is considered negative. The force peaks positions are dependent on the corrugated profile of the check strap's arm and on the position of the detents, and the same holds for the sinusoidal shape of the force curves. The plots relative to the closing sweep energy vs. angle curves are shown in Figure 5-11 and Figure 5-12. The final value of the energy ultimately depends on the type and configuration of the specific door. The force is the derivative of the energy (both in the closing and opening case); this relationship is shown and explained better in the following. From Figure 5-11 and Figure 5-12 it is possible to note a huge difference between the energies relative to the steel and to the aluminum door in the last degrees of closure (from 30 degrees to closed position); the curves relative to the aluminum closing sweep event are quite far from each other, indicating probably a dependence of the sweep test on the speed at which it is performed (that is never the same

for each test since they are performed manually); however, the difference between the end point of the tests on steel and aluminum (at about 3 degrees opening angle) is very big, regardless of which test is considered (see Figure 5-12).
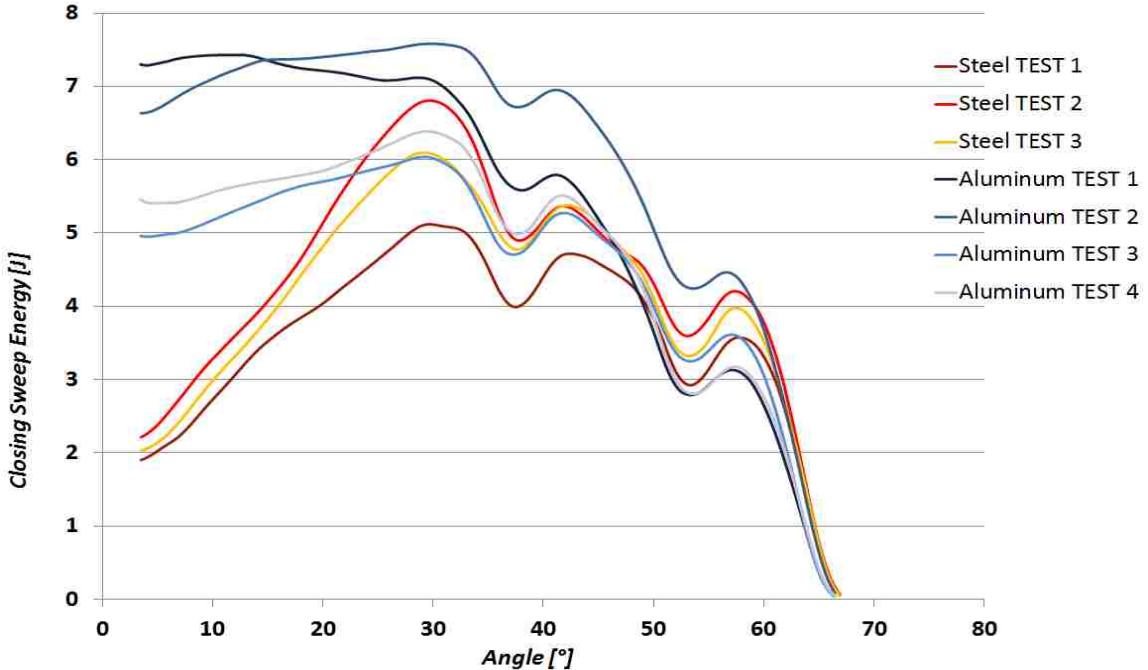
Figure 5-11: Steel vs. Aluminum Closing Sweep energy comparison. The shape of the energy curves depends on the shape of the force curves.
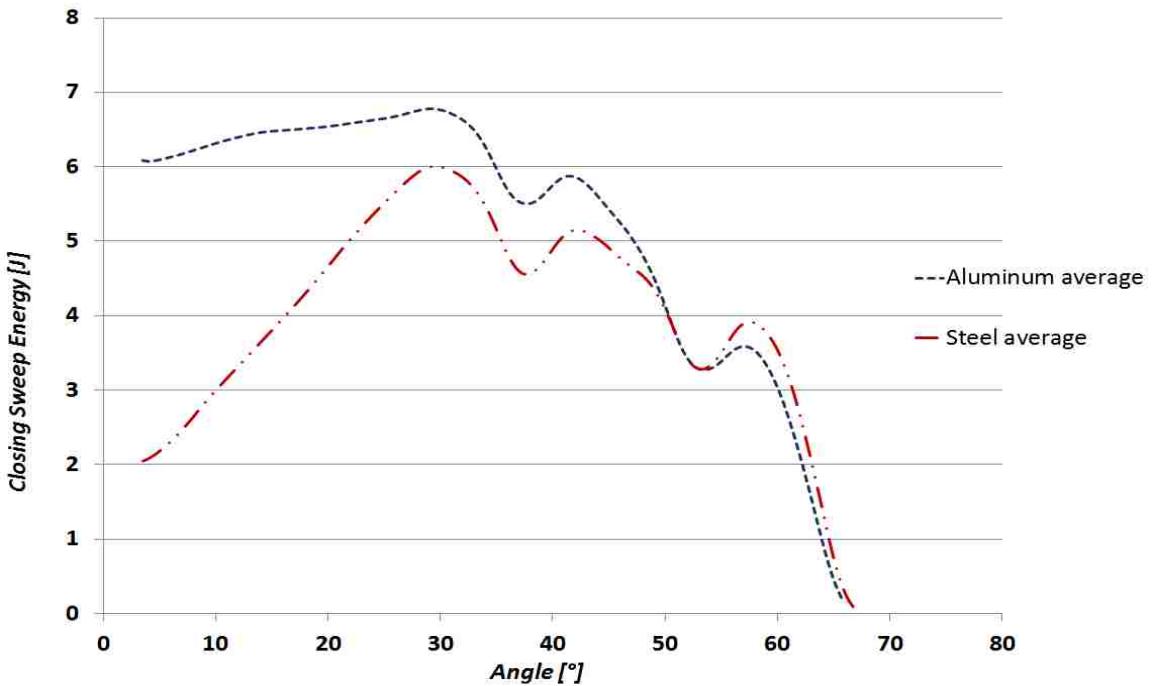
Figure 5-12: Average closing sweep energies for the steel and the aluminum door tests.

A first explanation of this difference might relate to the difference in weight of the two doors: the lower weight of the aluminum frame pulls the door less toward the closed position thus requiring less energy by the user to keep the speed constant (and therefore causing a smaller decrease in the energy in the first 30 degrees of swing). The opening sweep force and energy curves are presented in Figure 5-13, Figure 5-14, Figure 5-15 and Figure 5-16. All the plots are directly given as outputs from the opening sweep test performed with the EZ Slam. With regard to the closing sweep force and energy graphs, they have to be read from right to left, as for the minimum closing speed graph presented earlier, because the tests start from the fully open position of the door and end when the door is almost closed; the opening sweep force and energy graphs must be read from left to right because the tests start with the door in almost closed position and finish when the door is fully open. The graphs never start or end at 0 degrees because during all the sweep tests the door never reaches the fully latched position but the tests end when the door starts leaning on the seals.
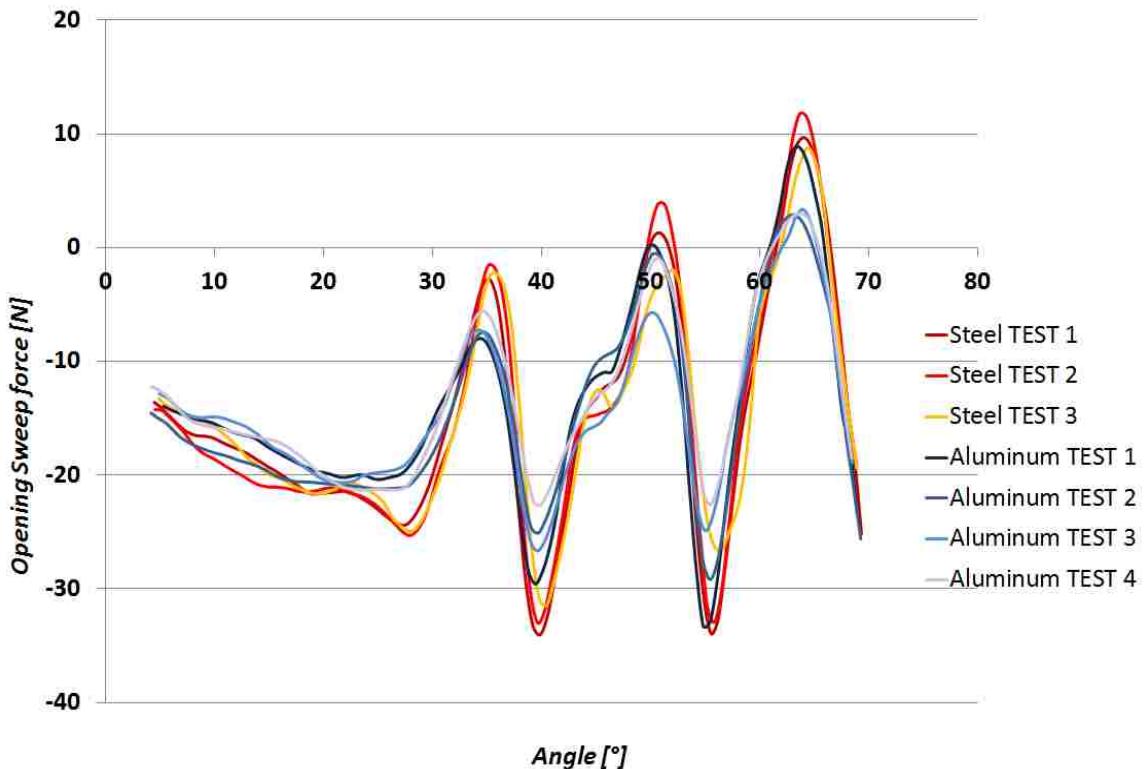
Figure 5-13: Aluminum vs. Steel Opening Sweep Force comparison. As in the case of the closing sweep force graphs, the sinusoidal shape of the curves is due to the corrugated profile of the check arm.
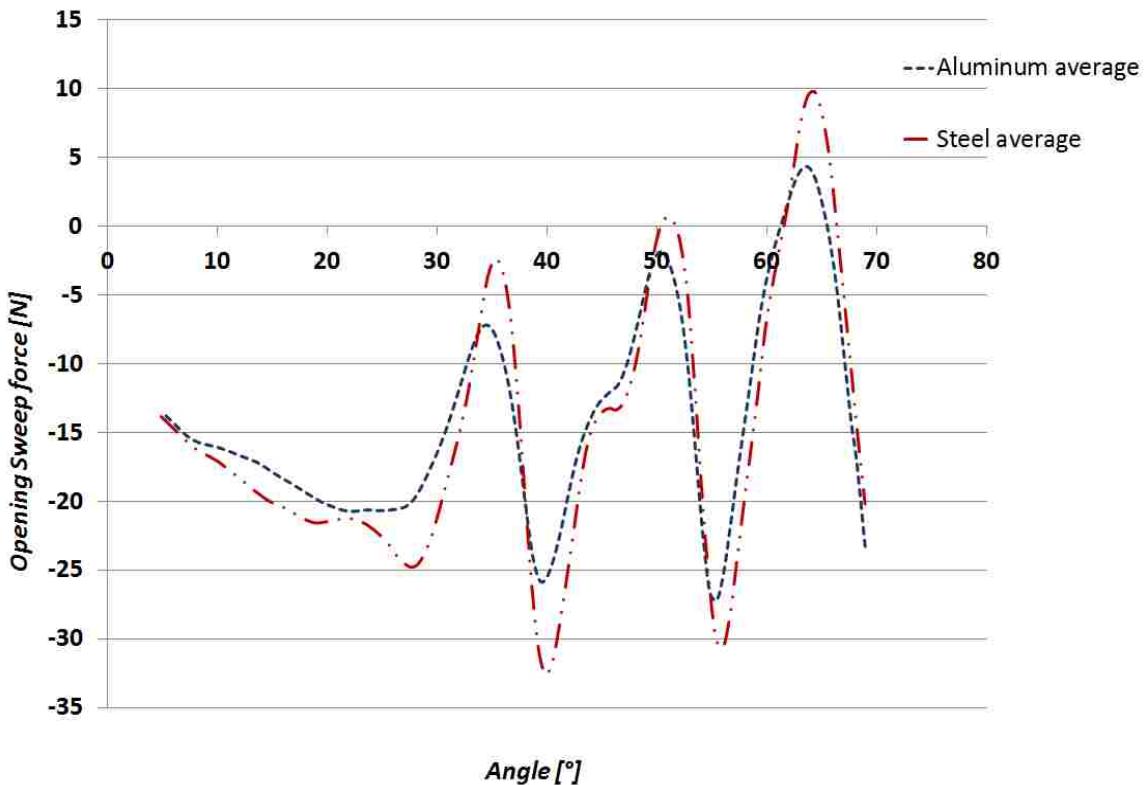
Figure 5-14: Average opening sweep forces.
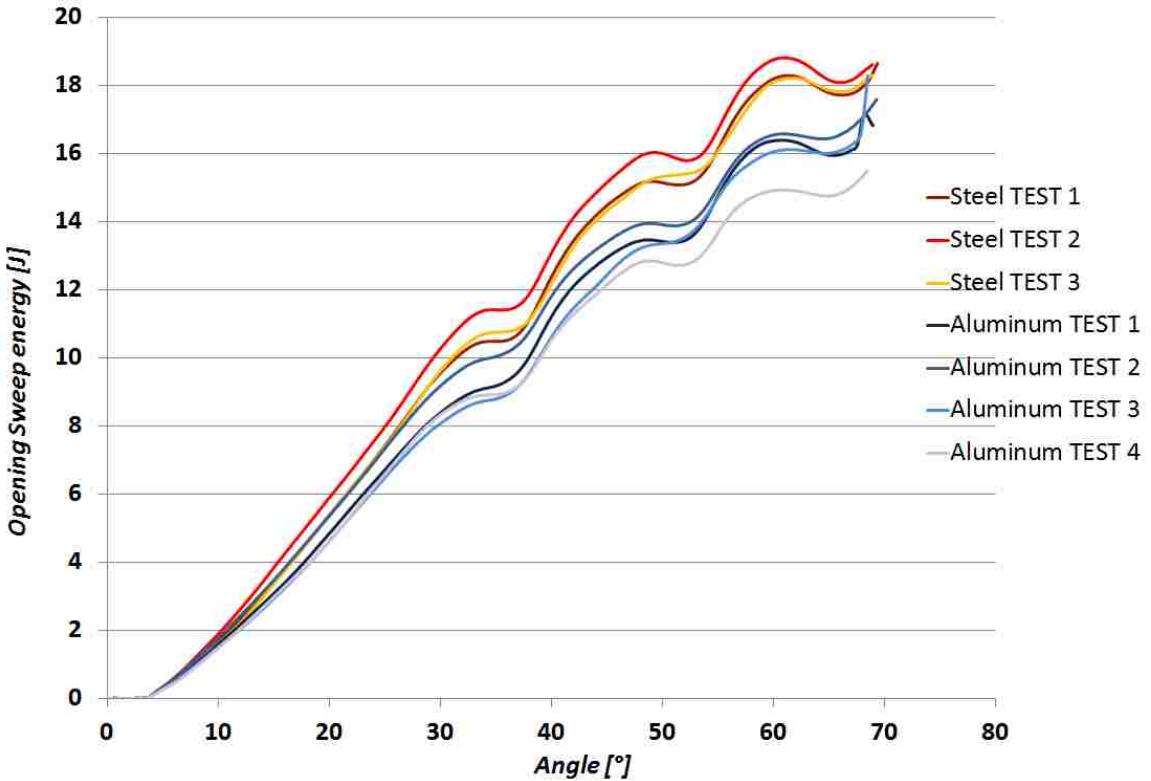
Figure 5-15: Aluminum vs. Steel Opening Sweep Energy comparison.

85
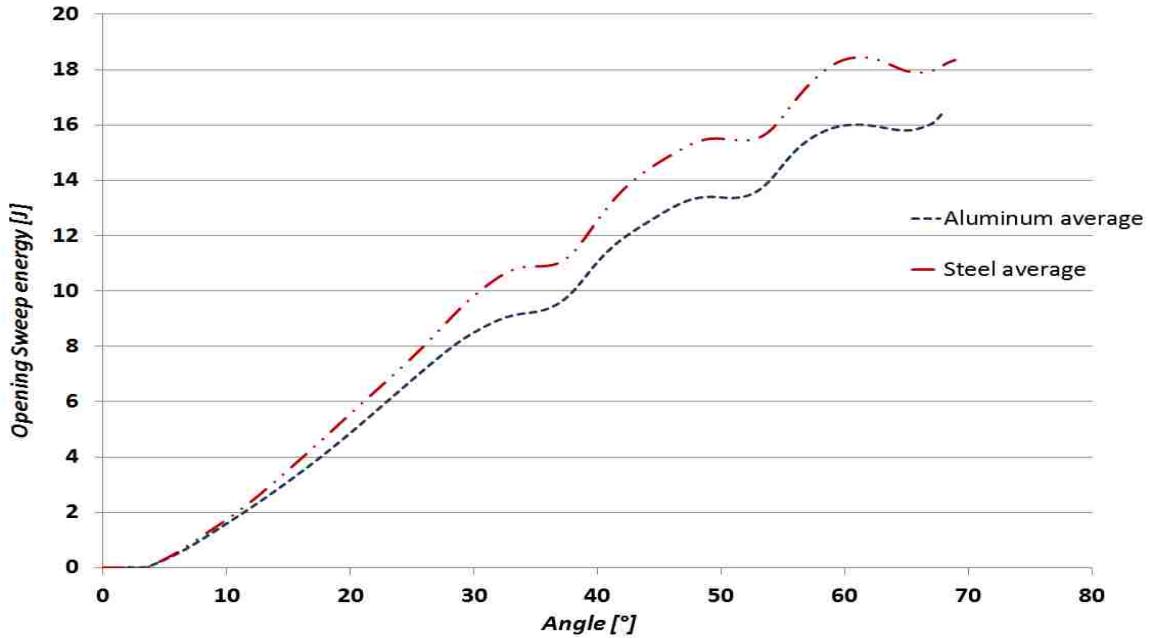
Figure 5-16: Average opening sweep energies.

To better assess the contribution of the check system alone, the component was tested at the check supplier's facility on a trace tester to obtain the Load vs. Angle curves. The machine used consisted of a light frame representing a door, driven by a motor at low constant speed and with negligible friction. The weight and center of gravity information were input to the machine to simulate the two doors, and the inclination of hinge axis was set as well, with the value relative to the real doors. A rotary potentiometer was used to measure the angle and a load cell to measure the force. This type of machine did mechanically what the EZ Slam user did manually during the opening and closing sweep tests.

Three configurations were tested:

- Frame without any weight and no hinge axis inclination (Flat Setup).
- Frame loaded with a weight equal to that of the steel door placed on the frame in a position representing the center of gravity of the real steel door (Steel Setup).
- Frame loaded with a weight equal to that of the aluminum door and placed on the frame in a position representing the center of gravity of the real aluminum door (Aluminum Setup).

86

In the last two configuration the hinge axis was tilted as in the real door tested with the EZ Slam. The closing and opening forces for the three configurations are shown in Figure 5-17 and Figure 5-18.
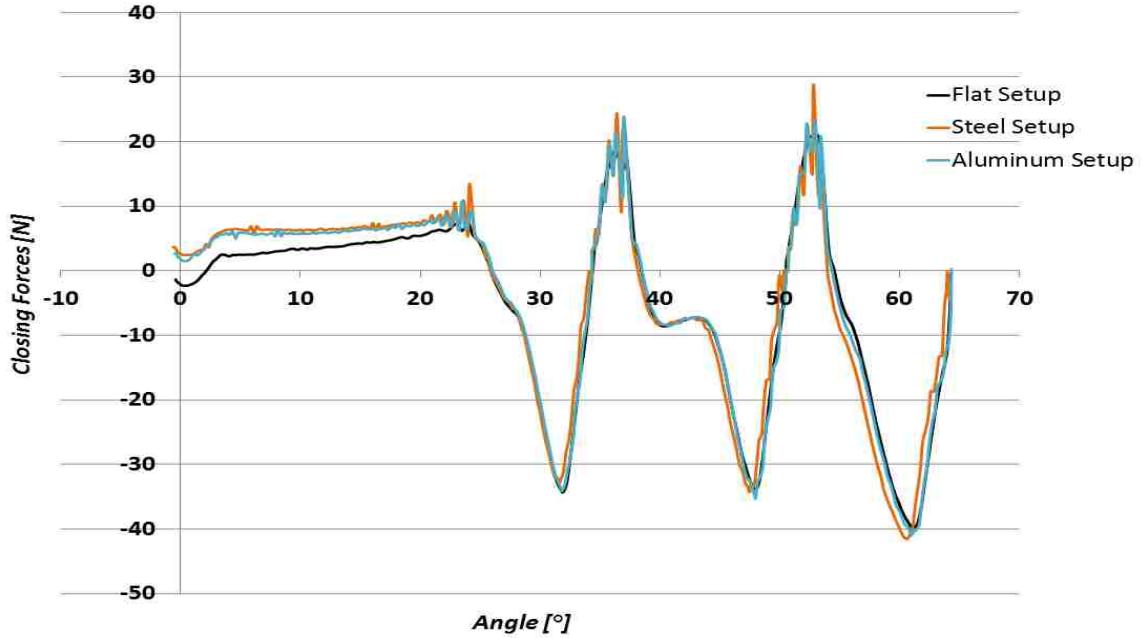
Figure 5-17: Production check closing force for the three configurations tested (Supplier tester).
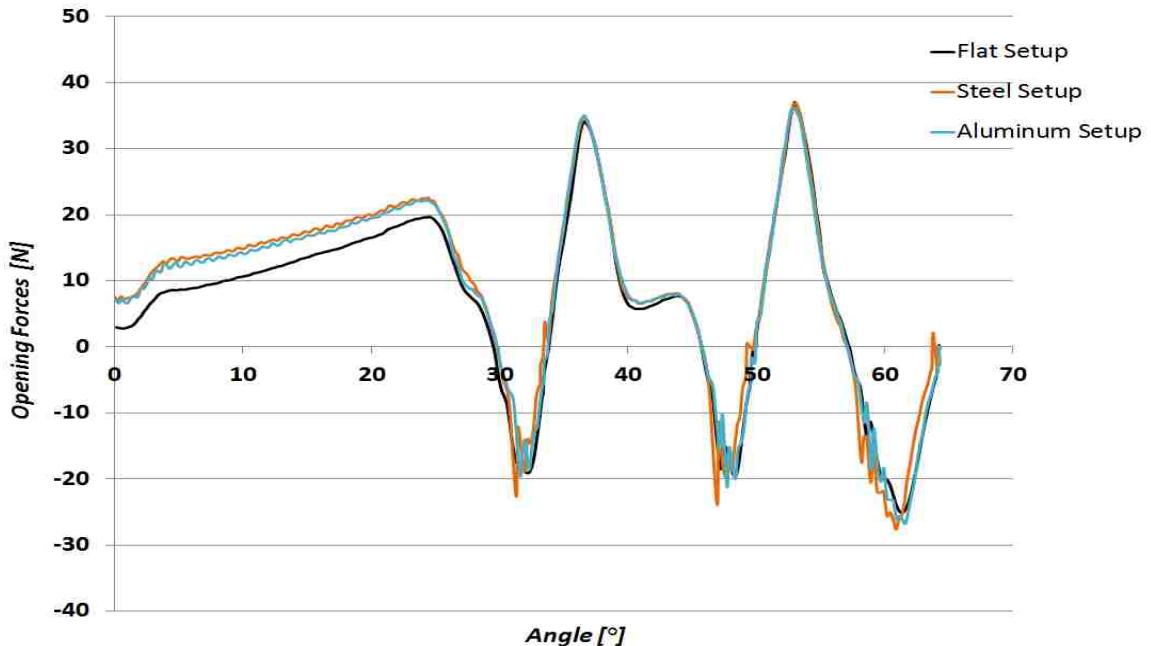
Figure 5-18: Production check opening force for the three configurations tested (Supplier tester).

For both the opening and closing actions of the three configurations tested the curves have the same shape throughout the entire swing of the door and the magnitude of the

forces matches for the three configurations from the fully open position up to an angle of around 25-30 degrees open. This angle represents the beginning of the last slope of the check profile where the difference in weight between the three configurations and the inclination of the hinge axis exhibit an effect on the check force. The curves relative to the steel and aluminum configurations match almost perfectly even if there is a significant difference in weight and center of gravity position between the two configurations. The opening and closing actions are directly compared in Figure 5-19. Since the weight of the door always acts in the same direction, the difference in force is given by the friction forces; in a frictionless system the two curves would look the same, however because of the friction at the check the opening and closing actions are different. During opening the friction is acting to hold the door closed, thus resulting in a higher curve, while during closing it is acting to hold the door open, resulting in a lower curve. It can be noticed that the curves of Figure 5-17, Figure 5-18 and Figure 5-19 are switched in sign with respect to the curves in Figure 5-9 and Figure 5-13; the reason is just a difference of convention between the two tests (trace tester and EZ Slam), but the meaning of the curves is the same.
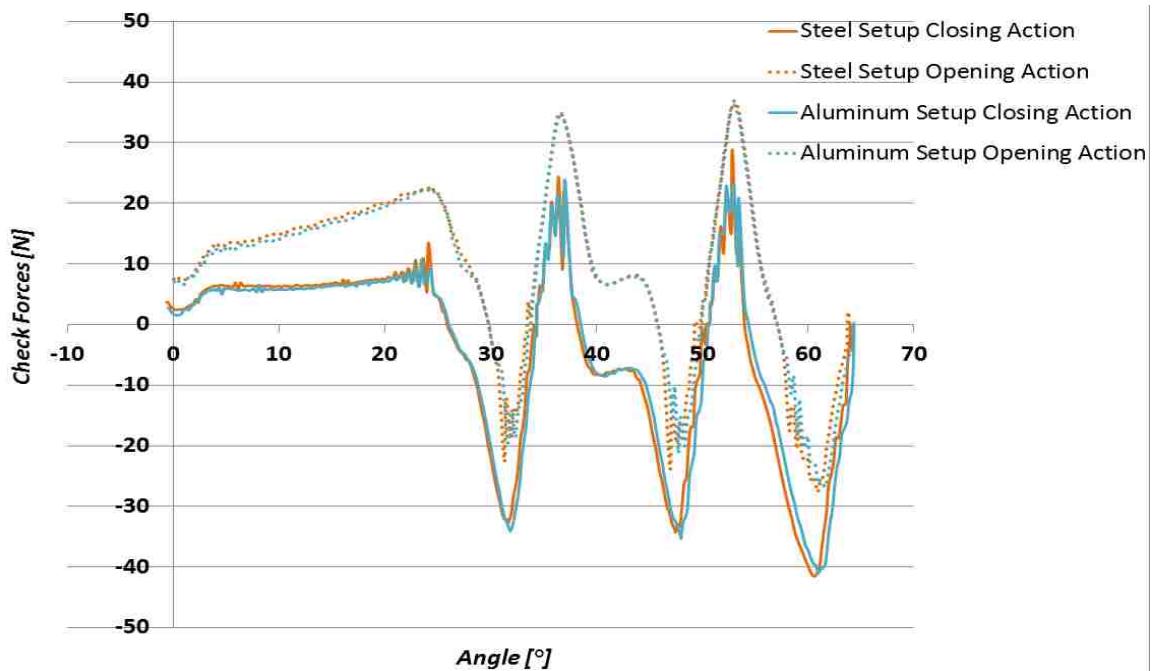
Figure 5-19: Opening and closing check forces comparison (Supplier tester). The force is expressed as a function of the opening angle.

The opening and closing force curves for the EZ Slam and the trace tester are compared in Figure 5-20. A difference in the magnitude of the forces can be noticed; the forces measured by the EZ Slam appear always smaller than the ones recorded by the trace tester. In particular the peaks of the forces measured by the tester are always higher, because the test was performed at very low and constant speed by the machine, while in the tests performed manually with the EZ Slam there was a damping effect given by the changes in speed during the tests, due to the difficulty of opening manually the door at a slow constant speed along the whole profile of the check. The plots of the energies are more similar because they represent the area under the curve that, being the force peaks greater for the tester measurements both in the negative and in the positive side, results to be quite similar.
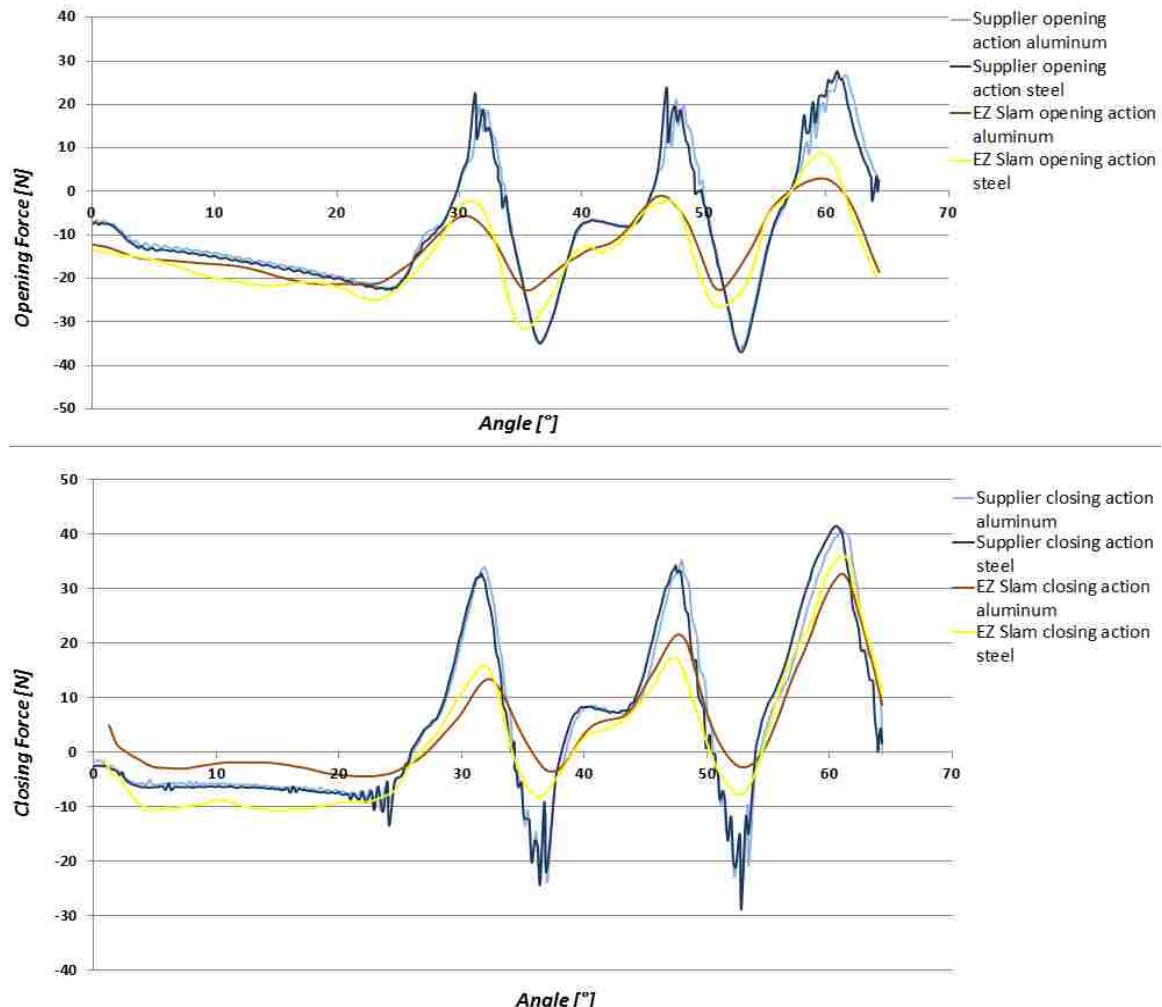
Figure 5-20: Trace tester vs. EZ slam forces comparison for opening and closing actions. The upper half of the graph is referred to the opening action, the lower half to the closing action.

89

The plots of the closing energies measured with the trace tester are shown in Figure 5-21. Comparing the orange and blue lines there is only a negligible difference between the energies (as was expected since the curves of the energy directly depend on the curves of the force) also in the initial 30 degrees of the plot, unlike the curves obtained with EZ Slam (Figure 5-11).

The results of the tests conducted with the trace tester showed that, when considering the static response of the check (very slow constant speed), in ideal conditions (no friction at the hinges), the weight and the position of the center of gravity don't affect strongly the forces exchanged with the door. On the contrary, as highlighted by the EZ Slam tests, when the real door system is considered, the action of the check system is no more independent from the type of door tested (steel or aluminum).
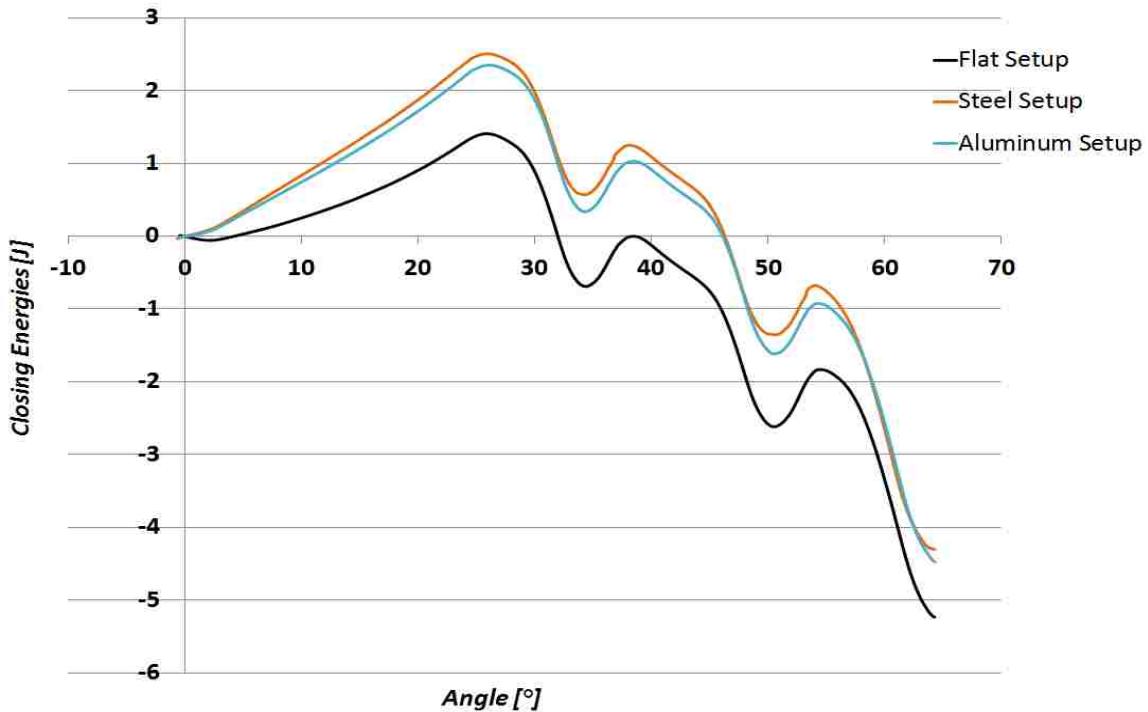
Figure 5-21: Closing energy for the three configurations tested (Supplier tester). The curves are obtained by numerical integration of the force curve starting from the fully closed position (at which point the check is not contributing any energy to closure).

In this non-ideal case three major aspects might have played a role in the difference between the performance of the two doors; the material properties (as for example door flexibility) were not taken into account in the supplier tests, because the frame used to simulate both aluminum and steel configurations was the same. Moreover the trace tester

90

frame and the real doors have different shape and geometry, and will therefore have different rigidity. Also a misalignment between the hinges and the check due to the remounting of the check on the body after having placed the aluminum door might be responsible for part of the difference in the EZ Slam tests (Figure 5-11 and Figure 5-12). The graphs in Figure 5-22 and Figure 5-23 directly compare the results obtained with the supplier's tester with the steel and aluminum configurations and the EZ Slam equipment on the real steel and aluminum doors.
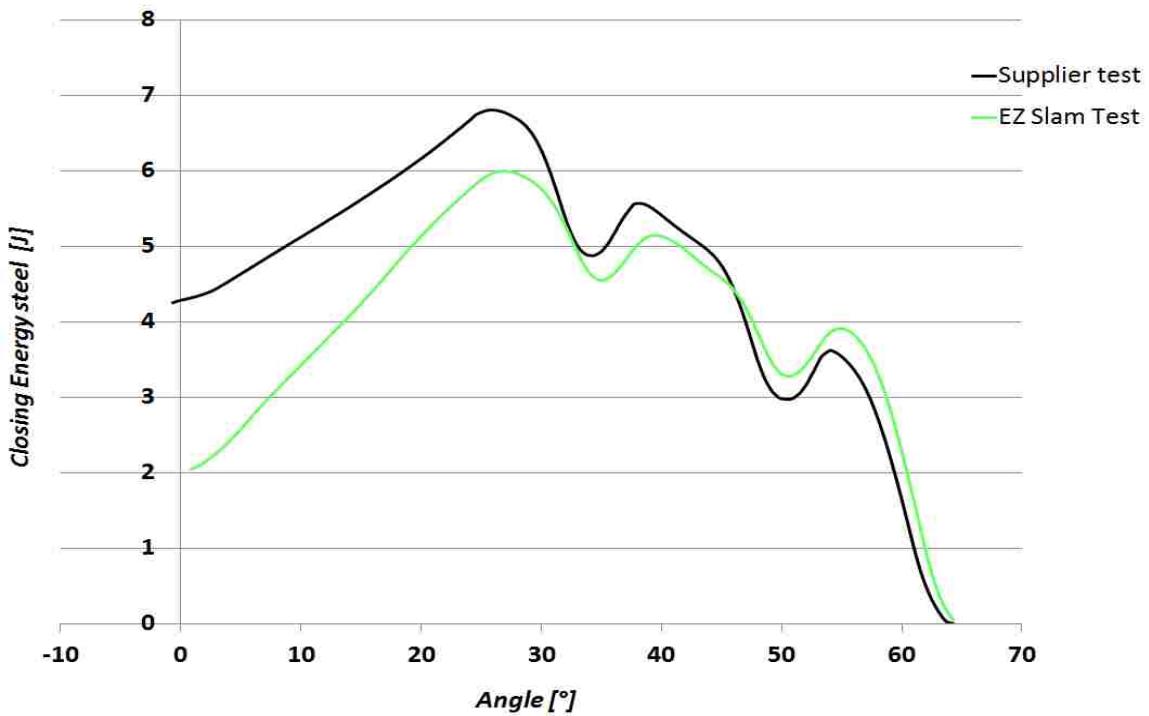
Figure 5-22: Closing energies comparison between the Supplier's tester measurements on the steel door setup and the EZ Slam measurement on the steel door.

It is possible to notice a greater similarity between the curves shown in Figure 5-23. This can be due to the fact that both the frame of the trace tester and the door were of the same material. It must also be pointed out that the EZ Slam tests, since they were performed manually in a well defined time window, were done at a greater speed; this might mean that increasing the speed of closure of the door, and so going into the "dynamics domain", the influence of weight and center of gravity position may increase.

As it can be seen, the same type of energy (closing sweep energy) is displayed differently in the graph of Figure 5-21; to be able to make a direct comparison with the EZ Slam graphs, the closing energies relative to the tests performed with the supplier's trace tester

have been recalculated with the numerical integration method on MS Excel, directly from the Force vs. Angle curves shown in Figure 5-19, and integrating from the fully open angle to the closed position.
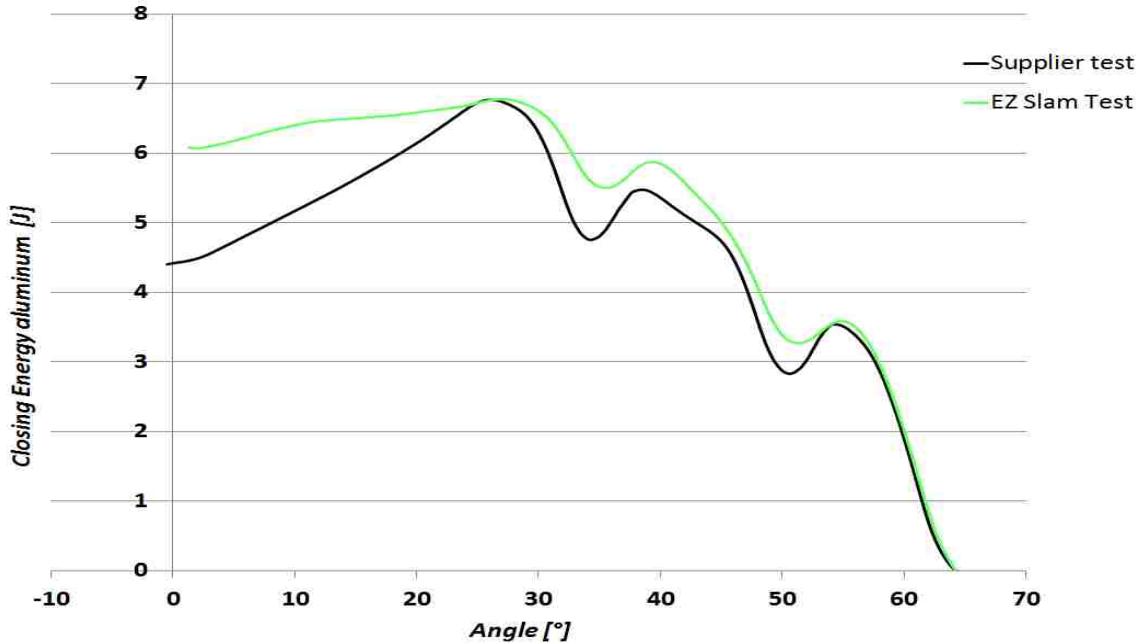
Figure 5-23: Closing energy comparison between the Supplier's tester measurements on the aluminum door setup and the EZ Slam measurement on the aluminum door.
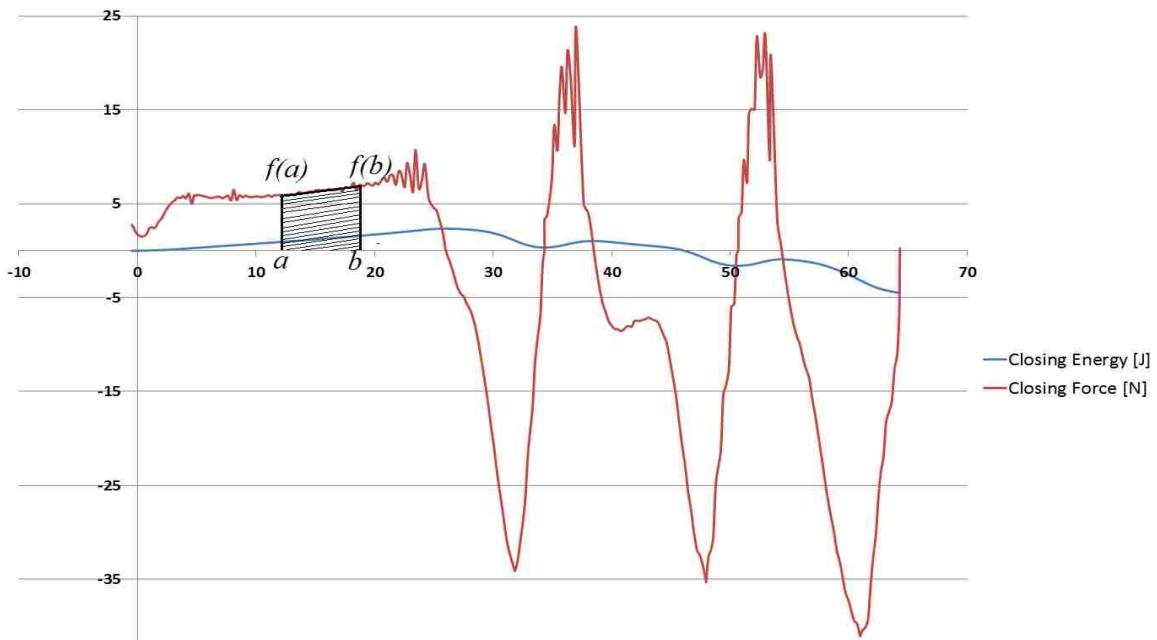
Figure 5-24: Closing force and closing energy for the flat check configuration The energy is the integral of the force.

The angles have been first converted in linear distance to calculate the energy. The numerical integration is the area under the curve. As shown in the example given in Figure 5-24, the method estimates the area under the curve using multiple trapezoidal elements, each of area:

$$A = (b - a) * \left(\frac{f(a) + f(b)}{2} \right) \qquad (5.1)$$

The elements are then summed one after the other obtaining the final shape of the curve. This method is an approximation, but the smaller the intervals are between points a and b, the more precise will be the calculation of the area.

Performing the integration of the force from 0 to full open angle, the energy curves will be of the type shown in Figure 5-21, while integrating from full open angle to 0 (always with the conversion to linear distance) the energy curves will look like those in Figure 5-11 (for the closing action).

The energy curves obtained with the EZ Slam have also been shifted, (see Figure 5-22), toward the left by approximately 3 degrees to make up for the fact that the EZ Slam closing sweep tests stop when a nearly closed (and not fully closed) position is reached, and to have the fully open angles coincidents in the two cases shown. The opening energies recorded by the tester and by the EZ Slam are shown in Figure 5-25.
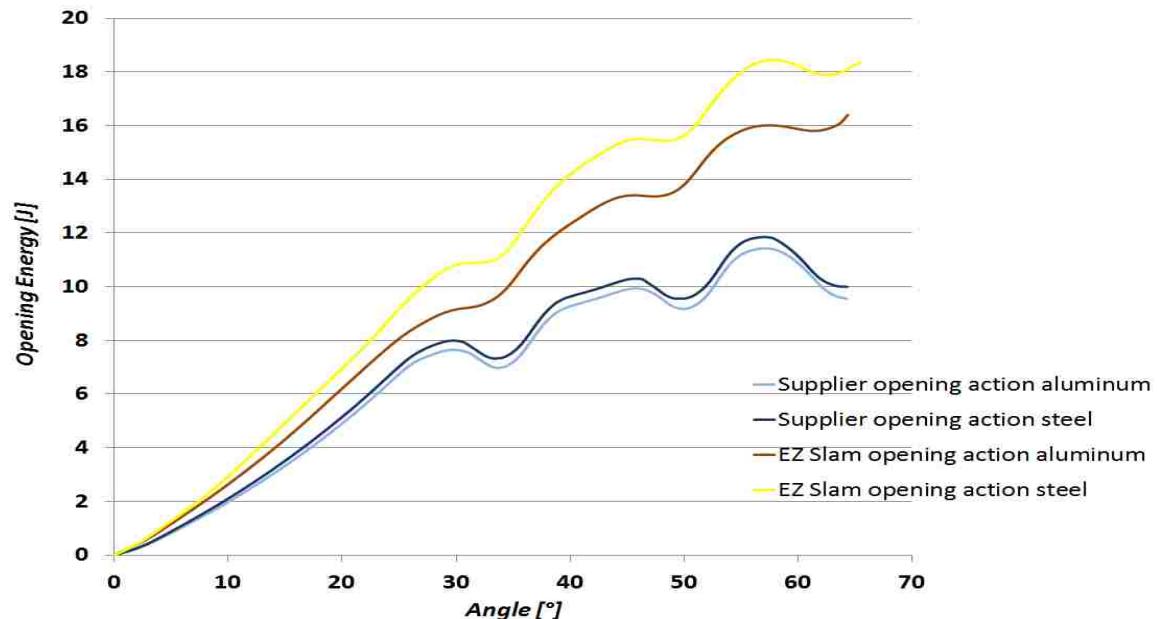
Figure 5-25: Trace tester vs. EZ slam opening energy comparison. The curves of the energy derive once more from the force curves.

The energy recorded by the EZ Slam is higher both for the steel and the aluminum case, but it must be recalled that the trace tester measures the energies in ideal conditions, including also the almost total absence of friction at the hinges, while the EZ Slam measures the energies coming from the real door system. The friction at the hinges of the door will cause a greater energy loss, in particular during opening when the inclination of the hinge axis acts against door motion. A good way to assess the effect of the difference in flexibility, or of other parameters related to the type of material, would be to test actual doors on the trace tester of the supplier and compare the results.

Amongst the energy sinking contributions, the air bind effect proved to have a significant influence on door closing effort; the pressure rise inside the cabin depends on the geometric characteristics of the door and of the cabin (door area, HVAC system area, cabin volume and ratio between cabin volume and door area). All of these parameters were left unchanged in the tests performed on the two different doors as the vehicle tested was exactly the same and the door geometric dimensions were the same even though the frame material changed. However, the energy sink due to air bind was 51% greater in the case of aluminum. The rise of pressure in the cabin is directly measured by the cabin unit at the level of the driver's seat, and depends also on door closing speed, increasing with the increase of this parameter. However the value of the pressure detected is not directly used for the calculation of the air bind energy sink but gives the trend of the pressure as a function of time. The pressure wave propagation inside the cabin is a dynamic event, the pressure that will act as an opposing force to closure should be measured at the door level. The minimum closing speed necessary to reach a fully latched position of the aluminum door was, as said before, around 50% faster than the speed necessary to close the steel door (Figure 5-5), so also was the level of pressure rise inside the cabin as shown in Figure 5-26 and Figure 5-27; this caused the larger value of air bind sink. The curves show the rapid increase in cabin pressure at the beginning of the contact between the door and the seals. As the area through which the air can escape from the cabin decreases due to the contact with the seals, the pressure rises. The peak pressure is reached in correspondence of the maximum overslam, after which it is possible to notice a slight depression due to the repositioning of the door in the rest position. The correlation between the closing speed and the pressure rise in the cabin can be understood

considering that the faster the door closes and the less time the air has to escape from the vent areas, thus being compressed in the cabin. This result can also be found from the outputs of the slam test; looking at the trend of the pressure inside the cabin as a function of the overslam, presented in Figure 5-28 and Figure 5-29.
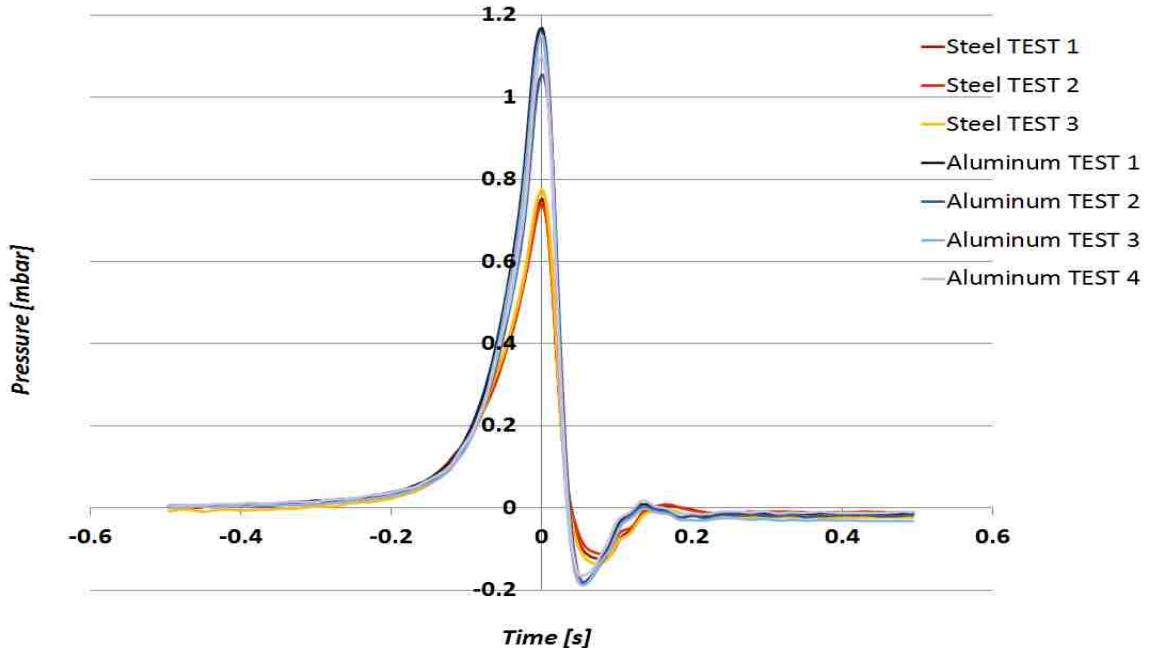
Figure 5-26: Pressure rise inside the cabin in function of Time. The peak of the curve is reached at time 0 when the door is fully closed and at maximum overslam.
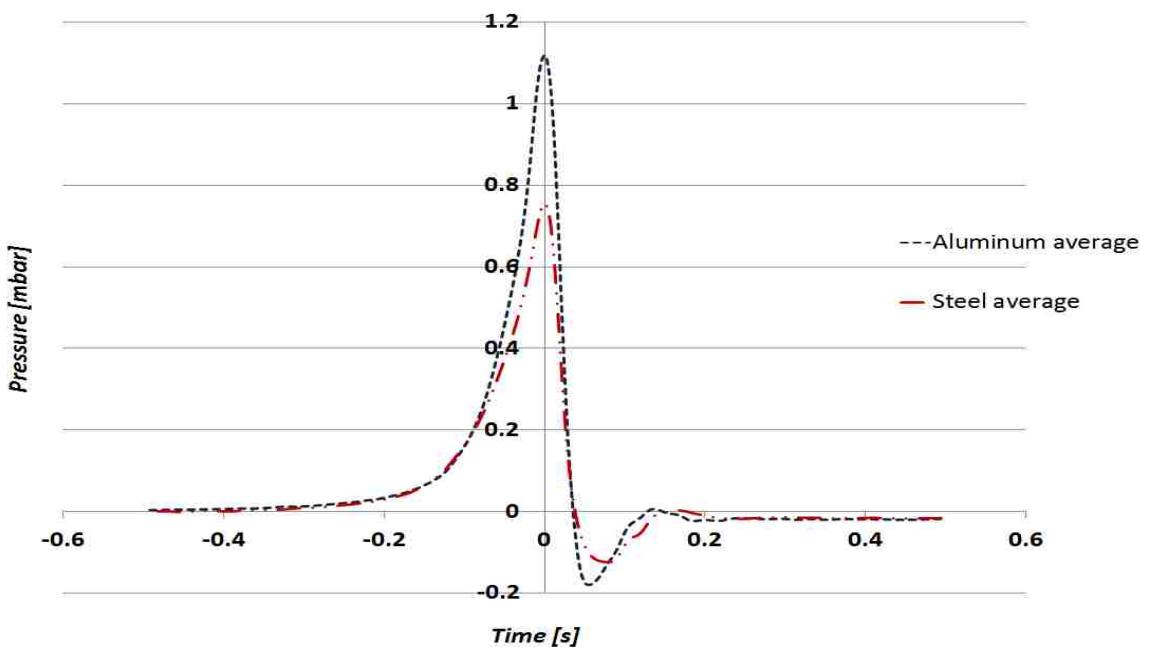
Figure 5-27: Average pressure rise in the cabin.

A test to verify if the cabin pressure peak can be considered constant throughout the cabin would be to perform the tests placing the pressure sensor, for example, on the back seats and watching the pressure rise results.
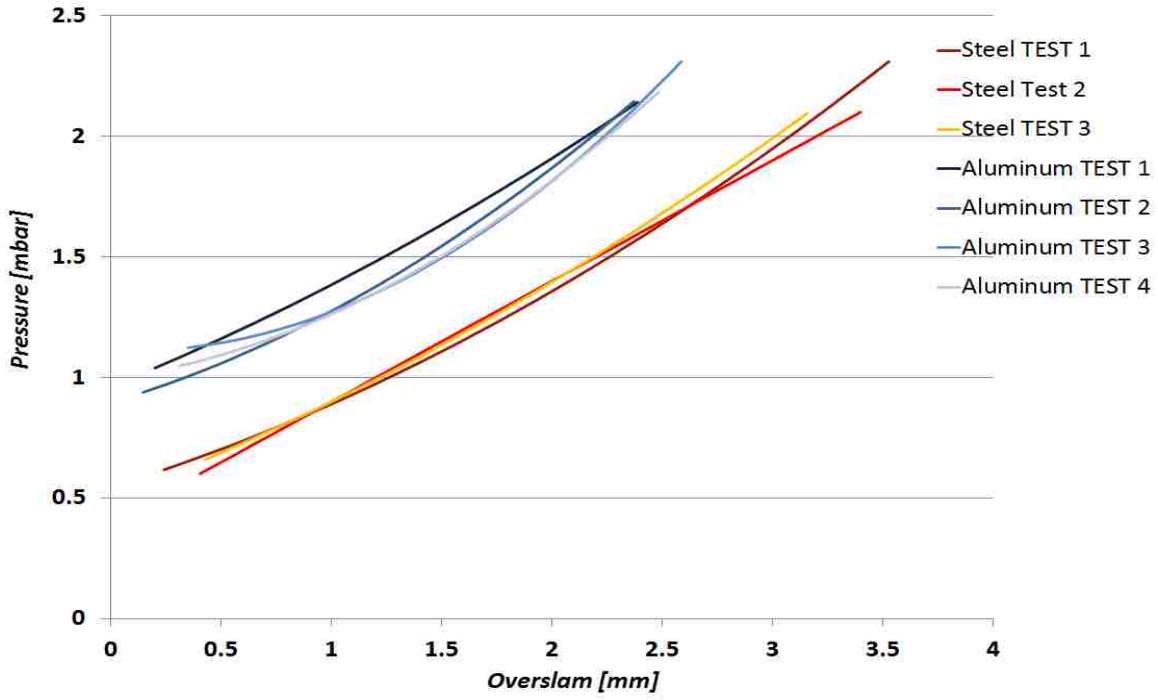
Figure 5-28: Pressure vs. Overslam trend for Steel vs. Aluminum comparison. The pressure is greater, for the same value of overslam, for all the aluminum tests as opposed to the steel tests.
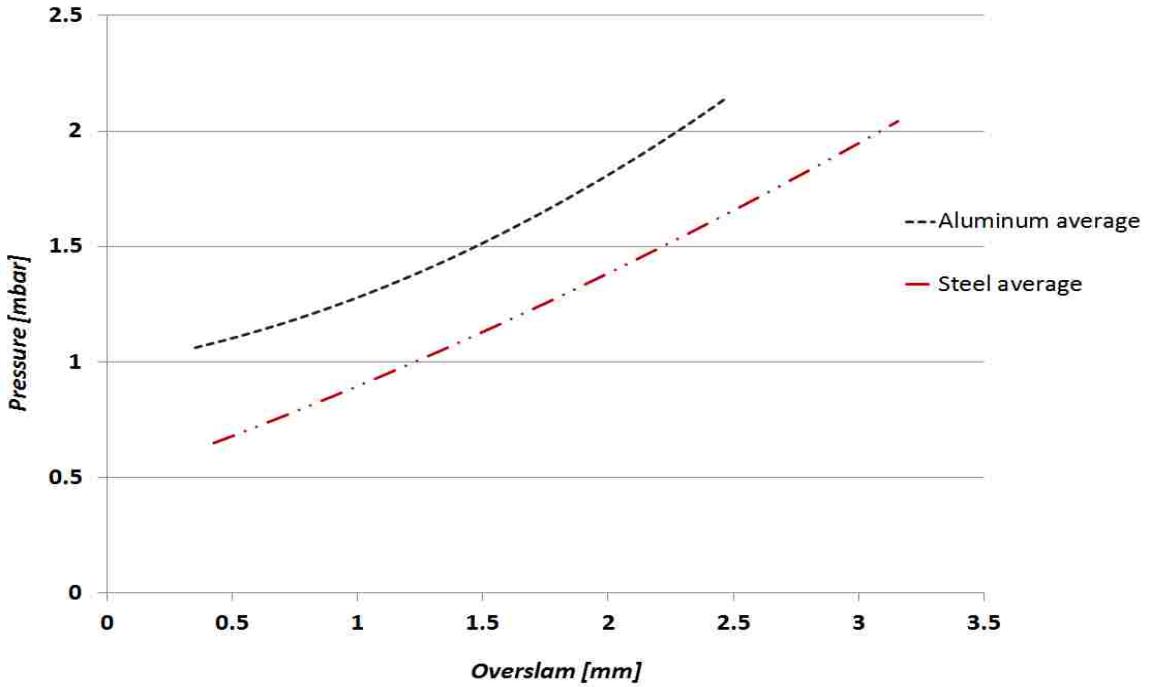
Figure 5-29: Average pressure vs. overslam curves.

It is clear that the pressure rise increases with increasing values of the overslam. This quantity, as shown in Figure 5-30 and Figure 5-31, is dependent on speed: the greater the closing speed, the greater the overslam recorded.
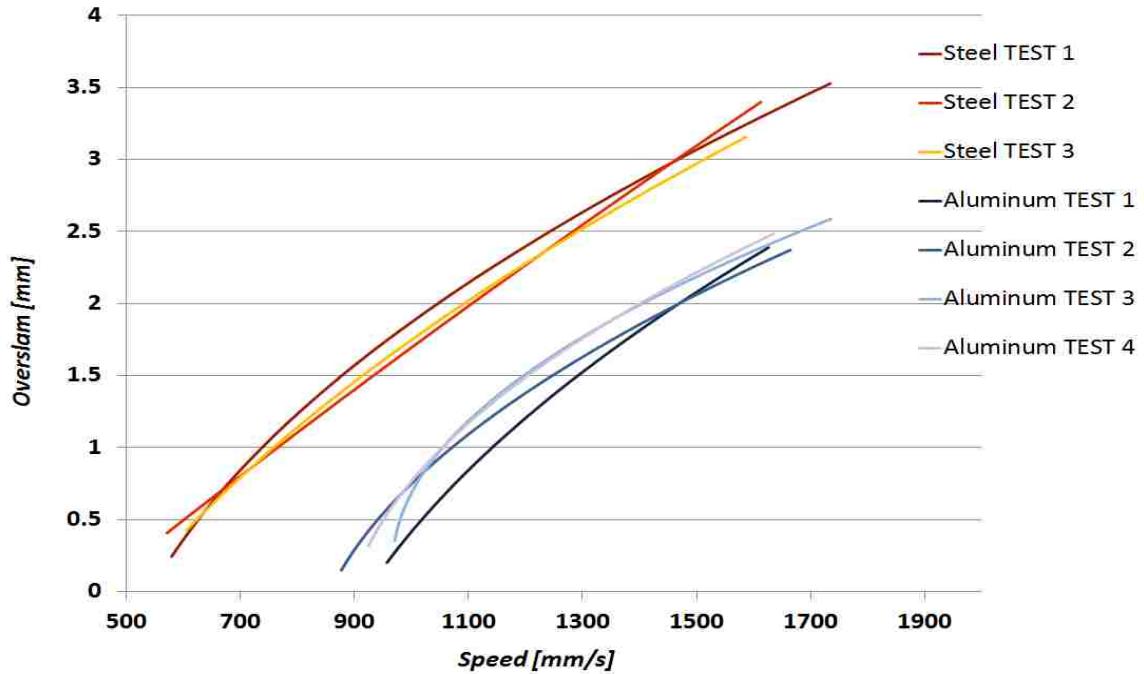
Figure 5-30: Value of the overslam as a function of the closing speed for the steel and aluminum tests. The same overslam was reached by the aluminum door with an higher speed.
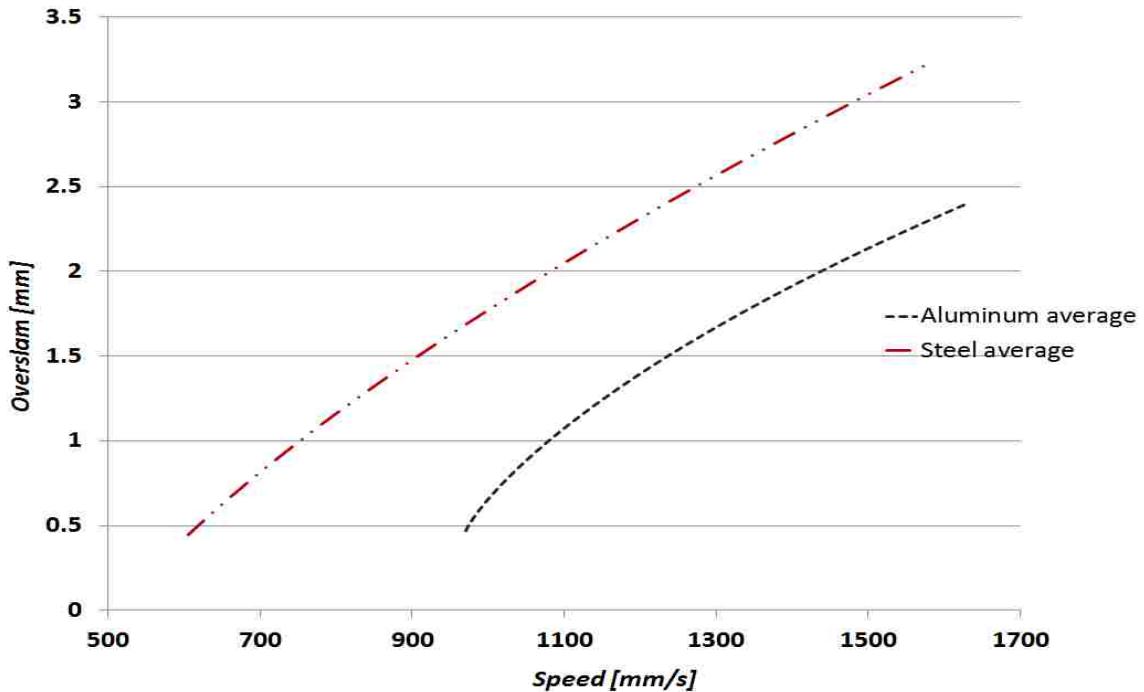
Figure 5-31: Average overslam vs. speed curves.

The plots presented above are the same type of plot shown in paragraph 4.1.2.4; the single runs are not shown but just the best fitting lines of each of the tests used to obtain the average values used in the discussion of the results. Another consideration on the air bind contribution is that, since the weight and the inertia of the aluminum door were lower than those of the steel door, the opposing action of air bind had more of an effect in the aluminum case (14.6% instead of 9.95% of the total energy sunk).
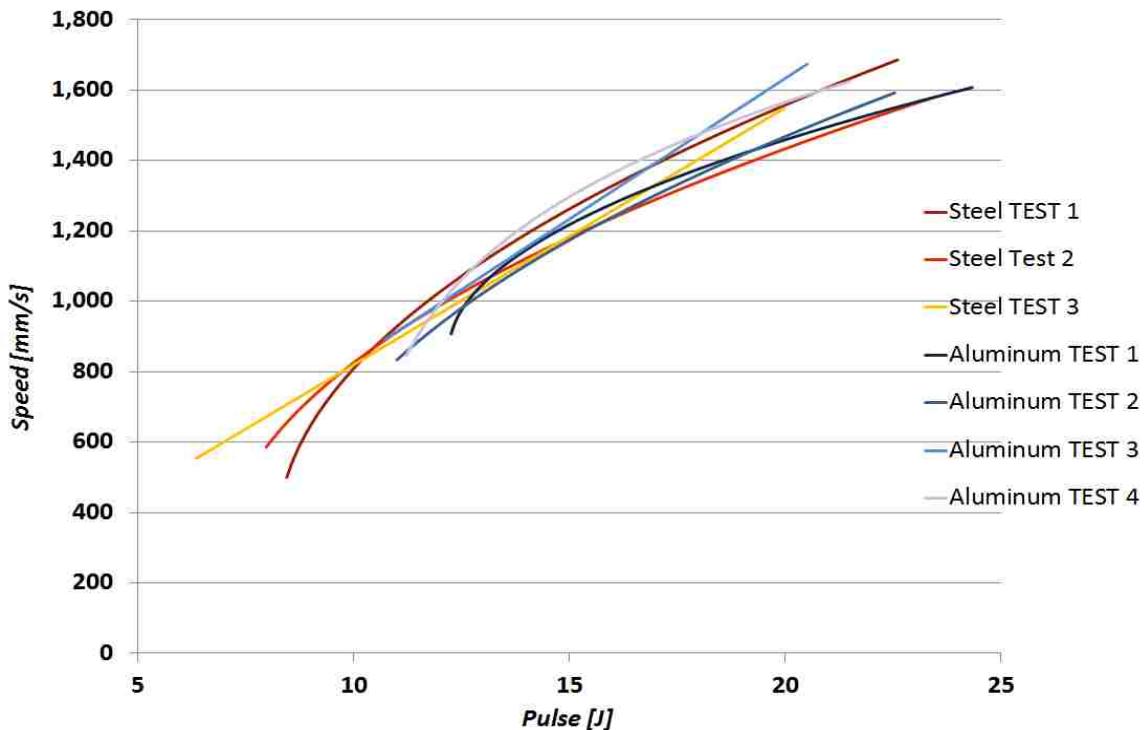
Figure 5-32: Speed vs. Pulse comparison graph for steel and aluminum.

From the graph in Figure 5-32 and Figure 5-33 it is possible to see how the velocities reached by the steel and the aluminum doors at closure for a certain input pulse given by the user were very similar; however, in order to reach a complete latching of the aluminum door a greater input by the user was needed. Finding a way to reduce the minimum closing speed would also have a positive effect from the energy perspective as it would mean lowering the air bind contribution to the effort.

From the quasi-static push test it is possible to evaluate what is the minimum overslam necessary to fully latch the door; Figure 5-30 shows that, when closing the aluminum door, to reach a given value of overslam the necessary speed is much greater. This is probably due once more to the lower inertia of the lighter aluminum door. As suggested

in [16] a possible solution to increment the contribution of the weight during closure without incrementing the mass of the door might be to shift the center of gravity position further from the hinge axis, changing the weight distribution of the door.
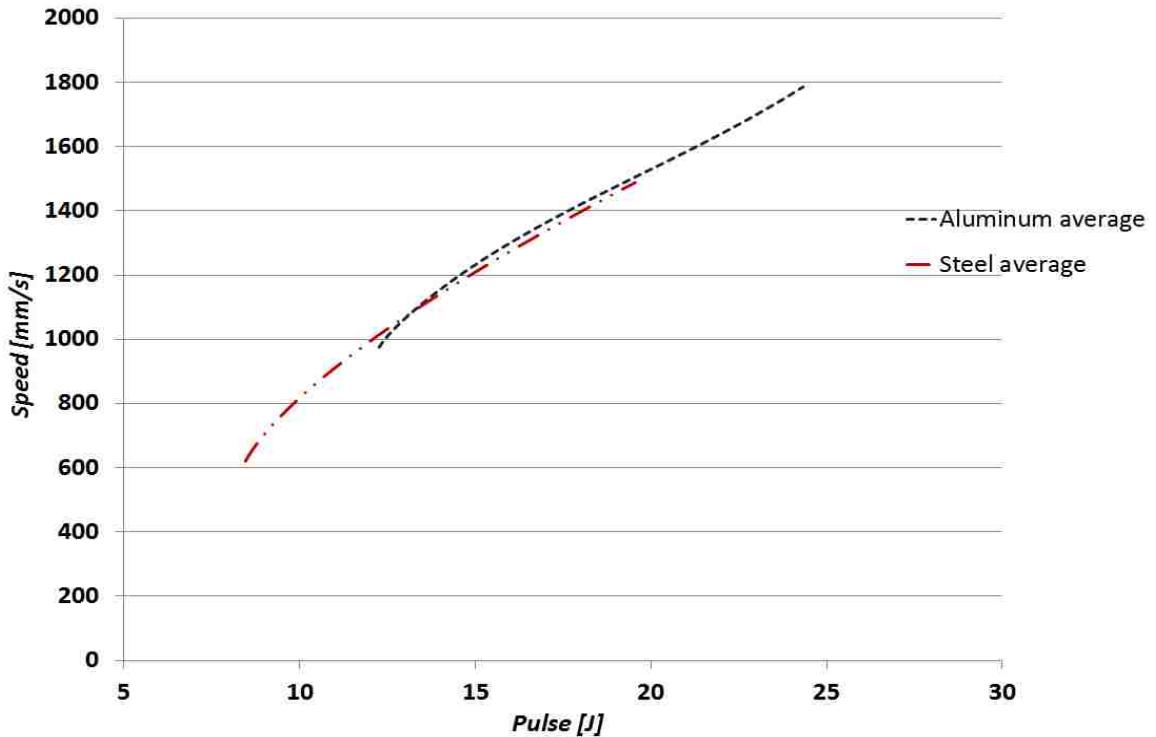
Figure 5-33: Average speed vs. pulse curves.

The center of gravity of the aluminum door was situated further from the hinges and in a slightly higher position with respect to the steel door. However, due to the complexity of the door's inner structure and all the components included, the distribution of the weights in the door represents a delicate matter to deal with.

The energy loss due to static compression (the reaction of the seals to the compression during the last few millimeters of closure from when contact starts taking place), consistently represented the smallest contribution to door closing effort. This value depends on the seals and on the seal gaps; the seals used in the two cases were exactly the same and the seal gaps, as highlighted before, were reasonably close (11% maximum deviation). The value of energy loss due to static compression almost doubled for the aluminum door when compared to the value recorded for the steel door, as shown in Figure 5-34 and Figure 5-35. Such a difference between the two tests cannot be justified by the sole difference in seal gaps, but the explanation must be found in a somewhat

different geometry of the aluminum frame with respect to the steel frame that caused greater compression of the seals from the aluminum door.
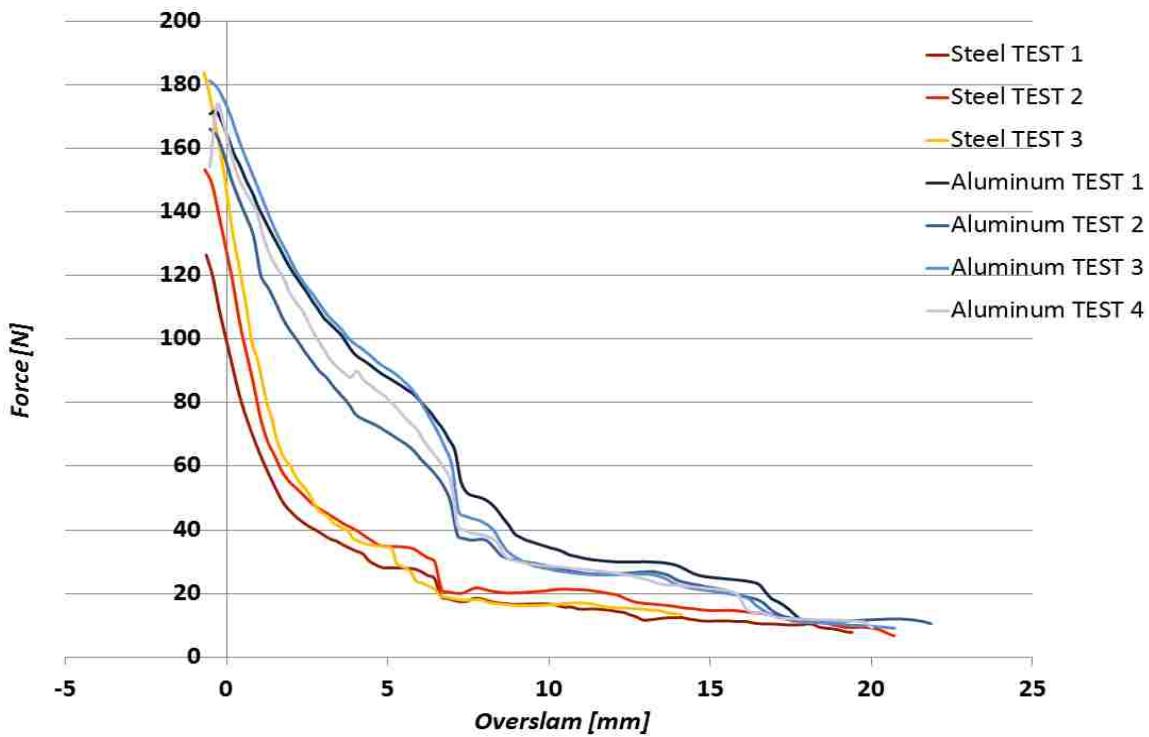
Figure 5-34: Static compression load curves for the steel and the aluminum doors tests.
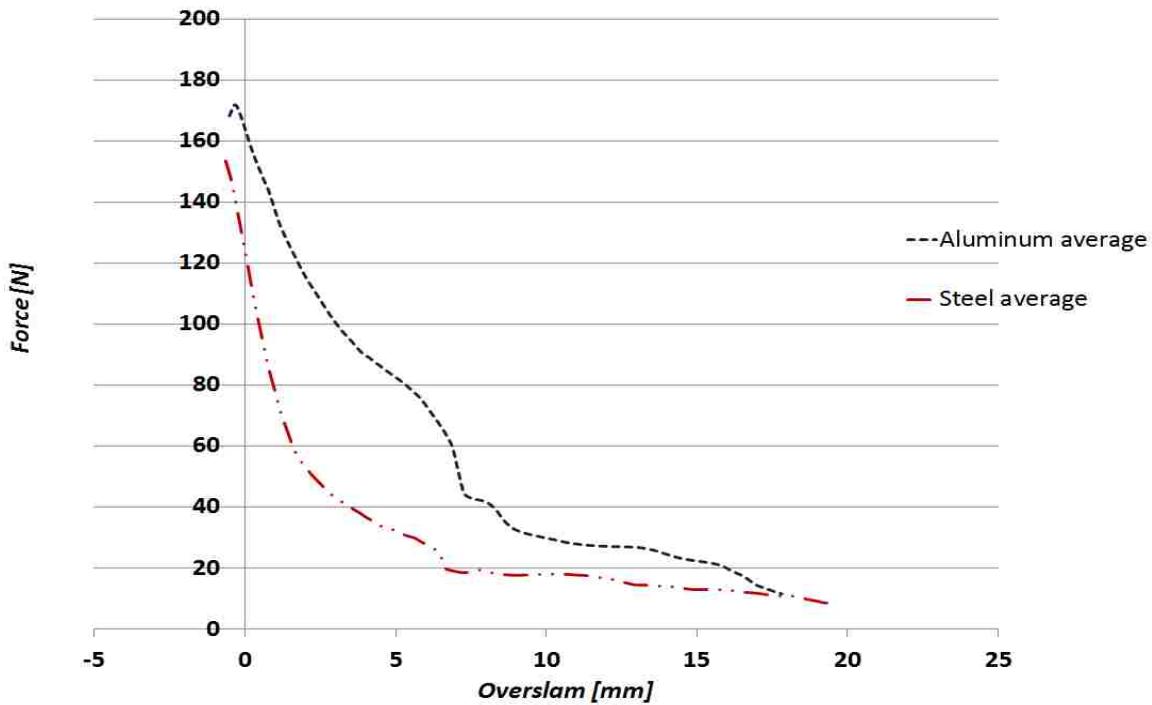
Figure 5-35: Average static compression load curves.

100

However, as pointed out before, the influence of the seals on the door closing effort is small as it only accounted for 3.3% and 6.4% of the total energy adsorbed in the closure for the steel and aluminum doors, respectively.

Even though, as mentioned before, the total energy required to shut the aluminum and steel door was within 5%, the tests highlighted how the quantity of energy to close the door that is required by the user is 42% greater in the aluminum case. This decrease in performance represents a major problem since the amount of energy required by the customer to close the door has a great influence on customers' impression about the quality of the door. Too big of an effort by the user therefore needs to be avoided. The input given by the user resulted in 51% and 69.4% of the respective total energies to close for steel and aluminum. This means that the positive contributions given by other factors (weight of the door, spring) in the aluminum case are lower. Looking at the trend of the curves of user input versus closing speed (Figure 5-32), a minimum necessary user input corresponds to a minimum necessary closing speed.

The greater flexibility of the aluminum frame needs to be considered because the door frame will bend more, when operated by the user, thus absorbing more energy. All the energy that is absorbed by the frame is not used by the door to close. In the steel case 41% of the energy to close was given by the spring of the check system and the last 8% of energy was provided by the weight of the door that, thanks to the inclination of the hinge axis, pulls the door towards the cabin helping the closure. Analyzing the closure event of the aluminum door, the spring and the weight contributed only 24.3% and 6.3%, respectively, of the necessary energy. The change in weight contribution (that becomes lower for the aluminum door) is obvious, because the aluminum frame weighs much less than the steel frame. However, the variation in energy provided by the weight was lower than expected.

The value of the contribution of weight in the steel case is just 16.5% greater than the value relative to the aluminum case. This can be explained with the fact that the weight energy contribution is based on the door rise value, in other words, on the total vertical displacement of the center of mass of the door during the entire swing of the door from fully open to fully closed. From the tests performed, the door rise was within 11% for the two cases. Moreover the absolute value of the door rise was very small (9.647 mm and

10.673 mm respectively for the steel and for the aluminum door) and so the overall weight contribution is small and does not change much even if the weight between the two doors is very different. Such a small value for the door rise is not common but it depends on the configuration of the door; increasing the value of door rise would therefore allow a greater help of the door's weight during closure.

In Figure 5-36 and Figure 5-37 the graphs of door rise for the aluminum and steel door tests are presented. The ideal door rise profile would see a constant decrease in the height of the center of gravity of the door in order to have a positive contribution given by the weight for the whole swing of the door from fully open to latched; however, from the graph it can be seen how, in the case of the door tested, the maximum height of the center of gravity is at around 45 degrees from closure instead of at the fully open position.

From the point of maximum height to fully closed, the Δh of the centre of gravity is negative, so the weight will pull the door towards the cabin assisting closure. The value of door rise also depends on the door opening angle which depends in turn on the door hinges and on the door check system (both kept the same for the two doors tested).
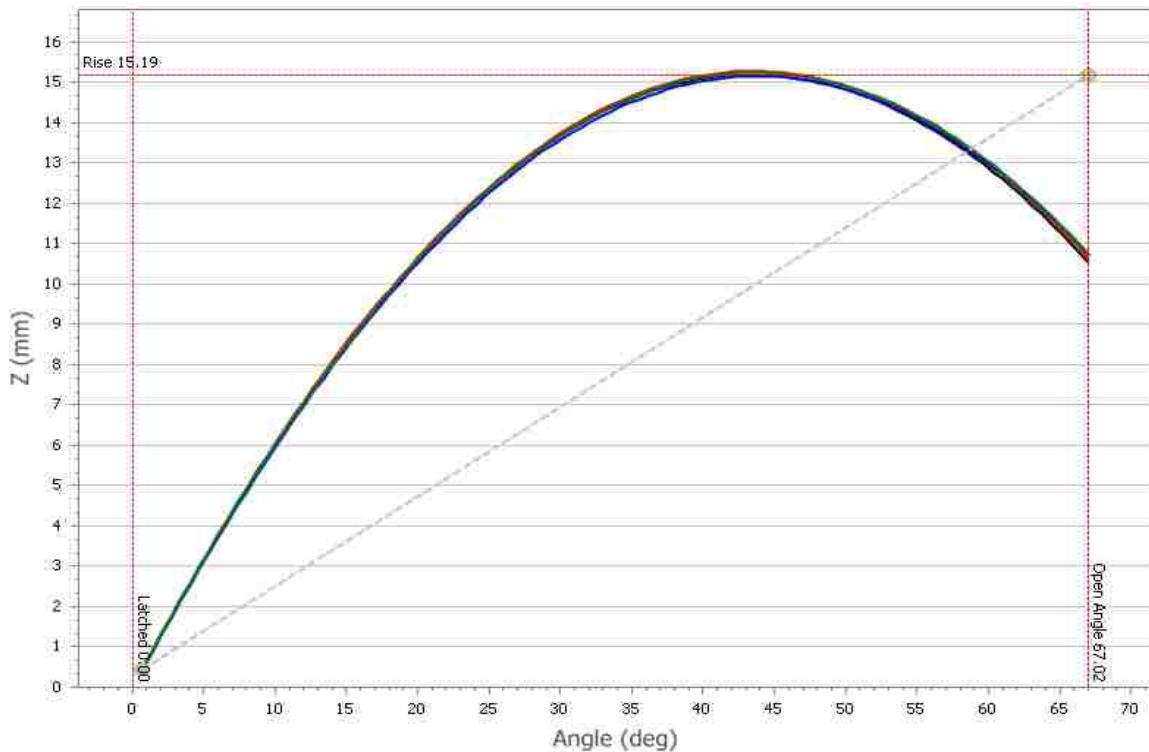
Figure 5-36: Door rise of the aluminum door during the closing event.
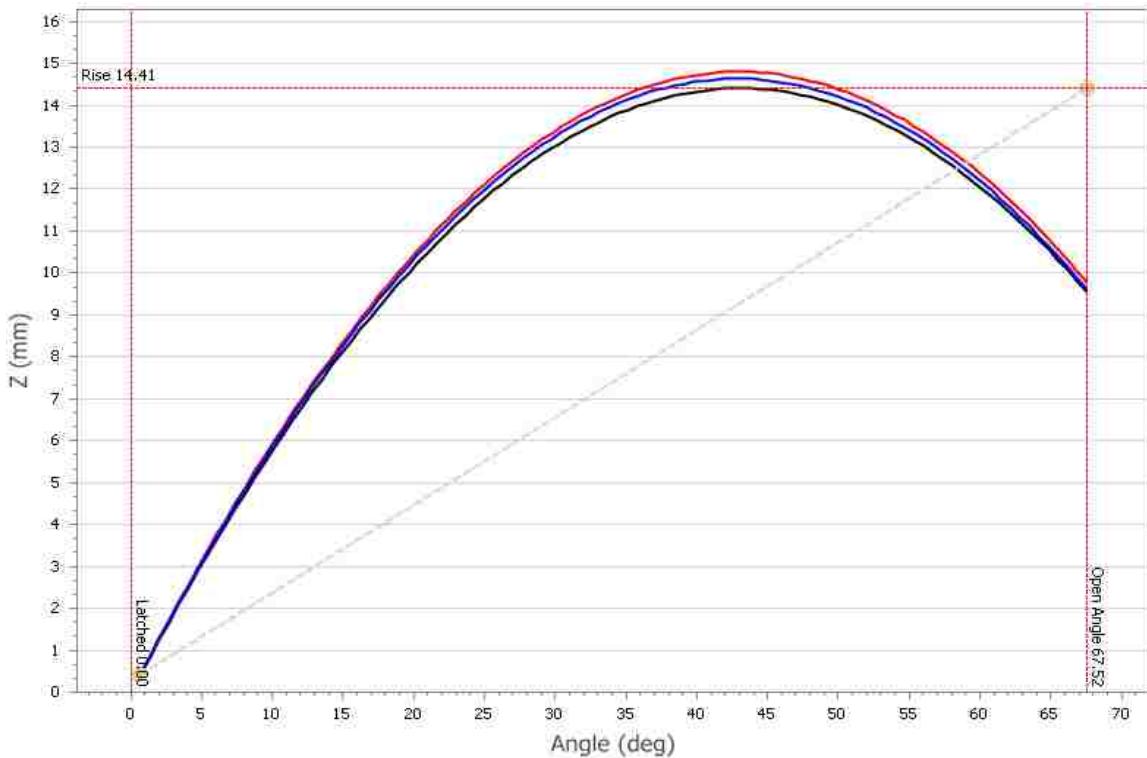
Figure 5-37: Door rise of the steel door during the closing event.

With regard to the positive spring contribution from the tests, a difference of -37.6% in the energy provided was recorded for the aluminum door. Based on the considerations done so far on the three contributors that bring the door to closure, the decrease in spring energy represents a crucial factor. As we saw from Table 5-2 the total energy to be provided to the two doors to reach a complete closure is very similar, but in the closing of the steel door the spring effect assisted much more than in the closing process of the aluminum door. Therefore the difference in spring energy had to be covered by a greater input by the user. From the analysis of the behavior of the check strap in response to the change of weight and material, the mass and the center of gravity position of the door don't appear to cause significant changes in the check forces and energies exchanged with the door in the static range (as shown by the tests conducted with the trace tester) but the change in material seems to have an effect in the last 30 degrees of closure of the door (as shown from the tests conducted with the EZ Slam). As a general means of comparison, the quality index assigned by the EZ Slam to both doors is shown in Figure 5-38 and Figure 5-39.
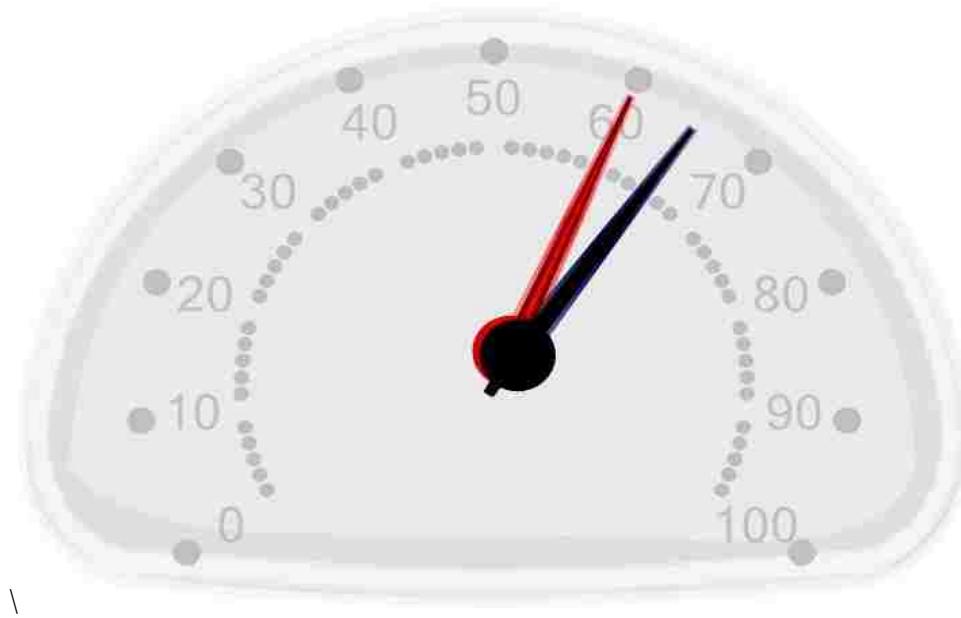
Figure 5-38: EZ Slam quality index of the three steel door tests. Black: steel test 1, Red: steel test 2 and Blue: steel test 3.
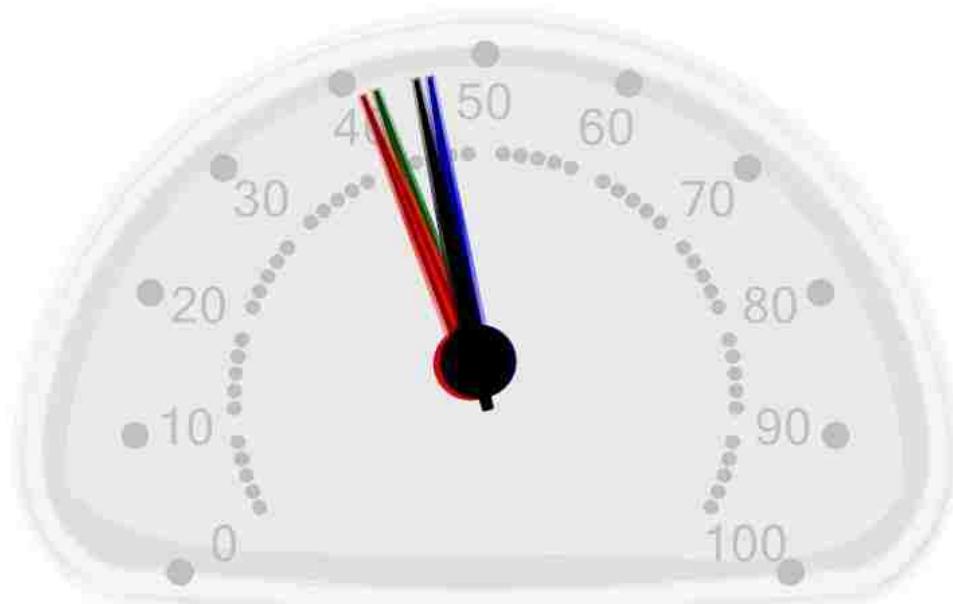
Figure 5-39: EZ Slam quality index for the four aluminum door tests. Black: aluminum test 1, Red: aluminum test 2, Blue: aluminum test 3, Green: aluminum test 4.

5.2.2 `OU Model comparison analysis

In this section the results obtained running the OU model with the steel door and aluminum door data are presented and compared to each other as well as with the EZ Slam testing results presented in section 5.2.1. The direct numerical comparison for the simulations relative to the two materials is presented in Table 5-4, while Table 5-5 shows the comparison with the EZ Slam tests. For this first simulation the torque vs. angle characteristics of the common check were used for both the steel and the aluminum door simulations, while in section 5.3.2 the influence of both checks were simulated for the aluminum door.

It is clear from Table 5-4 that the contributions to the closing effort considered by the OU Model are not exactly the same as the ones measured in the EZ Slam tests. The model is in fact a predictive tool of the minimum closing energy and closing speed necessary to fully latch the door from when the user releases it (nearly closed position), and does not take into account the whole swing of the door like the EZ Slam.

Table 5-4: Aluminum vs. Steel OU Model simulation.

	Steel Frame OU Model Simulation		*Aluminum Frame OU Model Simulation*		
	Predicted Value	*% of total energy*	*Predicted Value*	*% of total energy*	*Differential between aluminum and steel [%]*
E_{air} *[J]*	3.11	71.21	4.14	78.39	33.3
E_{seal} *[J]*	0.78	17.87	0.60	11.39	-22.9
E_{weight} *[J]*	-0.40	-9.16	-0.34	-6.38	-15.7
E_{hinge} *[J]*	0.10	2.24	0.10	1.84	-
E_{latch} *[J]*	0.78	17.84	0.78	14.76	0.2
E_{total} *[J]*	4.37	100	5.28	100	21.1
v_p *[ft/sec] (mm/s)*	2.78 (848)	-	3.263 (994.6)	-	17.3

Table 5-5: OU Model-EZ Slam comparison for the aluminum and steel tests.

	Steel frame			Aluminum Frame		
	OU predicted value	*EZ Slam measured value*	*Difference*	*OU predicted value*	*EZ Slam measured value*	*Difference*
E_{air} *[J]*	3.12	1.66	87.7%	4.15	2.50	65.9%
E_{seal} *[J]*	0.79	0.56	41.8%	0.60	1.10	-45.0%
E_{weight} *[J]*	-0.41	-1.33	-70.0%	-0.34	-1.10	-70.0%
v_p *[ft/sec]* (*mm/s*)	2.78 (848)	2.18 (664)	28.0%	3.26 (994.6)	3.20 (974.5)	2.0%

The contributions not considered by the OU Model are check friction (the model simulates door closure from "*when the check-link is assumed to cease to function*" [24]) and drag (that showed to be the two main energy sinks if the whole swing of the door is considered). As explained in section 5.2.1, the computation of the energy sink due to drag comes from an energy balance that takes into account all the energy input contributions, while the OU model calculates the effort differently. On the basis of the geometry of the door and of all the input data (see section 4.2), the model predicts the energy sink due to the four contributions considered and the energy that is given by the weight of the door caused by the tip angle of the hinge axis and gives as output the minimum closing energy and speed. The input of the user is not considered.

Looking at the results, the biggest part of the energy is absorbed in both cases by air bind (71.2% and 78.4% respectively for the steel and the aluminum cases), followed by latch and seals (about 17.8% each for steel and 11.4% and 14.5% for aluminum) and finally by hinge friction (2.2% and 1.8%). The energy indicated as total energy (E_{total}) to close the door includes both the positive and negative contributions to closure, the only positive contribution being in this case the weight of the door. The value of the weight contribution is negative because the energy sink is considered positive in the model. Analyzing the prediction on closing effort and closing velocity for the two frames, the total energy sink to reach complete closure was 21% greater for the aluminum door, while the EZ Slam tests showed a difference of less than 6% between the two results. The predicted value of air bind is much greater for both doors with respect to the value

calculated with the EZ Slam (almost double), but also the OU prediction highlights a strong increase in the air bind effect when switching to aluminum; in the OU model the value increases of about 33% (while in the tests the increase was of 50%). The air bind model in the OU predictive tool predicts the pressure inside the cabin based on the amount of air that will be compressed in the cabin during closure. This amount is calculated based on door geometry, cabin volume and vent area (from which the air escapes from the cabin). The EZ Slam measures the air bind sink based on energies considerations.

With reference to the seal compression contribution, the OU Model predicts a decrease in the energy absorbed by the seals, while the EZ Slam tests show an increase in the energy absorbed that is likely due to a greater seal compression. Even though the two methods are not consistent in the prediction of the seal contribution, recall that this energy is rather low if compared to the other energy sinks. With regard to the hinge energy contribution, since the value of energy displayed is positive, it represents a sink. This means that the energy given by the check to assist closure was less than the energy dissipated by friction at the hinges. For what concerns the positive contribution of weight both the EZ Slam and the OU Model are consistent in predicting a decrease in energy of about 16%. However, the absolute value of the energy is once more very different between the two methods; the weight contribution predicted by the OU Model is less than one third of that recorded by the EZ Slam. Since door closure from a small open position is considered, the change in the height of the center of gravity (that depends on door open angle) is much smaller than in the one recorded in the EZ Slam tests, performed from full open angle. This fact justifies the lower positive contribution of door weight in the OU model prediction. Considering the full swing of the door and the same overall door rise, since the weight model of the OU Model is geometrically exact, if the information input to the model regarding the hinges and center of mass position and the hinge axis inclination are correct, the positive contribution of the weight predicted by the model and the one measured during the physical tests should match.

The model overestimates the value of the minimum closing speed; however the value predicted for the aluminum door closure was within a 2% difference from the value measured during the physical tests. For what concerns the steel door, the predicted

minimum speed was rather high if compared to the measured value (21.7% higher), meaning that the steel door was able to close at a lower speed than the one predicted by the OU Model. The comparison performed on the particular door tested didn't show a strong correlation between the predicted results and the laboratory measurements, however both methods showed a decrease in door closing performance of the aluminum door when compared to the steel door.

5.3 Normal check vs. Prototype check Closing Performance on Aluminum

In order to evaluate if a check system with enhanced close assist would improve door closing performance of the aluminum door, a custom check strap was manufactured with a change to the slope after the last indent for a more aggressive profile during the last degrees of closure.

The values measured for dimensions a, b, d and δ of the normal and tailored check straps are listed in Table 5-6.
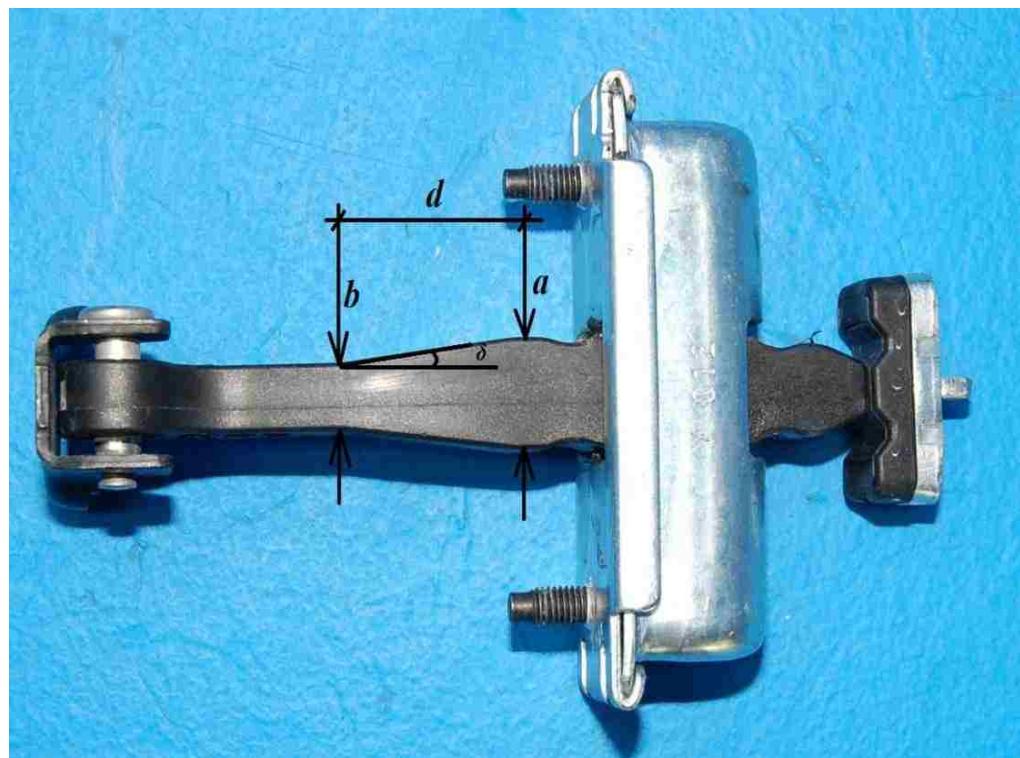

Figure 5-40: Check arm dimensions a, b, d and δ after last detent of the check arm [1].

Table 5-6: Check strap values of dimensions a, b, d and δ shown in Figure 5-40 for normal and prototype check straps.

Measure	Common check strap	Tailored check strap
a [mm]	15.99	16.46
b [mm]	9.57	7.20
d [mm]	32.81	32.81
Slope [%]	9.78	14.11
δ [deg]	5.59	8.03

To obtain a greater slope in the final part of the arm, right after the last indent the arm was made a few millimeters thicker (dimension *a* Figure 5-40), while it was made thinner in the last part, right after the end of the slope (dimension *b* Figure 5-40). The two check straps were tested on the aluminum frame. When considering the influence of the check system in door closing effort, it must be taken into account that the door needs to be easily opened and not just easily closed. Adjusting the check to assist closure may adversely affect the opening effort required; optimizing the check for both door operations is therefore necessary.

The same type of reasoning holds when considering the weight positive contribution; this contribution is important during closure, but it is important to recall that any assistance given by weight when closing the door adversely affects the user's ability to open the door. If the door is particularly difficult to open from the inside of the vehicle, the customer will not be satisfied by the overall performance of the door. As highlighted in the previous section, the total closing force comes from different sources during different moments of the closing process, so the best way to take full advantage of the positive contributions is to find the point in the closing event when they are most beneficial to the process. During closure, the user will push the door up to a certain point, after which it will be up to the weight of the door and to the spring's positive contribution to help bring the door to full latching; the maximum helping contribution of the check system is then needed from the point when the user releases the door.

A greater slope of the arm profile distributed along a smaller length might thus be a possible solution to maximize the contribution of the check system to door closure. It must be recalled that the maximum energy that the check can provide is always limited to

some point depending on the type of component, so the improvement in energy cannot go beyond a certain value.

Some considerations are necessary regarding the two check straps in order to understand the results obtained in the tests:

- The total opening of the door equipped with the custom check was 6 degrees greater because no hard stop was present on the check's arm; the door consequently stopped at the hard stop of the hinges. A greater total energy to open and close the door is then expected due to the larger travel that needs to be done on the check arm and the total friction at the hinges will also be greater. However, not all the contributions will be affected by the greater swing of the door; air bind and seal compression will not change while there will be a difference in the weight's positive contribution and in the energy dissipated due to friction from the check and the hinges.

- The material of the arm of the two check straps used is different; the normal check strap is made of mineral filled nylon while the custom one was built in glass filled nylon. This difference in materials means that also the friction between the roller bearings and the arm may be comparable, but will still be different.

- The normal check has been used much longer compared to the tailored prototype (brand new); it had therefore been exposed to many more closures and openings, undergoing a certain grade of wear.

5.3.1   EZ Slam Testing Comparison

The results of the normal and the prototype check door closing performance on the aluminum door are presented in Table 5-7, Figure 5-41 and Figure 5-42.

Table 5-7: Aluminum normal check vs. custom check door closing performance parameters.

	Aluminum (normal check)	*Aluminum (custom check)*	*Difference [%]*
Minimum closing speed [mm/s]	974.50	966.50	0.8
Total Energy to Close	17.47	18.55	6.2
Minimum user Input Pulse [J]	12.12	13.37	10.3
Closing Energy Sinks			
Energy Loss from Gravity [J]	0.00	0.00	-
Energy Loss from Spring [J]	0.00	0.00	-
Energy Loss to Air Bind [J]	2.51 (14.4%)	2.55 (13.8%)	2.3
Energy Loss to Check [J]	11.16 (63.9%)	12.72 (68.5%)	13.9
Energy Loss to Drag [J]	2.70 (15.5%)	2.11 (11.4%)	-22.2
Energy Loss to Static Compression [J]	1.10 (6.2%)	1.17 (6.3%)	7.1
Closing Energy Inputs			
Energy provided by Gravity [J]	1.11 (6.3%)	0.33 (1.8%)	-69.7
Energy provided by Spring [J]	4.24 (24.3 %)	4.85 (26.1%)	14.1
Energy provided by User [J]	12.12 (69.4 %)	13.37 (72.1%)	10.3
Opening Energies			
Energy provided by Gravity [J]	0.00	0.00	-
Energy provided by spring [J]	0.00	0.00	-
Energy provided by user [J]	16.51	17.90	8.4
Energy required by check [J]	11.16	12.72	13.9
Energy required by gravity [J]	1.11	0.33	-69.7
Energy required by spring [J]	4.24	4.84	14.1
Total Energy to Open [J]	16.52	17.90	8.4
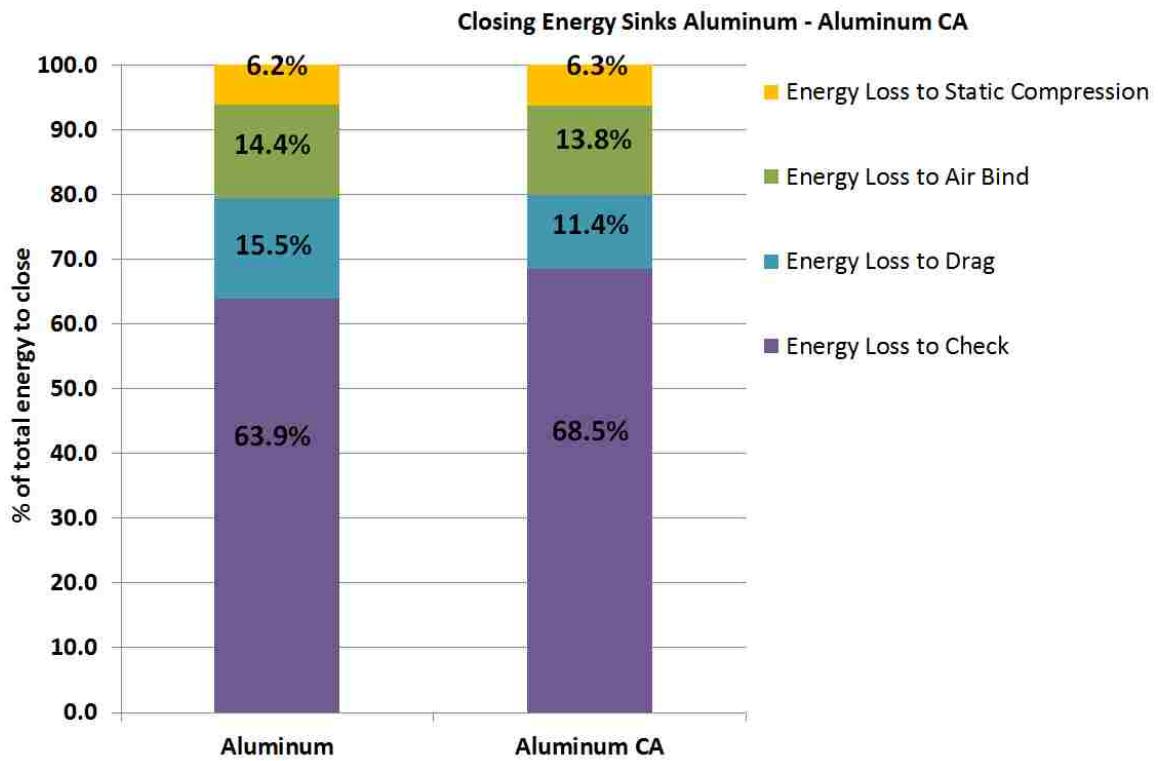
Figure 5-41: Direct visual comparison of the energy sink contributions for the tests performed on the aluminum door with the two different check straps.
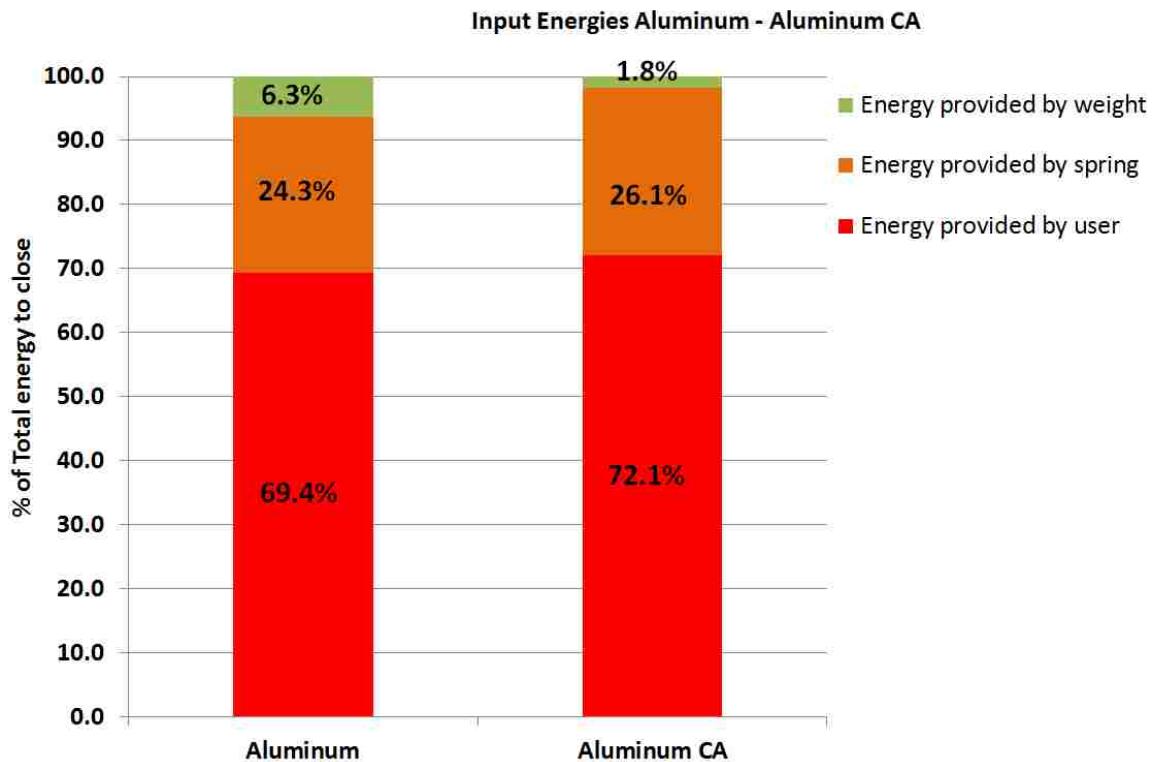
Figure 5-42: Direct visual comparison of the energy inputs for the tests performed on the aluminum door with the two different check straps.

112

Looking at the particular contribution of the check system, the losses with the second strap resulted around 14% greater (Table 5-7, "energy loss to check") than the ones obtained with the normal check. The bar charts relative to the energy dissipation in the two tests performed with the prototype check (CA) are shown in Figure 5-43. Analyzing the curves relative to the opening sweep energy, presented in Figure 5-44, the two checks show a good repeatability in the opening action.

The same cannot be said for the closing sweep energies (shown in Figure 5-46). The graphs relative to the closing sweep actions for the different runs performed are quite far one from each other even though the tests were performed in a consistent manner. The shape of the curves is the same obtained in the tests of the steel door but the prototype check allowed a greater opening angle as opposed to the normal check.
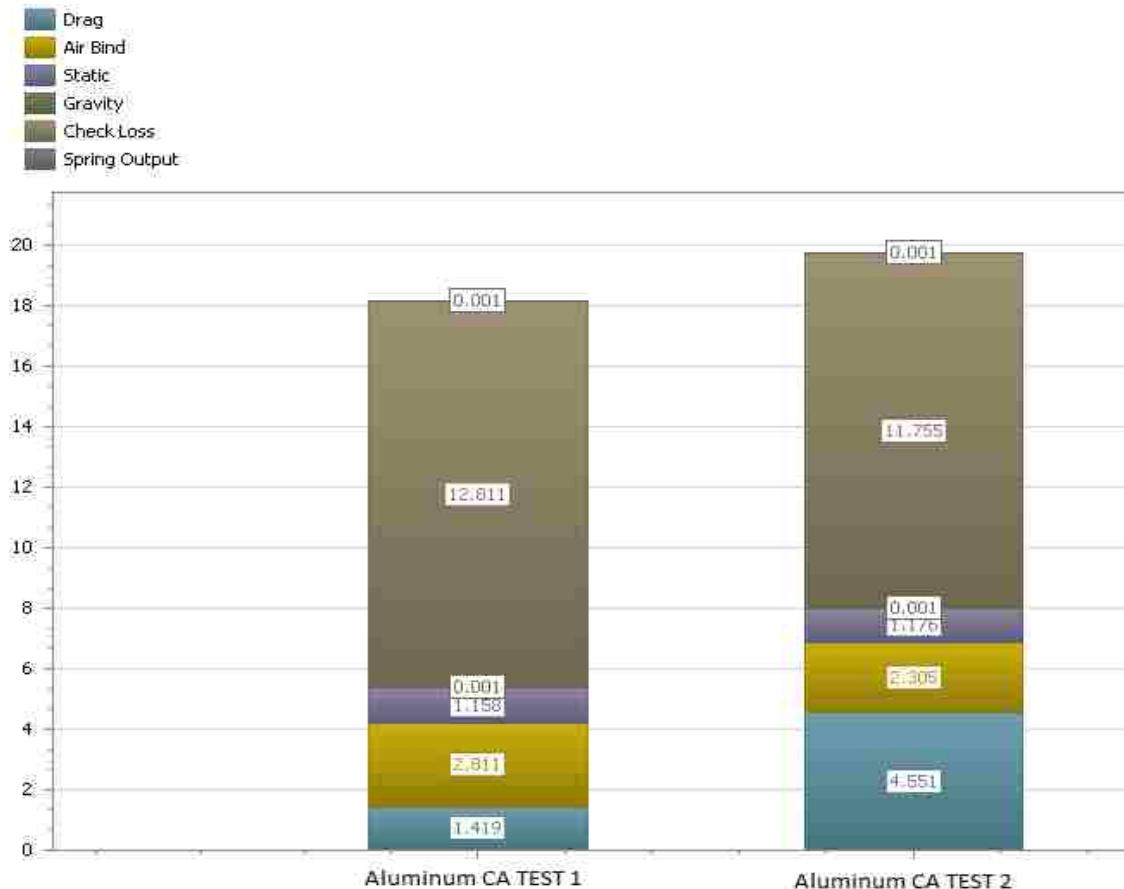
Figure 5-43: Energy sink contributions during the closing action of the aluminum door for the two tests performed with the custom check. The "CA" refers to close assist and indicates the tests performed with the prototype check.
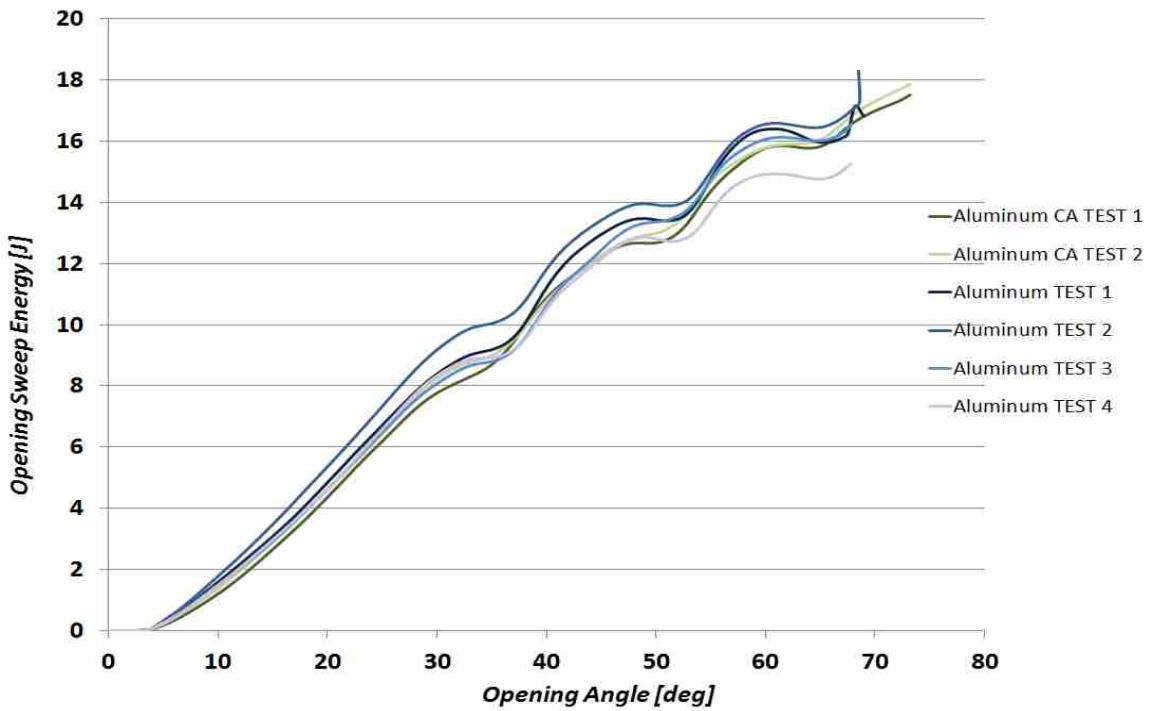
Figure 5-44: Opening Sweep energy comparison for the normal and the custom check. The plot comes from the numerical integration of the opening sweep force curves from the almost closed position to the fully open position.
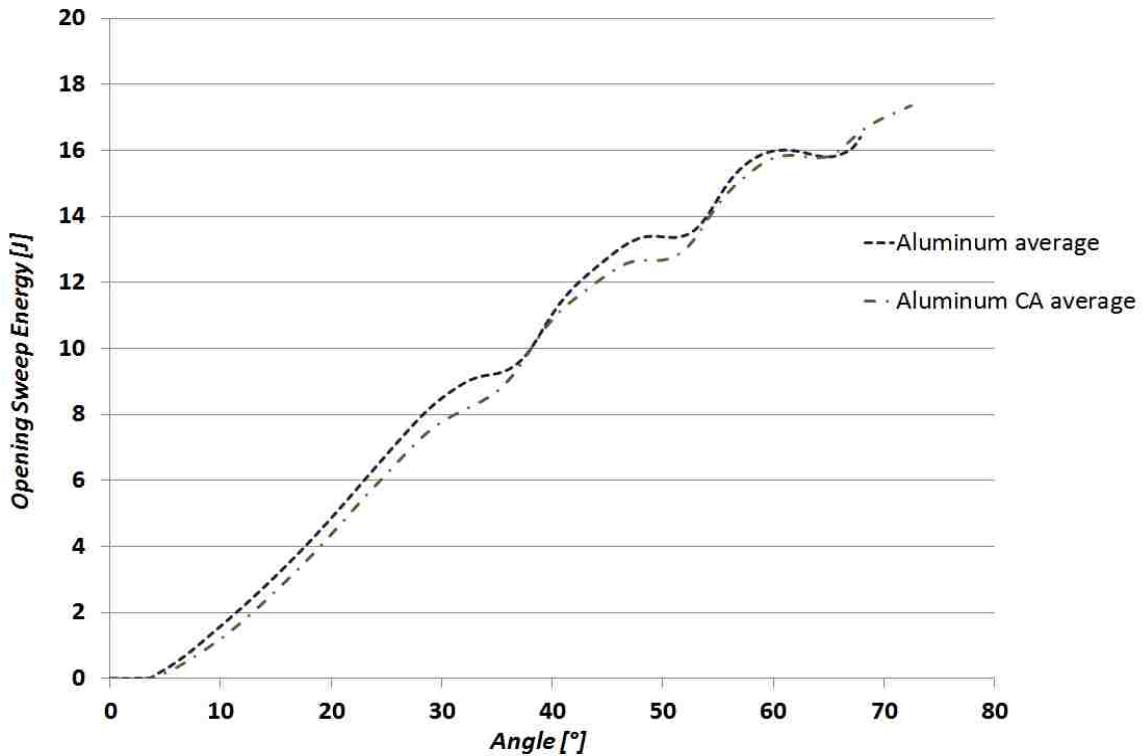
Figure 5-45: Average opening energy curves. Labeled in green is the curve of the custom check tests and in blue the curve of the normal check tests..
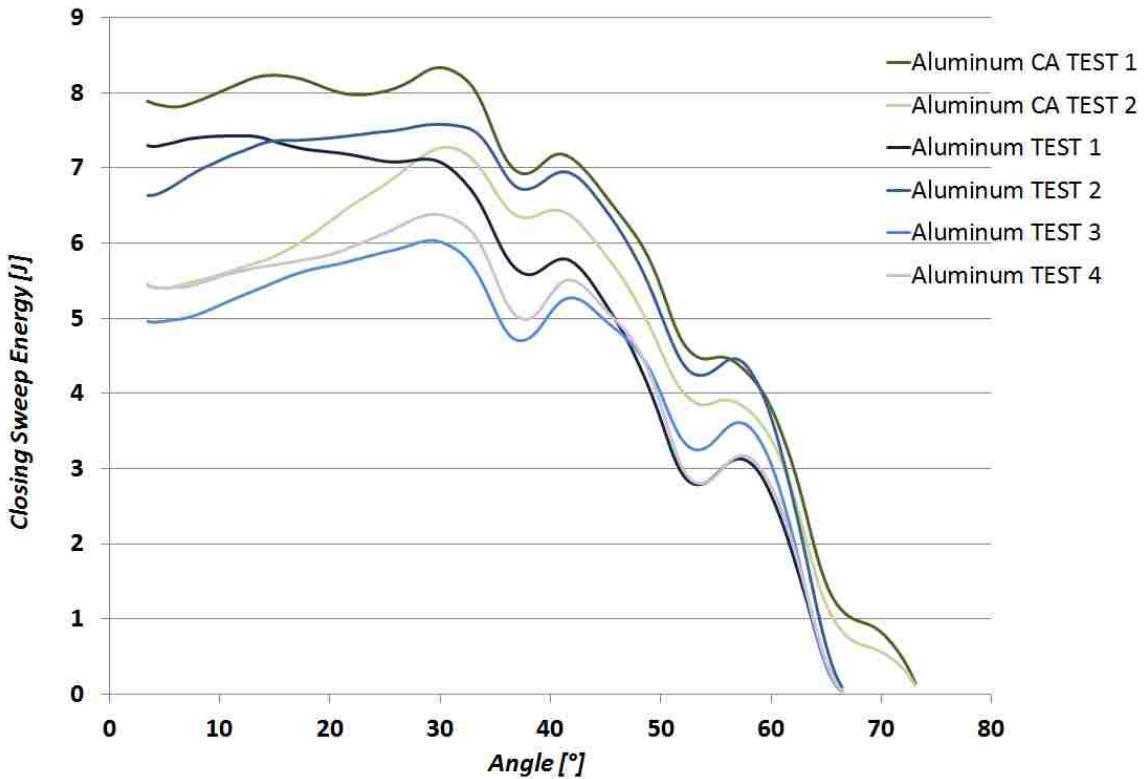
Figure 5-46: Closing Sweep energy comparison for the Production and the Custom checks. The full open angle is grater for the custom check (CA) because of the absence of the check arm hard stop.
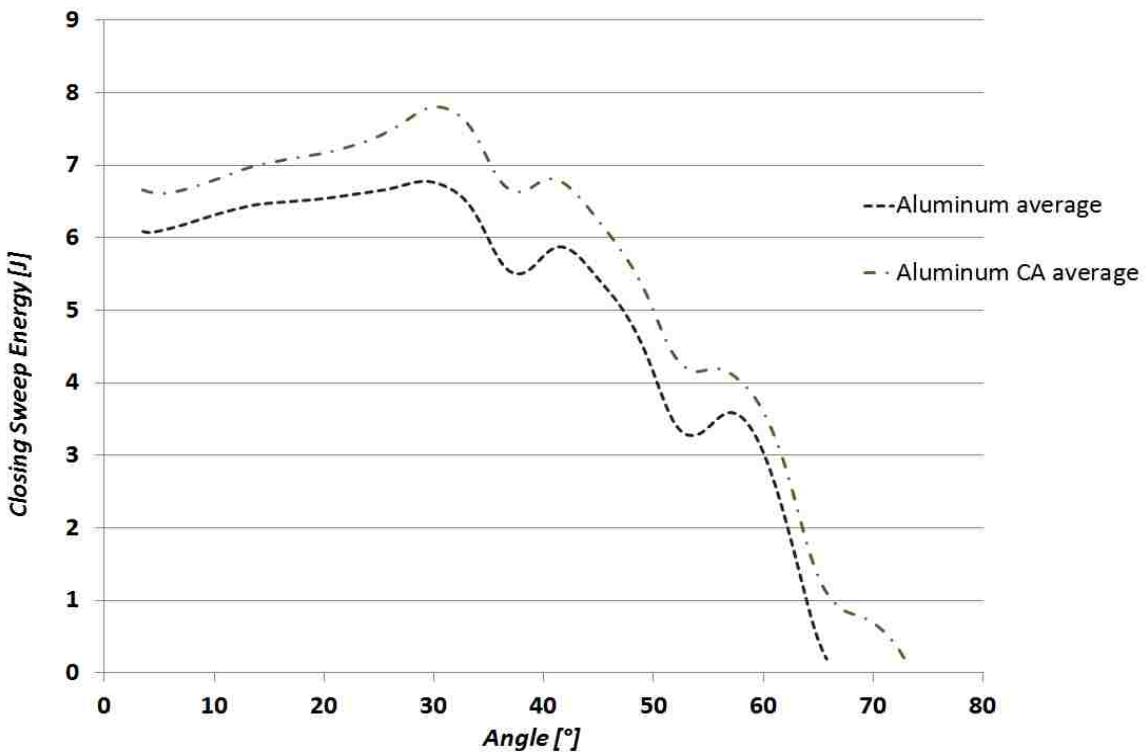
Figure 5-47: Average closing sweep energy curves.

115

In particular the higher value of closing sweep energy for the prototype check could be due to a stick-slip action caused by a check arm that is too dry (because it is being used for the first time). The effect of this stick-slip phenomenon is the increase in energy required to close the door at a constant speed during the sweep test. The same trace tester system used to assess the check contribution variation in the comparison between the steel and the aluminum frames was used also in this part of the study to fully characterize the custom check and evaluate the differences in its contribution to the closing effort of the aluminum door, compared to the production check. The closing forces and the closing energies for the two checks are compared in Figure 5-48 and Figure 5-49, after having transformed the energy curves per the EZ Slam method of calculating the closing sweep energy.
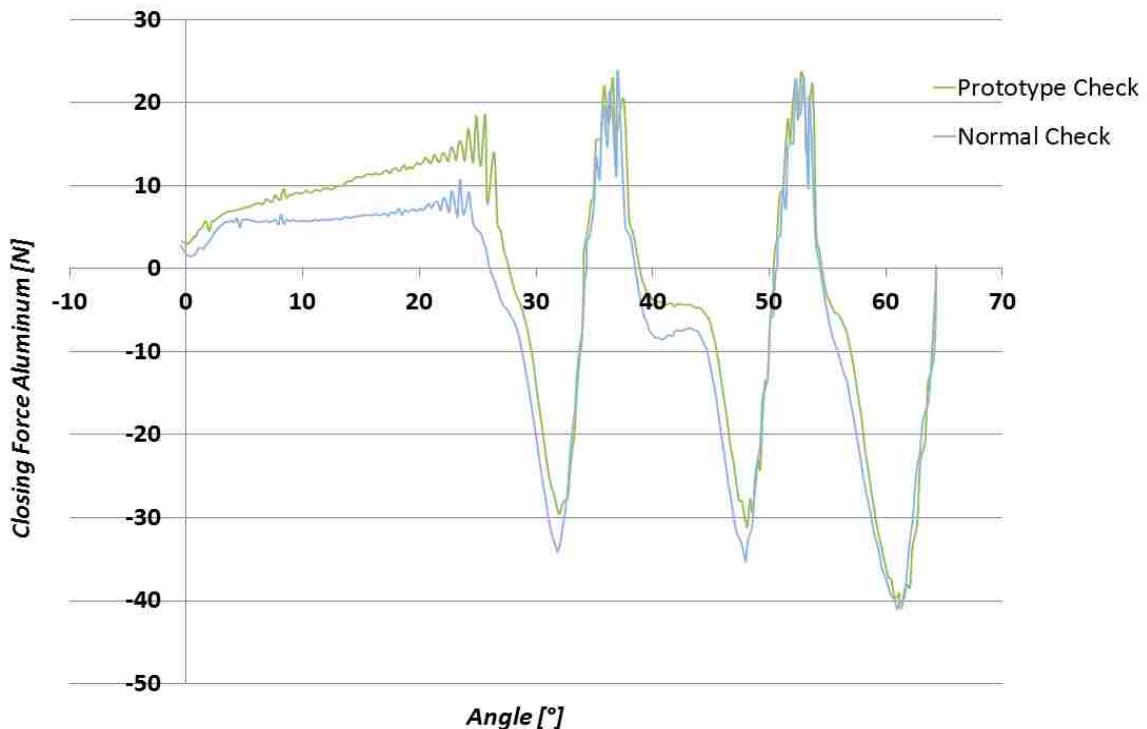
Figure 5-48: Closing force comparison for the production and the prototype check (Supplier's tester).

Recalling that, with the trace tester sign convention for the force graphs, a positive force means that the check is pulling the door towards closure, from Figure 5-48 it's clear how the prototype check improves assistance during the closing event. The difference between the performance of the production check and that of the prototype check is much greater than what can be seen from the closing sweep tests of Figure 5-46 in which the curves

seem very close for the two check straps. In particular the difference can be seen simply looking at the area under the curve of the two curves in Figure 5-48. The part of greatest interest is from 30 degrees open to 0 degrees, because it is in this part of the closing event that the greater close assist of the prototype check gives its contribution. The area under the prototype check force curve is almost twice as much as the area under the normal check force curve; recalling the relationship between the area under the force curve and the energy, this proves that a greater amount of energy will be provided by the prototype check to assist closure, as opposed to the normal check.
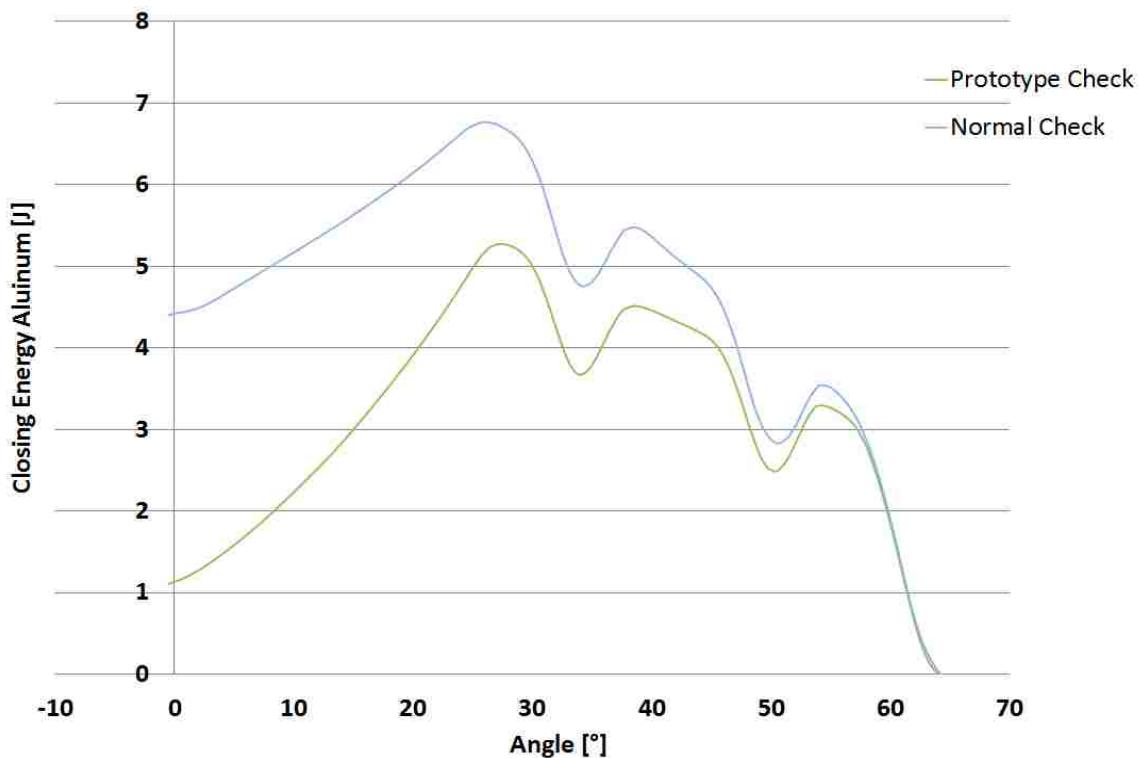
Figure 5-49: Closing energy comparison for the production and the prototype check (Supplier's tester).

To assess exactly the contribution given by the greater close assist in terms of door speed, the trace tester machine loaded with the weight and center of gravity information relative to the aluminum door was equipped initially with the production check and later on with the prototype check. The frame of the machine was manually brought to the edge of the final slope of the check's arm and let go in order to measure the velocity reached by the door thanks to the sole close assist of the arm. A speed trap was used to measure the speed. The speed trap was composed of a C shaped component equipped with two lasers

placed at a known distance from each other and pointing at two photocells. A light rod of metal was attached to the frame representing the door using a magnet, and in such a way that it passed through the cavity of the C shaped component when the door was closing. The sensor recognized the passage of the rod in the cavity because of the interruption in the connection between the lasers and the photocells. Knowing the distance between the two lasers and timing the passage between them, the velocity meter gave as output the velocity of the frame at closure.

The door velocity recorded with the production check installed was 710 mm/s while the custom check allowed a door speed of 875 mm/s. With a simple calculation, the increase in the kinetic energy at the end of the slope was:

$$E_k = \frac{1}{2} * m_d * \left(v_c - v_p\right)^2 = \frac{1}{2} * 28.12 * (0.875 - 0.710)^2 = 0.38\,J.$$

This increased amount of energy relates to the door movement at the last slope of the check arm and not the entire swing of the door but, from this result, one can conclude that the prototype check will assist in door closure more than the normal check.

In Figure 5-50 and Figure 5-51 it is possible to analyze the trend of the input force by the user as a function of the door open angle in the EZ Slam tests.
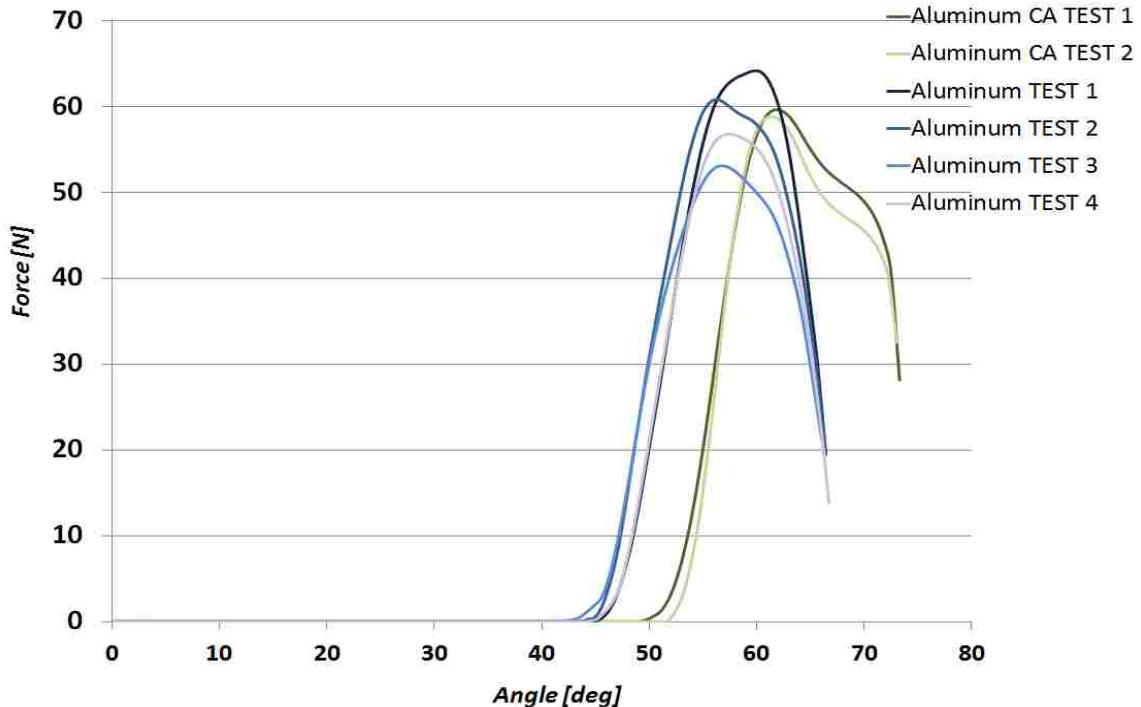
Figure 5-50: Force pulse vs. Angle for the two different check straps. The impulse starts approximately 6 degrees earlier for the custom check due to the greater swing allowed.

118
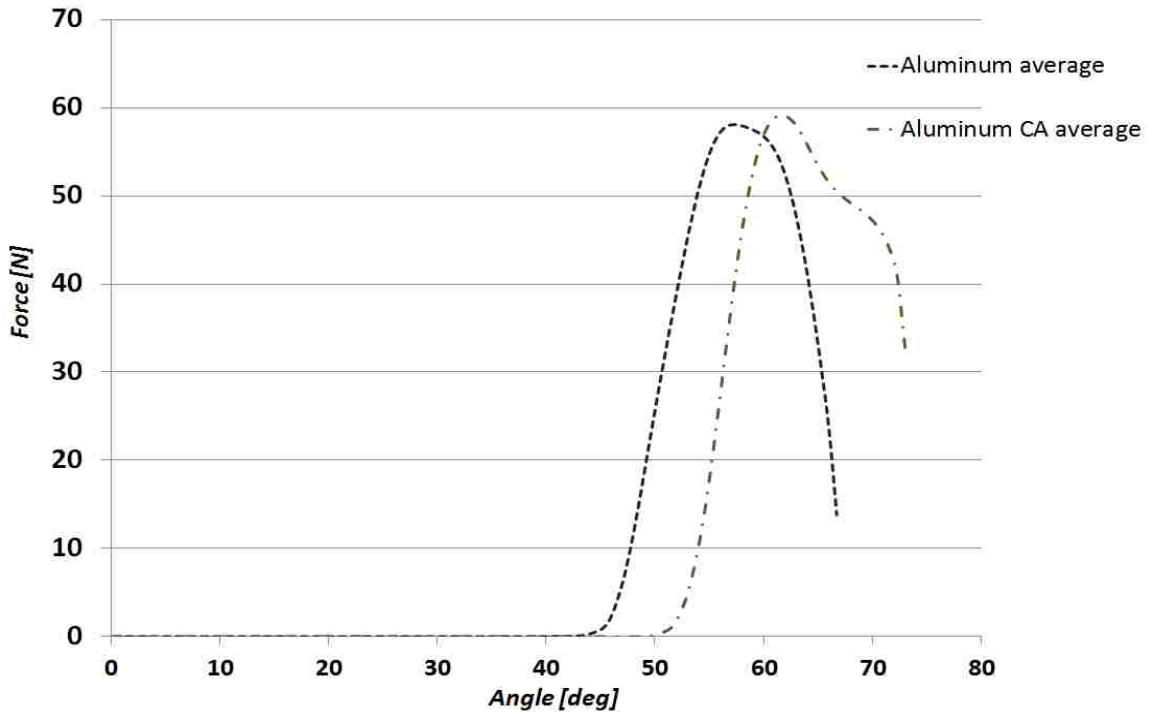
Figure 5-51: Average force vs. angle curves.

As it can be seen from Figure 5-50 and Figure 5-51 there was no difference in the type of input force to the doors during the tests, and the force was given always in the same window (in terms of angle) in the two tests (just shifted to the right by approximately 6 degrees for the prototype check strap). The type of force input to the door is that of an impulse; when the user released the door the force went to 0. The curves presented in Figure 5-52 and Figure 5-53 show the closing speed reached by the aluminum door equipped with the two checks as a function of the energy pulse input by the user to close the door.

All the curves relating the closing speed and the user input are quite close for the two cases, but to reach the same closing speed with the prototype check, a little higher input was required from the user with respect to the production check. Considering the wider swing of the door allowed by the prototype check, for a given impulse a greater amount of total energy sink is expected during closure due to increased friction, and so a lower speed is expected at the end of the closing event.

119
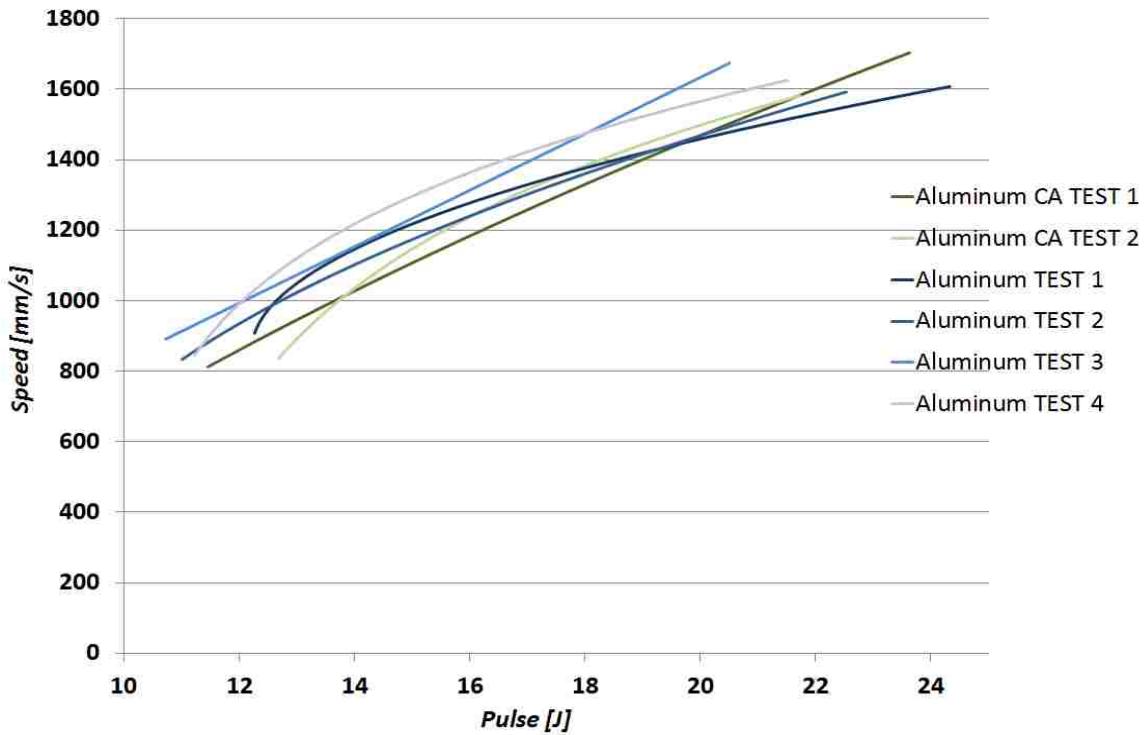
Figure 5-52: Speed vs. Input pulse curves for all the tests performed on the aluminum door with the normal check (blue curves) and with the prototype check (green curves).
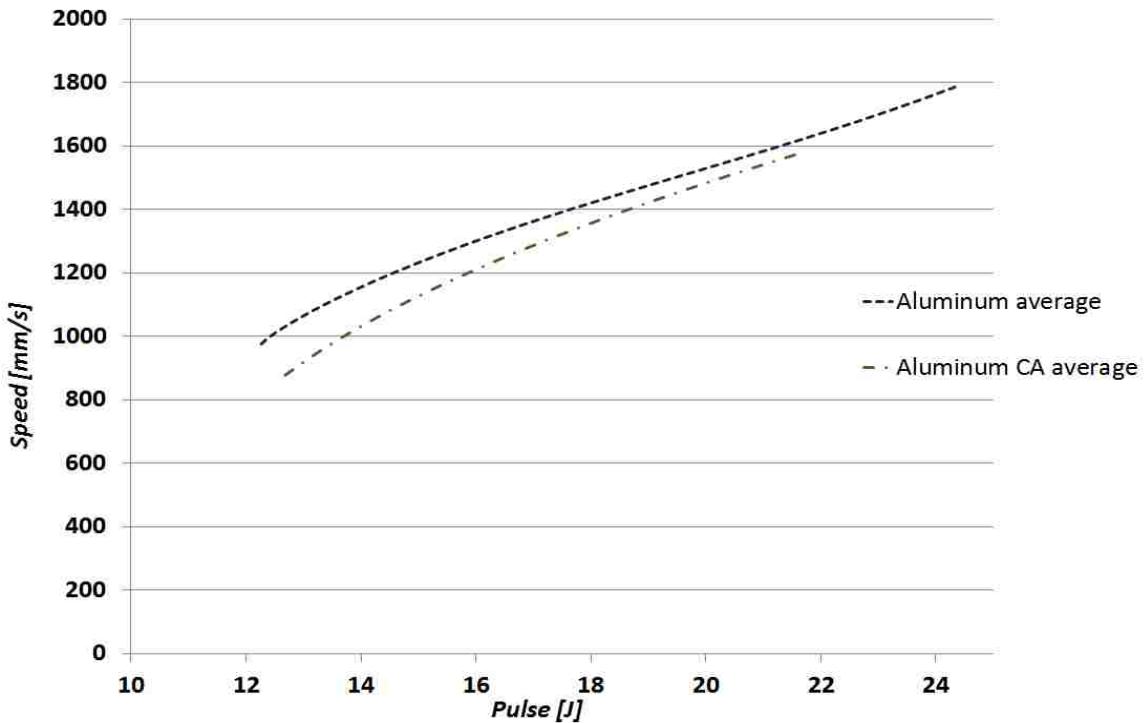
Figure 5-53: Average Speed vs. Input pulse curves for the tests performed on the aluminum door with the normal check (blue curve) and with the prototype check (green curve).

To better assess the effect on final closing speed and energy of the more aggressive arm profile, the tests should be performed starting from the same fully open position (using a prototype check equipped with the same hard stop of the production check).

In Figure 5-54 and Figure 5-55 the speed profiles relative to the two tests are presented.
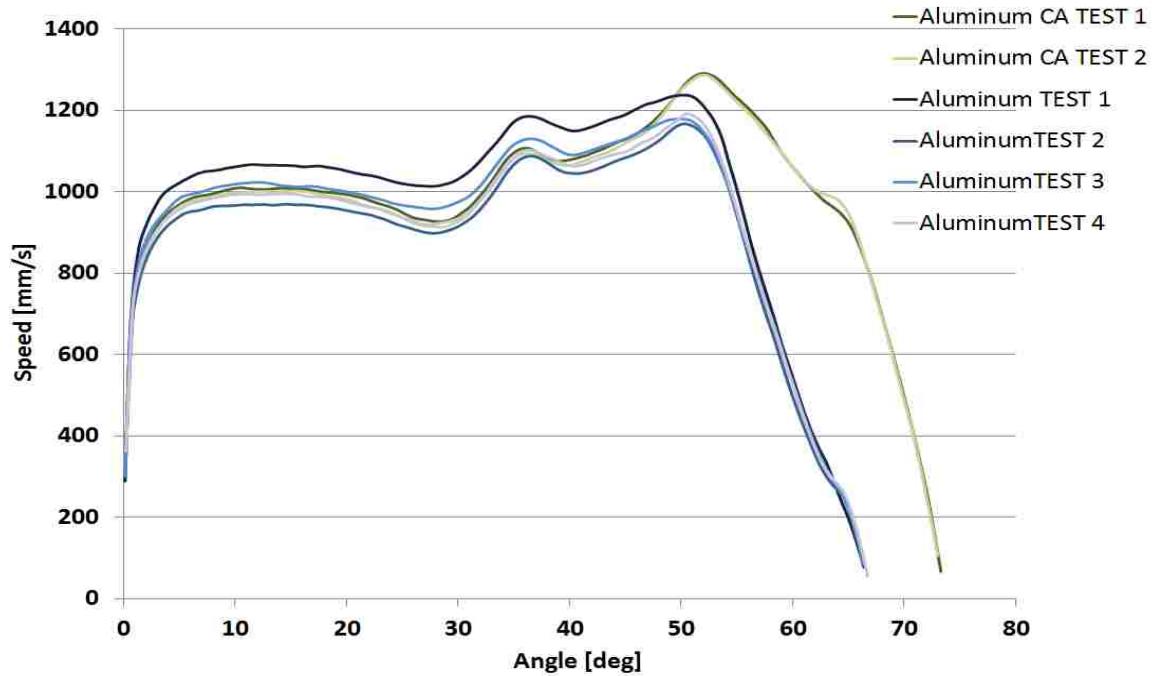
Figure 5-54: Minimum closing speed vs. Angle comparison for the Production and Custom check.
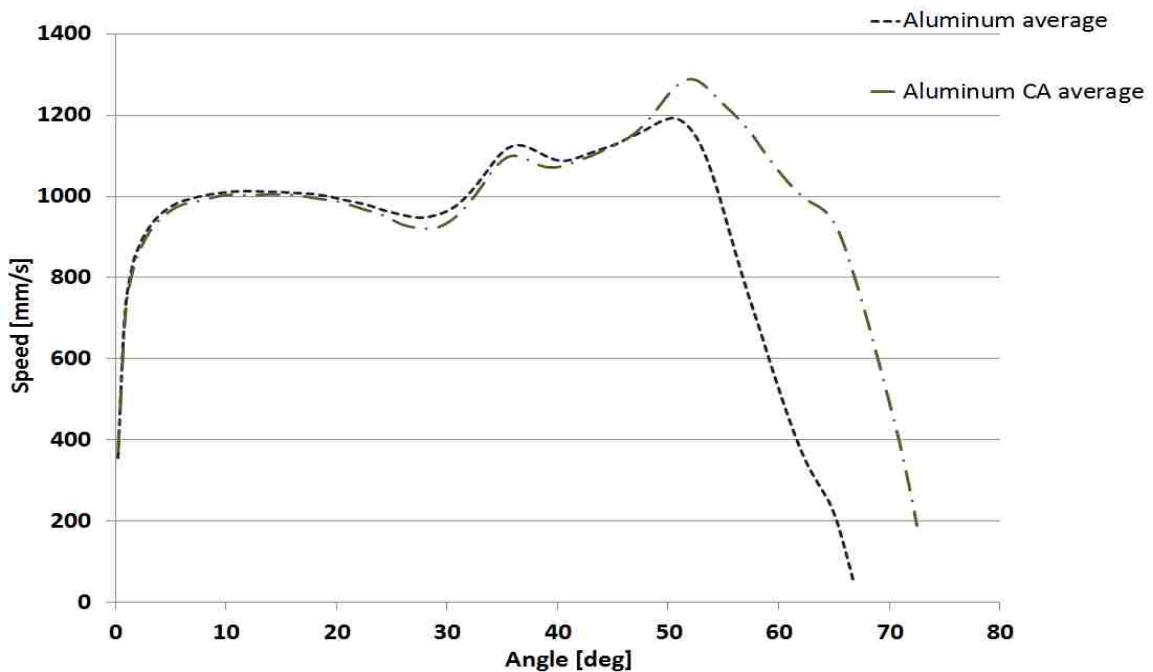
Figure 5-55: Average minimum closing speeds.

121

Even though the custom check provides greater assist, the speed profiles in the leftmost portions of the curves look the same in the two cases, with a greater speed being reached in the very first phase of door closure, between 50 and 70 degrees (Figure 5-55). A greater acceleration was expected in the last degrees of closure for the custom check due to the greater slope of the arm profile.

A parameter called door check linearity, that assess the difference between the minimum and maximum speed between the release of the door and the near latched point, was be more than 24% greater for the second check strap. This means that the door accelerated more during the closing event, after the user released it, when the prototype check was mounted.

The value of the energy provided by the spring during closure (and so also the value of the energy required by the spring during opening) resulted in approximately 15% more energy for the custom check strap, due to the greater compression of the springs in correspondence of the thicker part of the check's arm after the last detent. Recalling that the spring contribution was the factor that decreased the most in the comparison between the steel and aluminum door performance, an increase in its value is a positive result; however, the difference with the normal check test is of only approximately 0.6 J, not enough to allow a decrease in the energy contribution required to the user. As it is possible to see from Table 5-7, in the tests with the prototype check the spring contributed for 26.1 % of the total energy required to close the door (compared to a 24.3% contribution from the normal check), but also the user input increased, slightly, to 72% of the total energy (as opposed to the 69.4% of the normal check). This is due to the drastic decrease in the positive weight contribution that accounted only for 1.8 % of the total energy needed (as opposed to the already low 6.3 % of the aluminum door with normal check). This result is once more dependent on door rise, shown in Figure 5-56. As it can be seen from the graph, the maximum rise is only slightly lower in the case of the custom check, but the position of the centre of mass (at full open angle) is much lower, and because the overall door rise is calculated as the difference between the final and the initial height of the center of mass, it results much smaller in this second case with respect to the production check, thus making the door weight positive contribution even smaller.

122
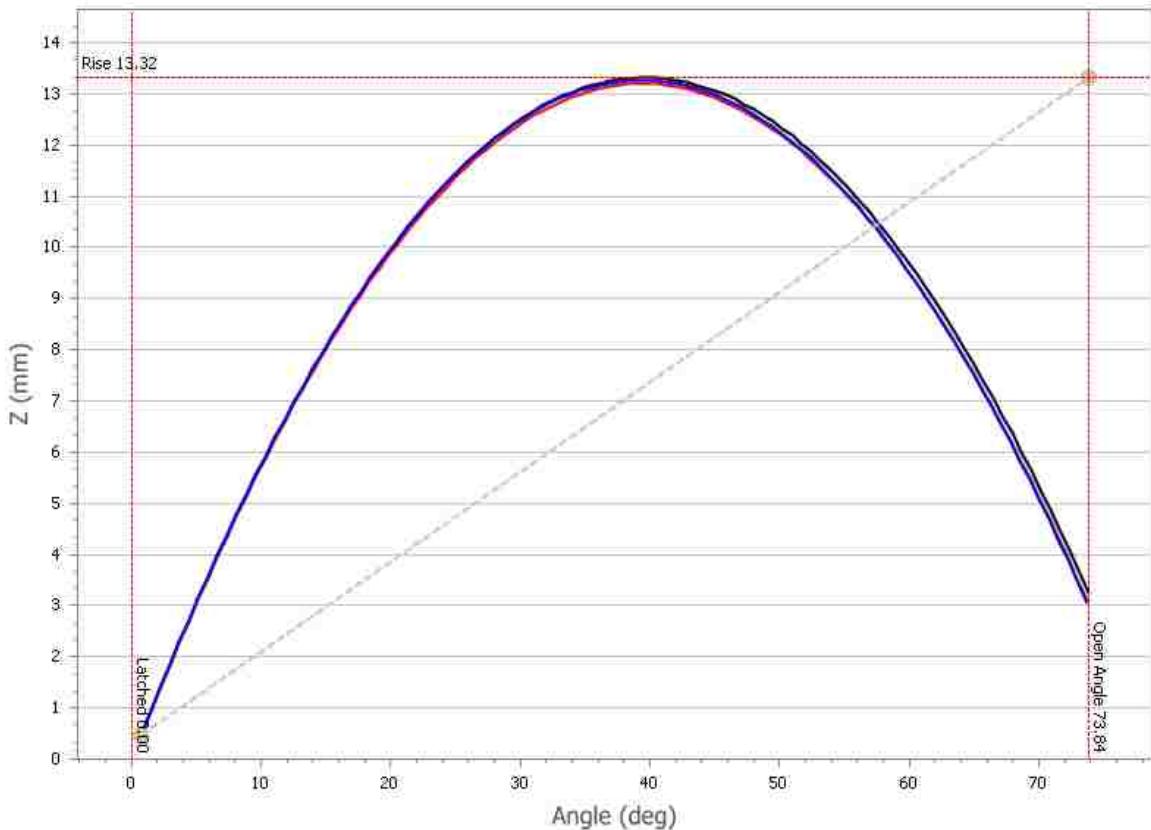
Figure 5-56: Door rise of the aluminum door with custom check during the closing event.

The difference in initial door height might depend on a different position of the check system in the two cases and on the wider opening angle allowed by the custom check. This extremely low contribution of the weight leads to an even worse result in terms of effort required to the customer to close the door. If the check is not positioned exactly at the same point with respect to the hinge axis, this will influence the check force applied on the door but a simple translation of the check strap in a higher or lower position, if along the hinge axis, should not change the forces. A smaller upward component of force might not have pushed the door as high in the case of the custom check. Even though a clear positive effect of the custom check on the overall closing event was not revealed from the EZ Slam tests, the difference in the amount of allowed swing of the door (6 degrees) caused by the absence of the hard stop on the custom check's arm affected the results of the tests, therefore a positive effect of the greater close assist cannot be excluded; looking at the speed test performed on the two checks and relative to the close assist action alone (considering just the last slope of the arm) it is expected that the greater kinetic energy that the door has at the end of the last slope of the custom check

123

will increment the positive contributions to close the door thus allowing a lower required energy input (i.e. effort) to the user. Moreover, the extremely low weight contribution can be increased by adjusting the fitting of the door and in particular of the check strap (using a hard stop like the one used on the normal check), to bring it back to the value obtained with the normal check mounted on the aluminum frame. Together with the 14 % greater spring contribution, this would lead to a decrease in the initial user input with respect to the tests performed with the normal check, thus reaching a value of user effort closer to that obtained with the steel door.

5.3.2   OU Model comparison analysis

The data of the prototype check strap was input to the OU model programmed for the aluminum door in order to run a comparison between the effect of the two check straps on aluminum door closure. The results are listed in Table 5-8 and discussed below. The check-torque characteristics of the two check straps are shown in Figure 5-57. The torque curves have the same shape of the opening and closing force vs. angle curves of Figure 5-17 and Figure 5-18 (note the polarity reversal for input to the OU Model); the value of the torque for each point is evaluated multiplying the force by the distance of the handle from the hinge axis (characteristic of the door tested).

Table 5-8: Normal check vs. Prototype check OU Model simulation on aluminum.

	Normal check OU Model Simulation		*Prototype check OU Model Simulation*		
	Predicted Value	*% of total energy*	*Predicted Value*	*% of total energy*	*Differential in predicted values [%]*
E_{air} *[J]*	4.14	78.38	4.08	80.55	-1.50
E_{seal} *[J]*	0.61	11.39	0.61	11.87	-
E_{weight} *[J]*	-0.34	-6.38	-0.34	-6.65	-
E_{hinge} *[J]*	0.10	1.84	-0.06	-1.19	-162.09
E_{latch} *[J]*	0.78	14.76	0.78	15.42	-
E_{total} *[J]*	5.29	100	5.07	100	-4.16
v_p *[ft/sec](mm/s)*	3.26 (994.64)	-	3.19 (973.75)		-2.10
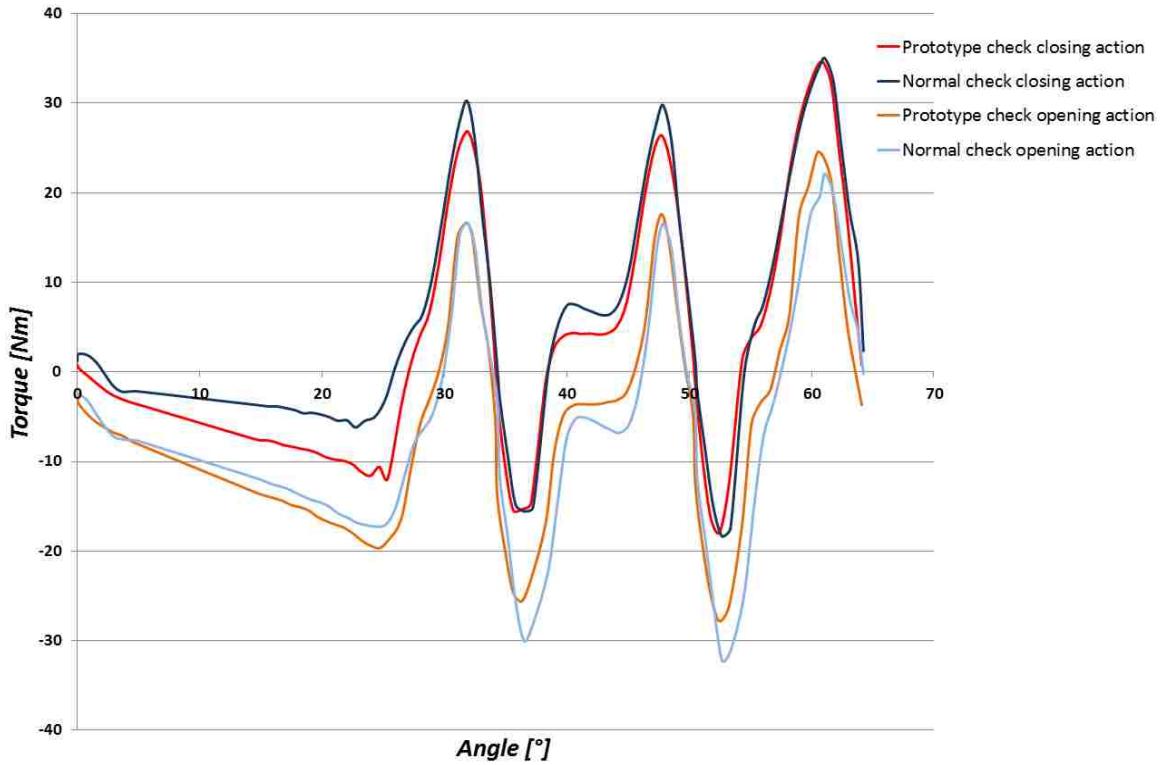
Figure 5-57: Torque characteristics of the normal check and of the prototype check

The total energy showed a slight decrease in the simulation with the prototype check (of about 4%), together with the minimum closing speed (-2%) and the air bind contribution (-1.5%). Seal and latch energy did not vary at all, as expected, while a greater positive energy contribution from the custom check (expressed through the torque vs. angle input curve) is highlighted by the decrease in the hinge contribution. In this simulation, since the value is now lower than 0, the energy given by the check was greater than the energy dissipated by the hinges due to friction. This result can be understood looking at the check torque characteristics (Figure 5-57); looking at the closing torque, the area comprised between the curve of the prototype check torque and the abscissa axis is much greater than that of the normal check, so the assist given by the custom check to closure was much greater as well.

As done for the normal check, the results obtained with OU Model for the prototype check are compared to the results measured with the EZ Slam in Table 5-9.

Table 5-9: Ou Model vs. EZ Slam comparison of the aluminum tests with the prototype check.

	Aluminum Frame with prototype check		
	OU predicted value	*EZ Slam measured value*	*Difference*
E_{air} *[J]*	4.082	2.555	59.8 %
E_{seal} *[J]*	0.602	1.170	-48.5%
E_{weight} *[J]*	-0.337	-0.335	0.6 %
v_p *[ft/sec] (mm/s)*	3.195 (973.75)	3.170 (966.5)	0.75 %

From the simulations, the weight contribution and the minimum closing speed are really close to the ones measured with the EZ Slam (within 1 %), while the air bind energy sink is again much higher than the one measured during the tests while the seal contribution is much lower. Also in this second case there was not a close correlation between the results of the predictive model and the results of the tests in terms of numerical values, particularly for the energies; however, it must be taken into account the fact that both methods have their approximations and don't refer to the exact same event. The prediction of the minimum closing speed matched the EZ Slam results.

6. SUMMARY

The door closing performance of an aluminum door was tested with the EZ Slam equipment to evaluate the behavior of the light material compared to the performance of a current steel door on a C segment vehicle. The same aluminum door was tested with two different check straps, the normal check in use for the car considered and a prototype check with enhanced close assist to evaluate a possible improvement in the closing performance with a more aggressive profile of the check's arm.

The door closing event was proved to be a complicated process that involves many different factors including the door's configuration and fitting on the body, door geometry and weight, cabin volume and material properties. With regard to the minimum closing speed, the aluminum door performance was still acceptable per specifications, as it closed at an average minimum velocity of 974.5 mm/sec (3.197 ft/sec). Even though this value is lower than the maximum allowed, it represents a decrease in performance of almost 50% with respect to the production steel door that closed at an average minimum speed of 664 mm/sec (2.178 ft/sec). Moreover, considering the studies on the IQS score presented in Chapter 2 ([16]), in order not to cause a decrease in the score, a speed lower than 900 mm/sec is required. From the test results, the total energy to close the door in the two cases was found to be almost the same (less than 5% greater for aluminum) but the contribution required of the user to close the lighter door was much greater; the minimum energy with which the user had to push the steel door to reach a complete closure was approximately 8.5 J, while the aluminum door required more than 12 J (about 42% greater impulse to fully latch the door). This result depended on the fact that the other two energy contributions that help the user in closing the door gave a much lower contribution closing the lighter door. The lower weight contribution was obviously expected due to the much lower weight of the aluminum door; however the difference in this energy contribution was only 0.22 J (16.5%). Moreover, depending on door rise during closure (a very small value), this contribution accounted only for 8% (for steel) and 6.4% (for aluminum) of the total energy input. This value was found to be rather low, also for the steel door, and depends on door configuration and hinge axis inclination, that affect the trajectory of the center of gravity of the door during closure. The biggest

difference in the closing events of the two doors was given by the spring contribution, which was, in the case of the aluminum door, 2.55 J less than for the steel (almost 38% difference). This represents a significant amount of the total energy necessary to close the steel door (40.83%) and a decreased assist when closing the aluminum door (only 24.3%). This contribution represents the assist given by the check system during closure due to its ability to store energy in the opening phase and to release part of it during closure. The loss in positive spring contribution strongly penalized the closing performance of the aluminum door and required the user to make a larger contribution to fully latch the door. Associated with the greater user input there was a higher minimum closing speed that caused an increase in the energy sunk by the air bind effect.

In terms of energy sink contributions, the value of air bind was 50% greater when closing the aluminum door (with a loss of almost 1 J more with respect to steel) and check friction was also increased by 1.2 J. The tests carried out specifically on the check system with the configurations simulating the steel and the aluminum door showed no major changes in the behaviour of the component, under ideal quasi-static conditions, due to a change in weight and center of gravity position. Considering that the same frame was used to test the check system in the steel and aluminum configurations, no change in material is really considered in those tests, while the EZ Slam measurements were taken on the actual steel and aluminum doors. Properties of the two materials other than the sole weight (as for example the different flexibility) seem to have affected the results in the closing event. The results obtained with the EZ Slam tests suggest therefore that the actions needed to improve the closing performance of the aluminum door are more concerning the input energies contributions than the energy sinks. The overall energy dissipation during closure is in fact fully comparable with the energy dissipated by the steel door, but the amount of this energy that is given by the user needs to be drastically decreased (by approximately 40% to achieve the same performance as the steel door).

For what concerns the capability of improvement of door closing effort given by a greater close assist on the check's arm, the tests with the EZ Slam did not show a major change in the overall closing effort of the aluminum door. However, looking at the sole spring contribution, the energy given by this factor increased by 14%. The total energy absorbed during closure was slightly higher, but the opening angle was 6 degrees greater due to the

absence of the hard stop on the check's arm of the prototype check. The door check linearity parameter showed that a greater acceleration was recorded between the release point of the door and the near latched point in the case of the prototype check. If the check system accelerates more the door during closure, it is expectable that a lower input of the user will be required to reach a certain closing velocity. The values of minimum user input, energy dissipated by check friction and energy provided by the spring slightly increased in the tests performed with the prototype check, but these results can probably be justified with the greater total swing of the door. The tests done with the trace tester on the prototype check highlighted instead an increase in the closing energy given by the greater close assist, so this solution is not to be abandoned. More specifically, this increase in closing energy was highlighted by the area under the force curves relative to the two check straps. This area resulted to be almost doubled in the case of the prototype check.

The simulations performed with the OU Models showed that a direct numerical comparison between the results of the tests and the prediction is not possible, at the moment, due to the different type of event considered by the two methods (closure from full open angle and closure from small open position). However, both methods predicted a worsening of the closing performance when comparing the aluminum door and the steel door, and the prediction of the speed, in particular for the aluminum door, matched the results obtained with the tests. The amount of decrease in weight energy contribution predicted by the tool and measured with the value was the same (16-17%). The prediction of the OU Model can be improved dropping some of the approximations that are made, for example, not taking into account the flexibility of the material and considering the door a perfectly rigid body. The air bind model for the calculation of the pressure variation inside the cabin can be improved as well; the air bind contribution is in fact predicted based only on considerations on the Bernoulli law for incompressible flows and on the conservation of mass law, therefore it introduces an approximation.

7 CONCLUSIONS AND RECOMMENDATIONS

The work presented is a necessary step to evaluate, and fully compare, the closing performance of an aluminum door with the performance of a steel door and gives important information on the closing behavior of an aluminum door as opposed to that of a steel door. The methodology used is particularly useful since it allows to quantify the closing performance of the doors in terms of energy and closing speed values and to perform an immediate comparison between the contributions to door closing effort. The configuration tested was that of a door fully dressed and therefore allowed the evaluation of the overall performance during closure, both in terms of speed and closing effort contributions. The vehicle needs to be tested in several different configurations that allow a distinction, with greater precision, between the effects of all the different contributions during the closing event. The tests done on the check system and presented in this work allow the determination of the forces exchanged by the check alone during closure, but to better assess the effect of this component on the overall closing event, in particular in the dynamic range of closing speeds, the EZ Slam test has to be repeated after having removed the check from the door and comparing the results. Another way to prove the influence of the different material of the frame in terms of its interaction with the check system would be, as previously suggested, to test the actual doors on the trace tester instead of using the light aluminum frame in place of the doors. Since on the trace tester the door is allowed to swing with negligible friction, the comparison of the results of this last test with the EZ Slam tests performed in this work would also give important information on the contribution to the effort of the hinges alone. More specifically, to assess the variation in door flexibility, the two doors could be tested by applying constraints to the hinges and applying and measuring the force necessary to reach (the same) given value of displacement pulling the door. This information can also more easily be obtained building a CAD model of the two doors and using the Finite Element Analysis to simulate the test. To improve the results of the EZ Slam sweep tests, it would be better to operate the door from the door unit handle with a hydraulic arm that allows to keep a constant, low speed during the tests thus eliminating the variability due to a human operator.

To eliminate the effect of air bind, the EZ Slam test can be performed opening the doors of the opposite side of the vehicle thus allowing the air to escape from the cabin without increasing the pressure inside the vehicle. To assess the influence of seal compression and reaction to door closure, the tests can be performed removing the seals from the body, from the door or from both. Performing all this tests will also give important information on the mutual effect that the different factors might have one on the other. Another aspect that must be included in future work is the analysis of the dynamic response of the door during the closing event. This type of study is usually made with FEM and modal analysis. Due to the change in the mass and stiffness matrices, dependent on the change in material, the vibrational response of the door will change and needs to be analyzed. This aspect is particularly important to be considered from the sound of closure perspective. As briefly explained in the introduction and analyzed in some researches presented in the literature review ([18]), the sound of the door during closure is a fundamental aspect that contributes to the customer's first impression about the quality of the car. Another aspect in which the dynamical response of the door will probably have an effect (and so the change in material needs to be considered) is the fatigue analysis of the slamming of the door.

BIBLIOGRAPHY

[1]   "Autoreverse," a2mac1. [Online].

[2]   A. Gilberg, J. Marcosky, L. Sherman and R. Clarke , "Door Latch Strength in a Car Body Environment," *Society of Automotive Engineers,* pp. 137-153, 1998.

[3]   S. Thanagasundram, G. Dhadyalla, R. McMurran, R. P. Jones and A. Mouzakitis, "Physical Modelling of a Door Locking Mechanism for a Vehicle Application," *SAE International paper,* 2010.

[4]   A. W. Bur, P. P. Dierauer and L. F. Ricks, "Honeywell's Automotive Door Latch Design is Ideal for Corporate Latch Strategy," *SAE technical paper series,* 2003.

[5]   R. Gehm, "Heavy on Lightweighting," 2012.

[6]   R. Guo, N. Wu and G. Zhang, "New Materials for Auto-body Lightweight Applications," Department of Automobile Engineering, Shandong University, China, 2011.

[7]   A. Kelkar, R. Roth and J. Clark, "Automobile Bodies: Can Aluminum Be an Economical Alternative to Steel?," *JOM,* August 2001.

[8]   T. Ruden, R. Murty and W. Ruch, "Design and development of a Magnesium/Aluminum door frame," 1993.

[9]   S. Luckey, S. Subramanian, C. Young and P. Friedman, "Technical and Cost Study of Superplastic Forming of a Lightweight Aluminum Door Structure," *Journal of Materials Engineering and Performance,* vol. 16, 2007.

[10] J. G. Schrot, H. M. Brueggeman and N. P. Grewal, "Quick Plastically Formed Aluminum Doors: Design and Performance," *ASM International,* 2007.

[11] P. E. Krajewski and J. G. Schroth, "Overview of Quick Plastic Forming Technology," *Material Science Forum,* pp. 3-12, 2007.

[12] "Ultralight Steel Auto Closures, Overview report," Porche Engineering Servicec, Inc, May 2001.

[13] B. K. Zuidema, "Bridging the Design-Manufactoring-Materials Data Gap: Material Properties for Optimum Design and Manufactoring Performance in Light Vehicle Steel-Intensive Body Structures," *JOM,* pp. 1039-1047, 2012 .

[14] A. Bhagwan, P. McKune, T. Faath and L. Knoerr, "InCar - Advanced Door Design," ThyssenKrupp Steel USA LLC, 2012.

[15] M. Grujicic, G. Arakere, V. Sellappan, J. C. Ziegert, F. Y. Kocer and D. Schmueser, "Multi-Disciplinary Design Optimization of a Composite Car Door For Structural Performance, NVH, Crashworthiness, Durability and Manufaturability," *Multidiscipline Modeling in Mat. and Str.,* vol. 4, 2008.

[16] A. J. Jei, "A study on the Methodology for improving IQS Score for Door Opening/Closing Effort," *SAE International, Hyunday and Kia Corp.,* 2011.

[17] E. Parizet, E. Guyader and V. Nosulenko, "Analysis of car door closing sound quality," *Elsevier - Applied Acoustics,* vol. 69, pp. 12-22, 2005.

[18] S. Kuwano, H. Fasti, S. Namba, S. Nakamura and H. Uchida, "Quality of Door Sounds of Passenger Cars," in *ICA*, 2004.

[19] Y. Nagayama and R. Fujihara, "A consideration of Vehicle's Door Shutting Performance," Nissan MOtor Co., Ltd., 1981.

[20] R. Nayak and K. Im, "Optimization of the Side Swing Door Closing Effort," *SAE International,* 2003.

[21] G. Yunkay, X. Ruiyao, G. Dawei, M. Junjie and Y. Lei, "Development of Calculation Software for Automotive Side Swing Door Closing Energy," *Chinese Journal of Mechanical Engineering,* 2010.

[22] H.-i. Moon, H. Kim, S. B. Kim, D. H. Kim and H. Y. Kim, "Predicted minimum door closing velocity based on a three dimensional door-closing simulation," *Finite Elemnt Analysis and Design,* 2010.

[23] P. A. Schweitzer, Metallic Material. Physical, Mechanical, and Corrosion Properties, New York: Marcel Dekker, Inc., 2003.

[24] J. Li and Z. P. Mourelatos, "Prediction of Automotive side Swing Door Closing Effort," Oakland University, Rochester, MI, 2007.

[25] Y. Gur and K. N. Morman, "Modelling the Dissipative Effect of Seal Air Hole Spacing and Size on Door Closing Effort," *Society ofAutomotive Engineers,* pp. 249-254, 1997.

[26] D. A. Wagner, K. N. Morman, Y. Gur and M. R. Koka, "Nonlinear analysis of automotive door weatherstrip seals," *Finite Elements in Analysis and Design,* vol. 28, no. 1997, pp. 33-50, 1997.

[27] T. Zou, S. Mahadevan , Z. Mourelatos and P. Meernik, "Reliability analysis of automotive body-door subsystem," *Reliability Engineering and System Safety,* vol. 78, pp. 315-324, 2002.

[28] "Pendulum, encyclopedia2 The free dictionary," Farlex, [Online]. Available: http://encyclopedia2.thefreedictionary.com/_/viewer.aspx?path=mgh_cep&name=Schematic-diagram-of-a-pendulum.jpg. [Accessed May 2013].

[29] D. A. Russel, "The simpe pendulum," 2011. [Online]. Available: http://www.acs.psu.edu/drussell/Demos/Pendulum/Pendula.html. [Accessed 2013].

[30] [Online]. Available: http://farside.ph.utexas.edu/teaching/301/lectures/node141.html. [Accessed 2013].

[31] T. Van Esch, EZ Slam 2 user manual, EZ Metrology, 2009.

APPENDIX – UNCERTAINTY

Table A-1: Maximum range of variation with respect to the average values of the quantities measured during the EZ Slam tests of the steel and aluminum frames.

	Steel	*Aluminum (normal check)*	*Aluminum (prototype check)*
Minimum closing speed	3.3%	8.5%	0.5%
Total Energy to Close	5.9%	6.1%	3.8%
Minimum user Input Pulse	11.6%	8.4%	1.3%

Closing Energy Sinks

	Steel	*Aluminum (normal check)*	*Aluminum (prototype check)*
Energy Loss from Gravity	-	-	-
Energy Loss from Spring	-	-	-
Energy Loss to Air Bind	20.5%	30.4%	20.0%
Energy Loss to Check	9.3%	14.1%	1.4%
Energy Loss to Drag	38.1%	33.5%	65.4%
Energy Loss to Static Compression	23.6%	12.8%	1.7%

Closing Energy Inputs

	Steel	*Aluminum (normal check)*	*Aluminum (prototype check)*
Energy provided by Gravity	9.1%	20.8%	14.9%
Energy provided by Spring	3.4%	20.3%	11.8%
Energy provided by User	11.6%	8.4%	1.3%

Opening Energies

	Steel	*Aluminum (normal check)*	*Aluminum (prototype check)*
Energy provided by Gravity	-	-	-
Energy provided by spring	-	-	-
Energy provided by user	5.7%	11.9%	2.0%
Energy required by check	9.3%	14.1%	1.4%
Energy required by gravity	9.1%	20.8%	14.9%
Energy required by spring	3.4%	20.3%	11.8%
Total Energy to Open	5.7%	11.8%	2.0%

In Table A-1 the same quantities presented in Table 5-2 and Table 5-7 are presented with the percentages of difference with respect to the medium values of the tests performed on the steel and on the aluminum frames. As mentioned in Chapter 5, three, four and two values were averaged respectively for the tests on the steel frame, on the aluminum frame and on the aluminum frame with the prototype check. The values shown in Table A-1 are obtained from:

$$[\%] = \frac{VAL_{max} - VAL_{min}}{AVG} \tag{A.1}$$

Where VAL_{max} is the maximum measured value, VAL_{min} is the minimum measured value and AVG is the value obtained averaging all the tests performed. The standard deviation is not used in (A.1) because of the small number of tests performed.

As a comment on the repeatability of the tests, it needs to be underlined that, even though the tests are performed always by the same user, since they are performed manually a perfect replication of the human action can't be obtained. The maximum window of variation of the measurements is shown also for the plots presented in Chapter 5 together with maximum absolute interval of variation of each curve.

Minimum Closing Speed
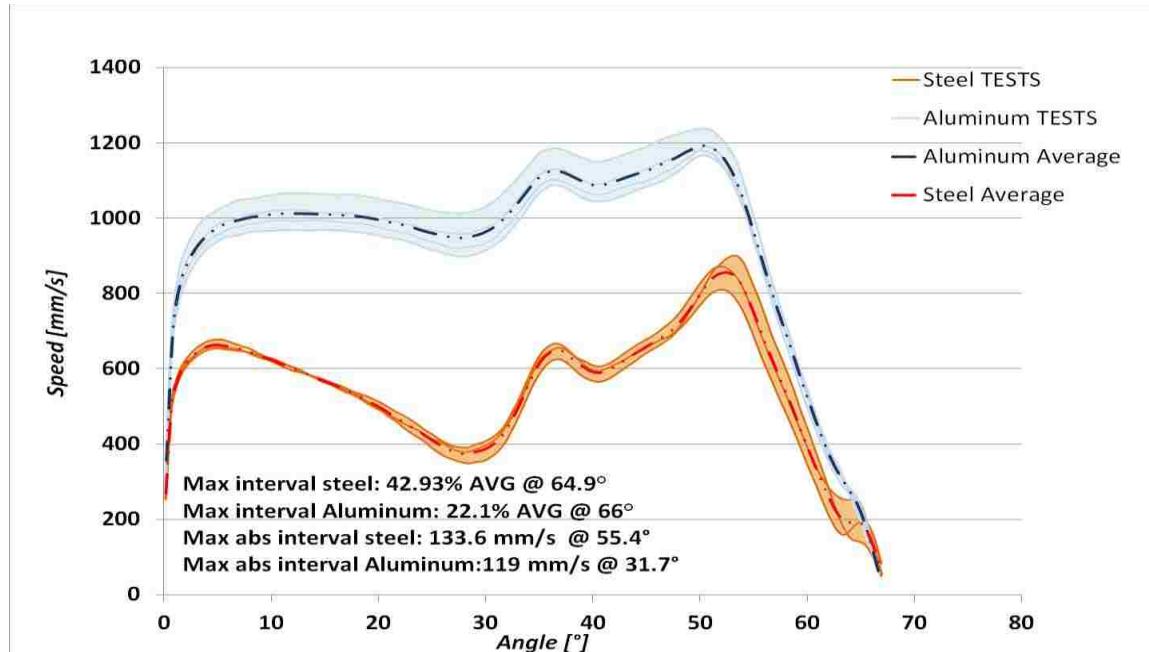
Figure A-1: Intervals of relative and absolute variations of the minimum closing speed curves for the steel and aluminum tests.

136
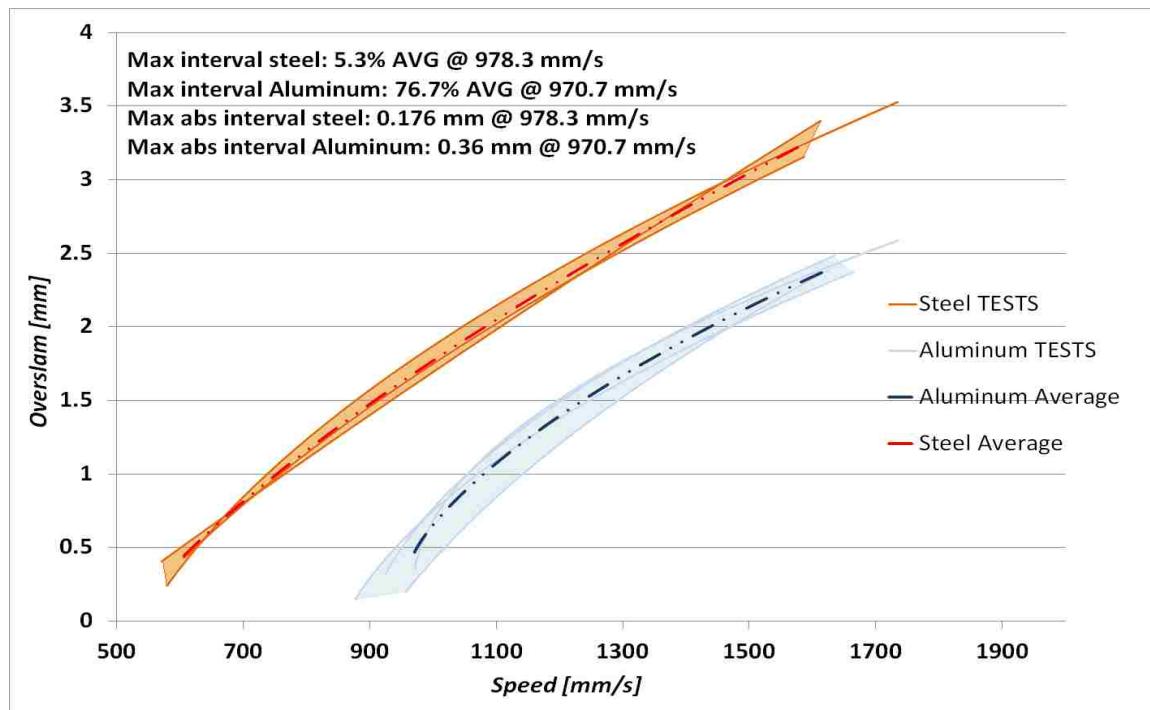
Overslam vs. Speed

Figure A-2: Intervals of relative and absolute variations of the Overslam vs. Speed curves for the steel and aluminum tests.

Pressure vs. Overslam
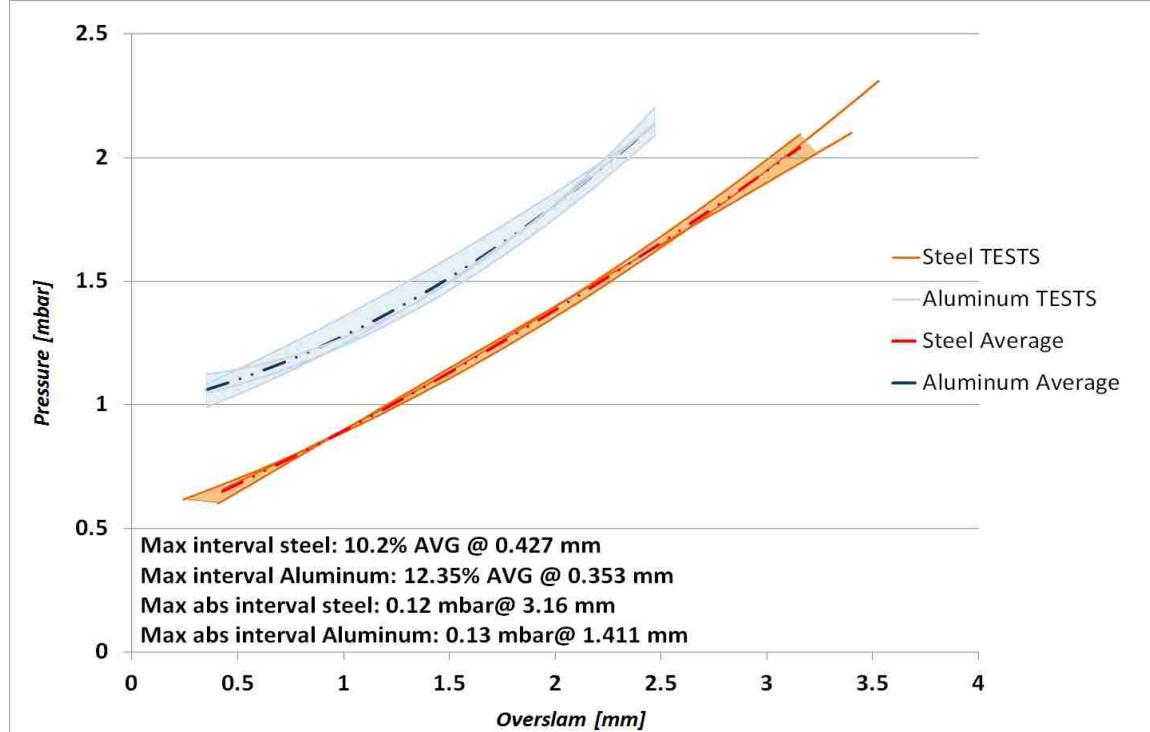
Figure A-3: Intervals of relative and absolute variations of the Pressure vs. Overslam curves for the steel and aluminum tests.

Speed vs. Pulse
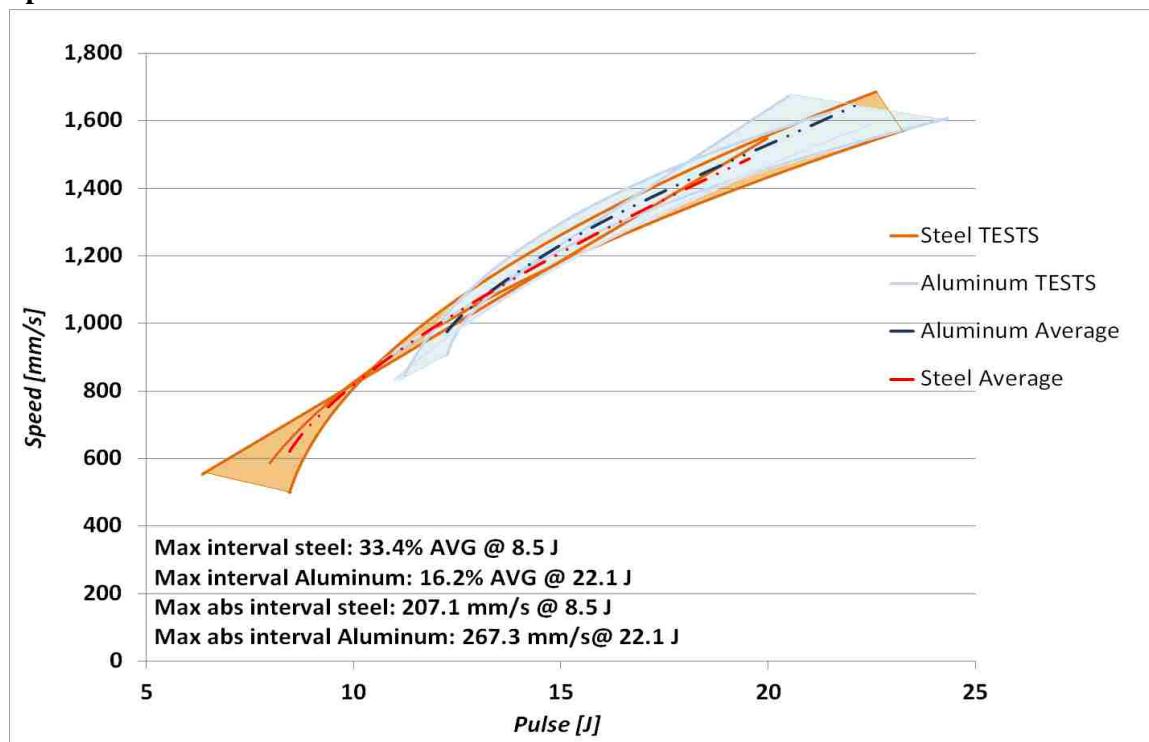
Figure A-4: Intervals of relative and absolute variations of the Speed vs. Pulse curves for the steel and aluminum tests.

Static Force
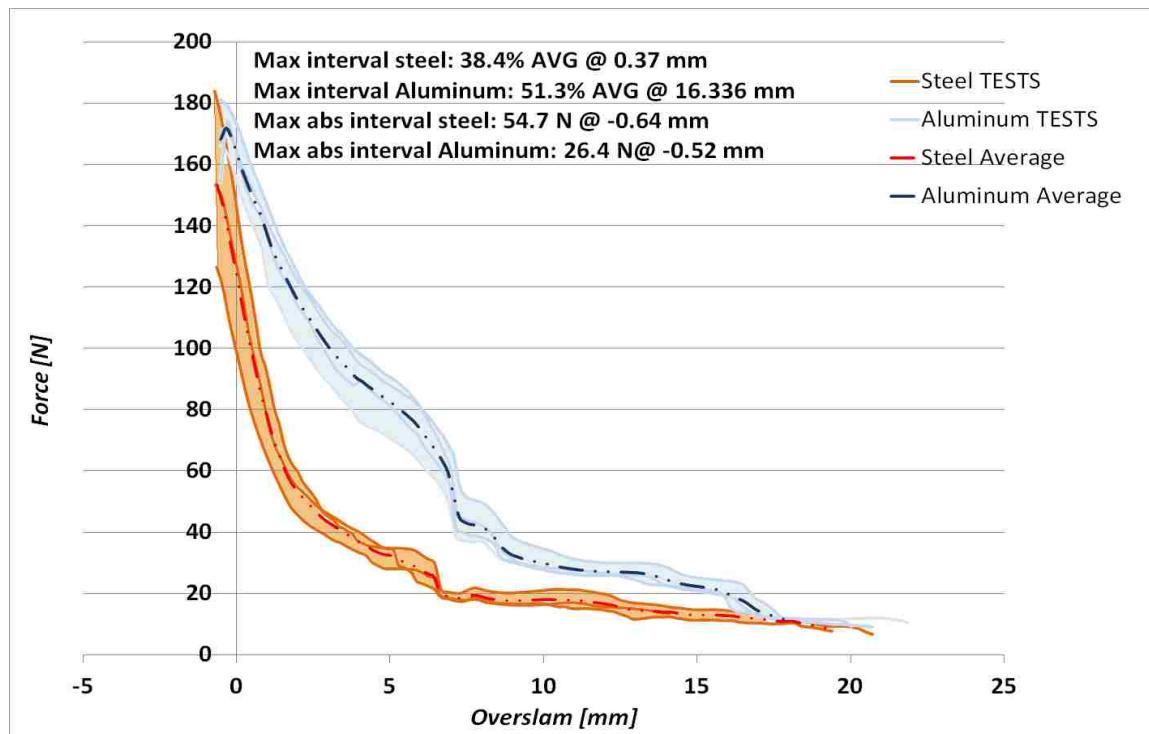
Figure A-5: Intervals of relative and absolute variations of the Static force curves for the steel and aluminum tests.

138

Pressure vs. Time

Figure A-6: Intervals of relative and absolute variations of the Pressure vs. Time curves for the steel and aluminum tests.

Opening Sweep Force
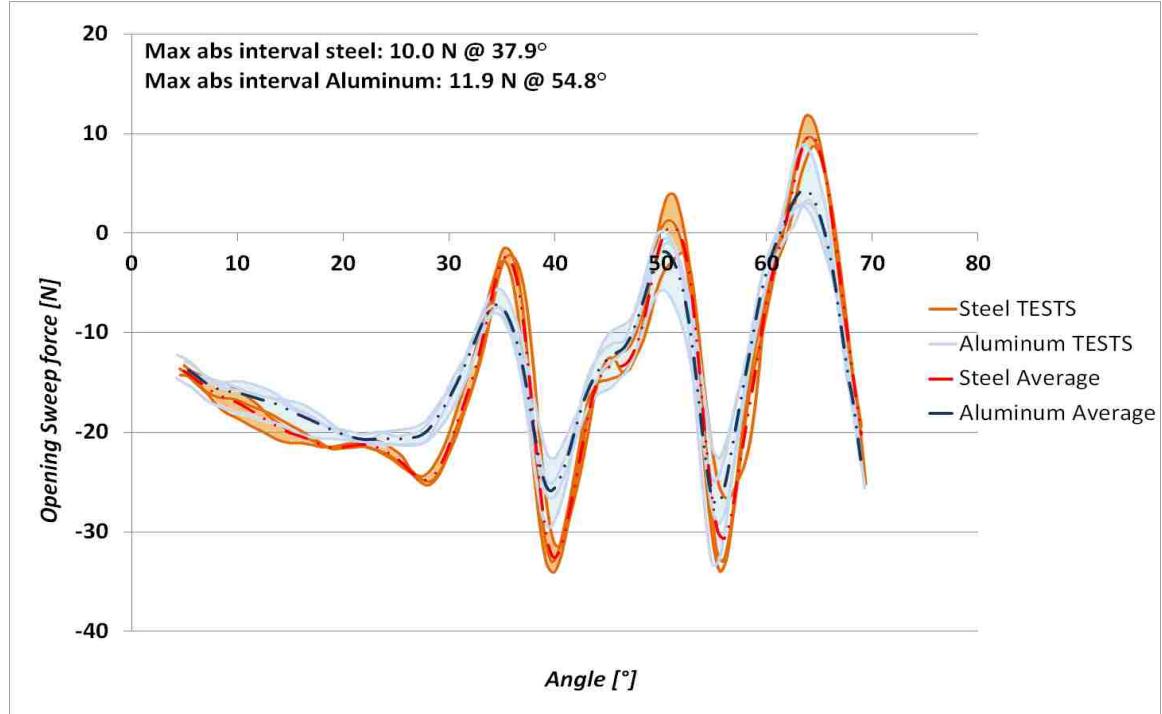
Figure A-7: Intervals of relative and absolute variations of the Opening sweep force curves for the steel and aluminum tests.

Opening Sweep Energy
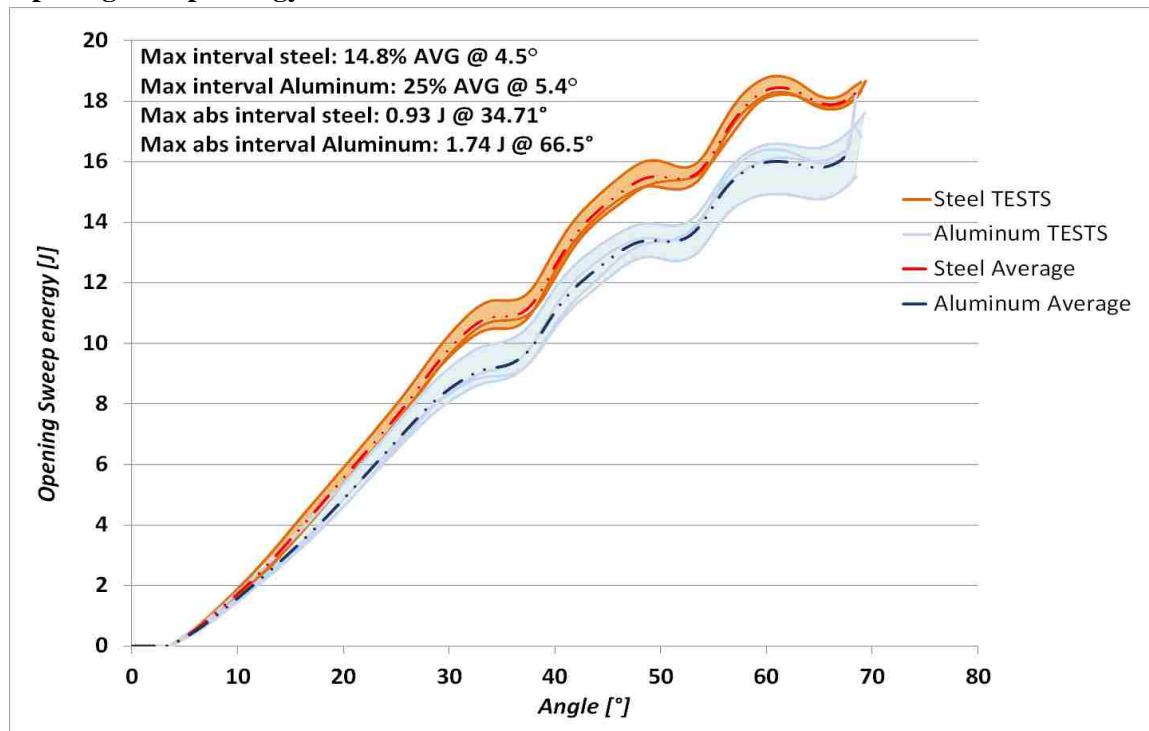
Figure A-8: Intervals of relative and absolute variations of the Opening sweep energy curves for the steel and aluminum tests.

Closing Sweep Force
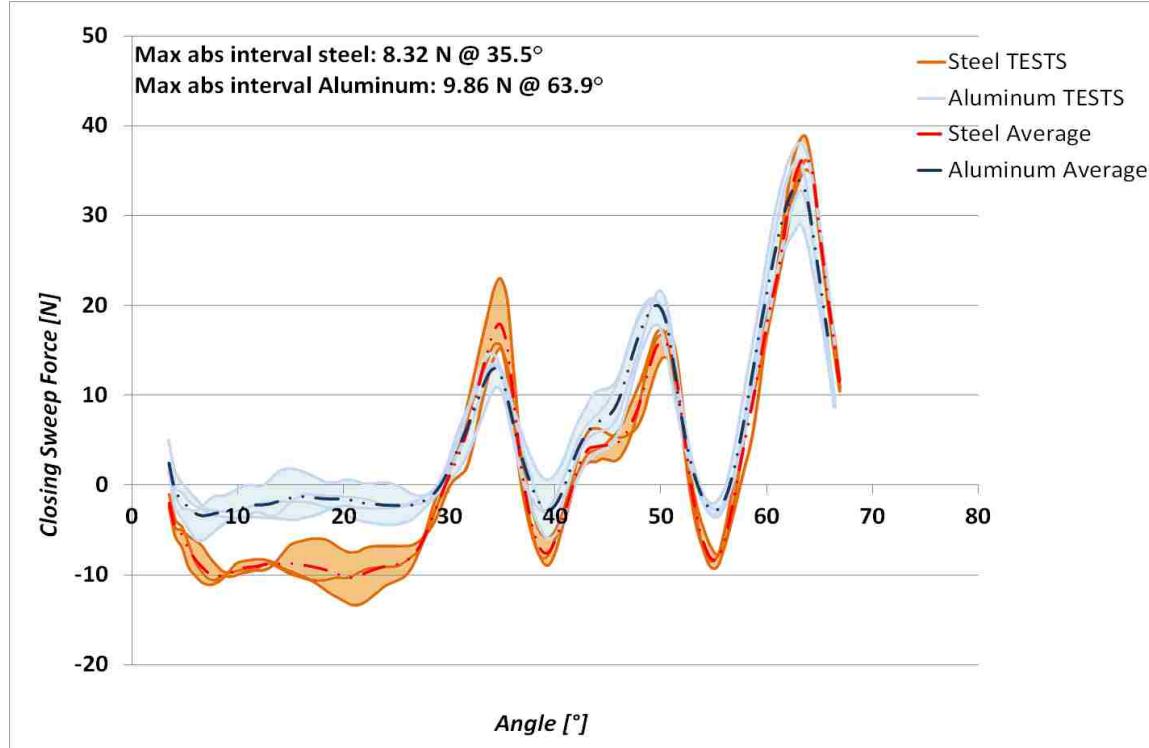
Figure A-9: Intervals of relative and absolute variations of the Closing sweep force curves for the steel and aluminum tests.

140

Closing Sweep Energy
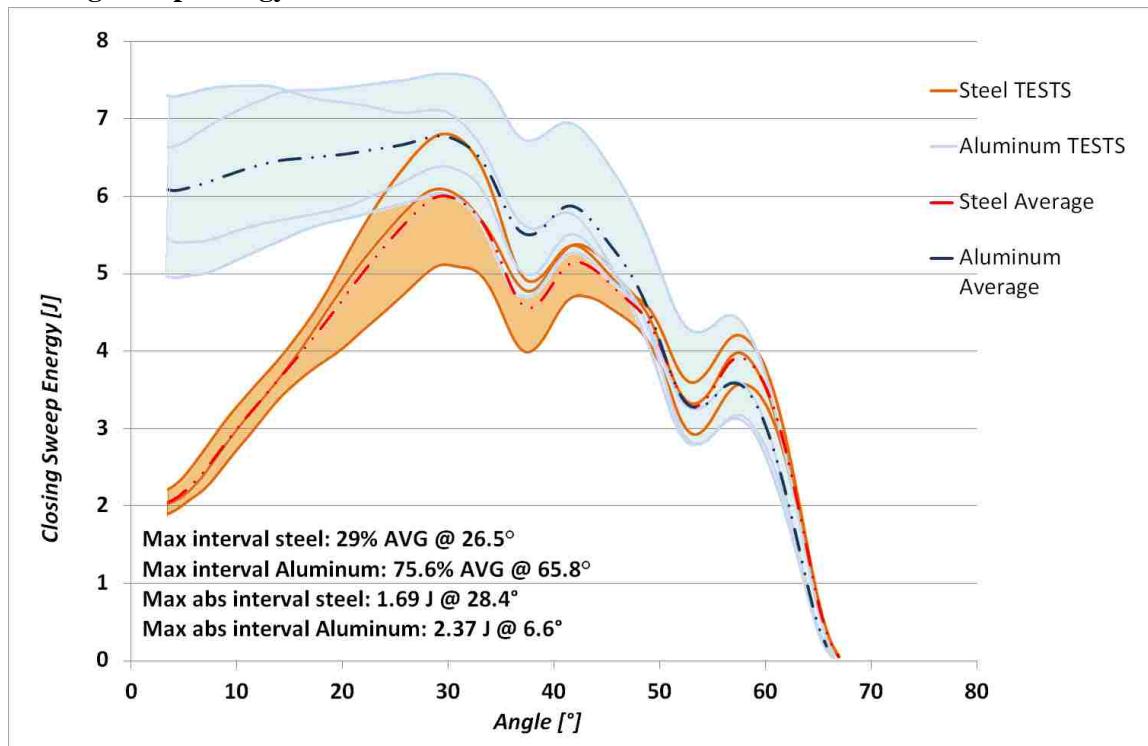
Figure A-10: Intervals of relative and absolute variations of the Closing sweep energy curves for the steel and aluminum tests.

Minimum Closing Speed
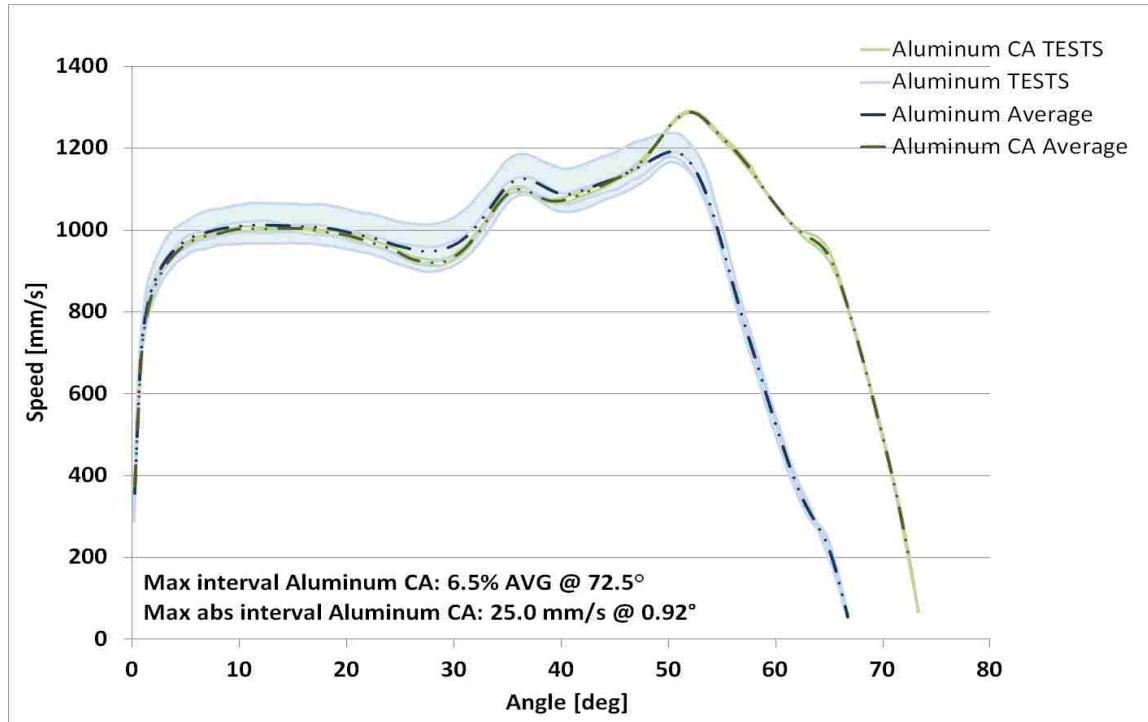
Figure A-11: Intervals of relative and absolute variations of the Minimum closing speed curves for the aluminum and aluminum CA tests.

Speed vs. Pulse
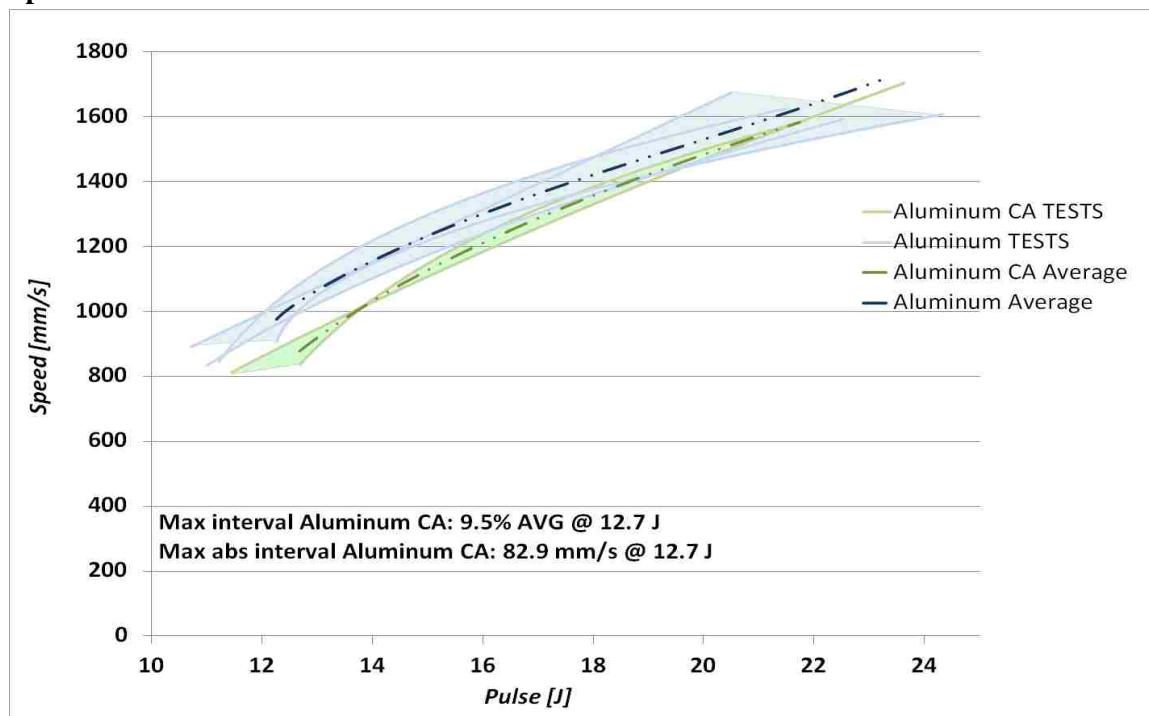
Figure A-12: Intervals of relative and absolute variations of the Speed vs. Pulse curves for the aluminum and aluminum CA tests.

Pulse Force vs. Angle
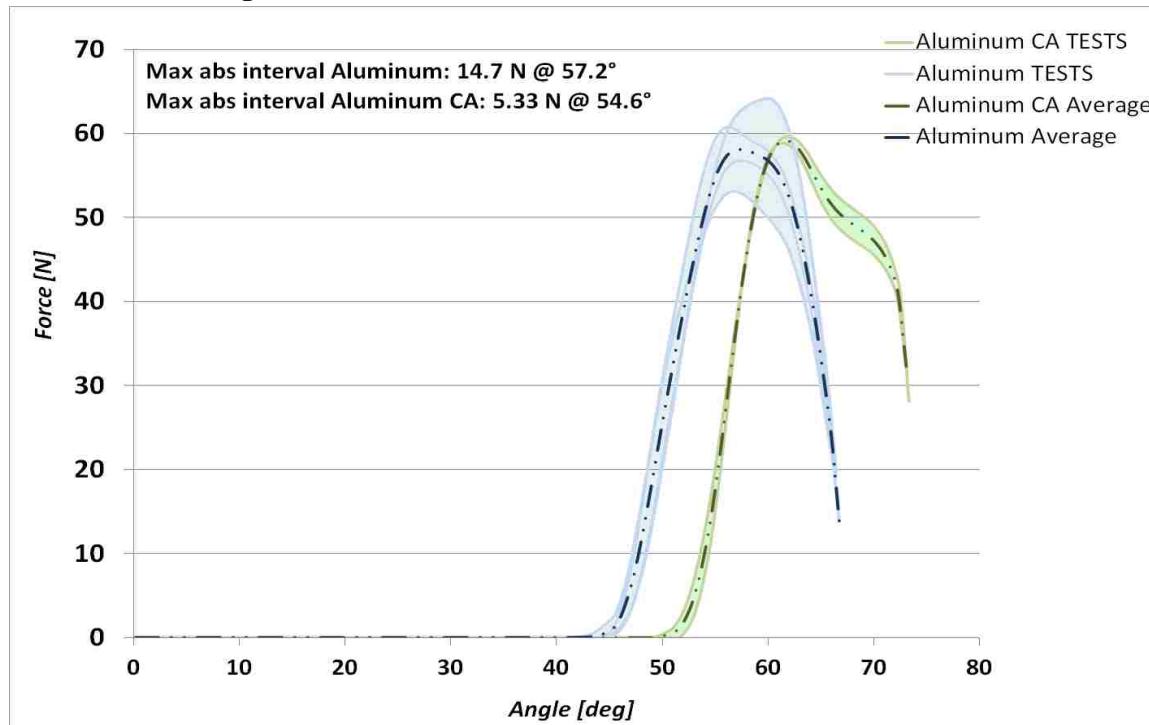
Figure A-13: Intervals of relative and absolute variations of the Pulse force vs. Angle curves for the aluminum and aluminum CA tests.

Closing Sweep Energy
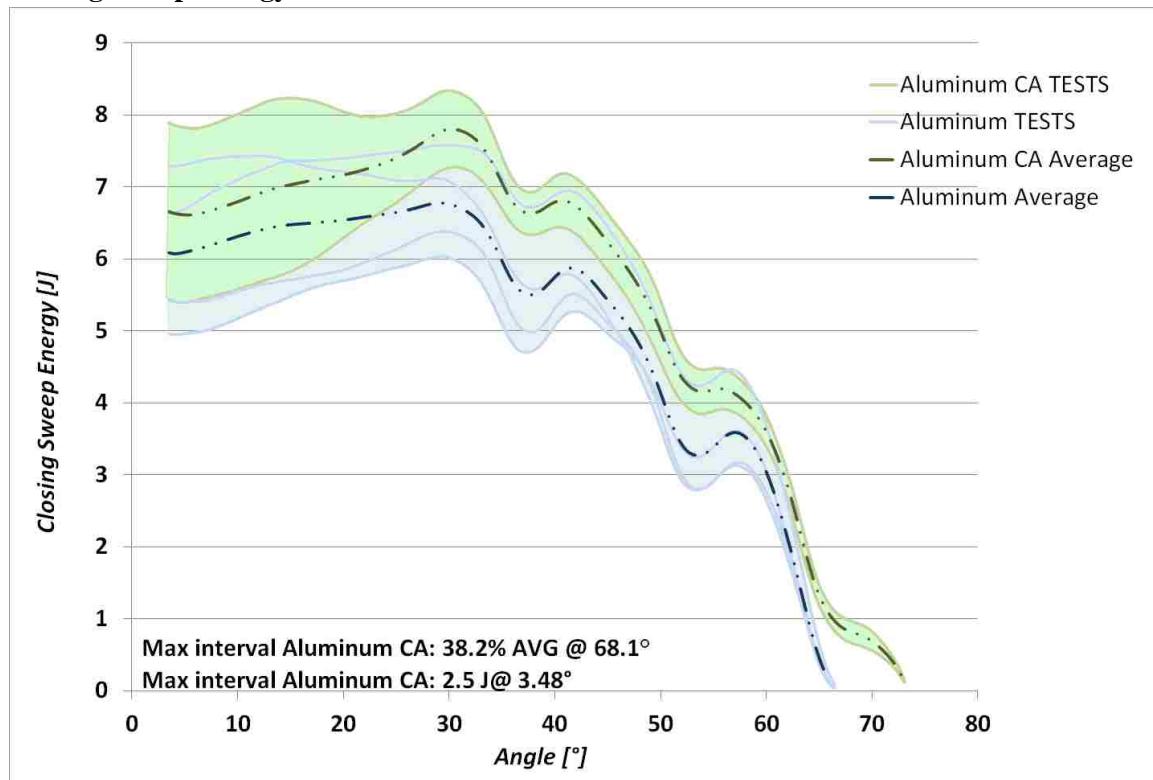
Figure A-14: Intervals of relative and absolute variations of the Closing sweep energy vs. Angle curves for the aluminum and aluminum CA tests.

VITA AUCTORIS

Maurizio Mozzone was born in Torino, Italy, in 1989. He graduated from Liceo Scientifico Ettore Majorana in Torino in 2008. From there he went to the Politecnico di Torino where he obtained the first level degree in "Ingegneria dell'Autoveicolo" ("Automotive Engineering") in 2011. He is currently a candidate for the the Master degree in Automotive Engineering at the Politecnico di Torino, Italy, and for the Master degree in Applied Science at the University of Windsor, Ontario.